INVESTIGATION INTO THE DESIGN AND OPTIMISATION OF MULTIDECK REFRIGERATED DISPLAY CASES

A Thesis Submitted for the Degree of Doctor of Philosophy

by

David Stribling
B.Eng. (Hons)

Department of Mechanical Engineering, Brunel University

July 1997

ABSTRACT

The refrigeration energy load in a modern day supermarket makes up a large proportion of the total energy bill. Better design of refrigerated display cases would reduce this load and also have a corresponding effect on the running costs of the refrigeration plant. Further enhancements such as the reduction of air overspill from the case would also influence the aisle temperatures and therefore the comfort levels in the store.

This research project uses the technique of computational fluid dynamics (CFD) to investigate the contemporary design of a vertical multideck refrigerated display case. From a two dimensional computational model conclusions were drawn as to the principles of operation of the case.

During the course of the project, a custom designed experimental facility was constructed, capable of testing the display case according to the relevant test standards. Using this facility, experimental validation was carried on a number of the design modifications to assess the actual refrigeration load against that predicted by the CFD model. The success of this validation allowed further work into the feasibility of certain design changes by making modifications to the CFD model.

The work presented in this thesis makes a contribution to the global effort towards the reduction of the energy consumption by retail refrigeration systems. It does this by showing that possibilities do exist for an improvement in the energy efficiency of multideck refrigerated display cases and that CFD provides a useful tool towards this goal. It also demonstrates the design modifications which proved to yield a saving in energy. These were a reduction in the mass flow rate of air around the case, the inclusion of a honeycomb section on the air curtain outlet of the case the addition of a front upstand and the introduction of a second air curtain thus applying a velocity gradient across the curtain.

ACKNOWLEDGEMENTS

I wish to express my sincere thanks to my supervisor Dr. Savvas Tassou for his suppport and guidance during the course of this research project.Thanks also to Debra for her help in constructing the test room at Brunel and may she one day, in the not too distant future, also reach this point in her own research. Safeway Stores plc proved to be the driving force behind the idea for this particular project and I would like to thank Doug Marriott for his ideas, commercial awareness and confidence that something tangible would come out at the end.

Any project of this kind has many ups and downs in the feint hope that eventually one of the summits of academic achievement will be reached. There have been many false summits on the eventual path to completing this thesis and I am indebted to all of my friends and family who have not merely asked me how I am doing but encouraged me along the way. In particular, Fiona deserves a special mention for her help, patience and understanding during the last year or so.

I would like to acknowledge the Engineering and Physical Sciences Research Council and Safeway Stores plc for their financial support.

Finally, I would like to dedicate this thesis to my parents who have supported me financially and otherwise throughout my decision to embark on further education. Without them none of this would have been possible and I am truly indebted to them for their belief in me.

CONTENTS

LIST OF FIGURES

LIST OF TABLES

PRINCIPLE NOMENCLATURE

b_o	Width of jet at x = 0 (metres)
b	Width of jet at some distance, x (metres)
C_p	Specific heat at constant pressure (J/kgK)
$C\mu$	Empirical constant in k-ε turbulence model
$C_{1\varepsilon}$	Empirical constant in k-ε turbulence model
$C_{2\varepsilon}$	Empirical constant in k-ε turbulence model
$C_{3\varepsilon}$	Empirical constant in k-ε turbulence model
D	Characteristic length scale (m)
g	Acceleration due to gravity = $9.81 m/s^2$
H	Height of air curtain (metres)
h	Enthalpy per unit mass (J/kg)
i, j, k	Integers appearing as subscripts
k	Turbulent kinetic energy
k_t	Thermal conductivity (W/mK)
p	Pressure (N/m^2)
Q	Heat transfer (Watts)
Re	Reynolds number = $\frac{\rho u D}{\mu}$
S_m	Mass source term
S_h	Enthalpy Source Term
T	Temperature (K)
t	Time (s)
u,v,w	Velocities in the x,y,z directions (m/s)

u',v',w' Instantaneous velocity fluctuations in the x,y,z directions (m/s)

$\bar{u},\bar{v},\bar{w}$ Mean velocities in the x,y,z directions (m/s)

u_τ Friction Velocity (m/s)

x,y,z Rectangular cartesian coordinates in space

y^+ Dimensionless distance of near wall cell from wall

δ_{ij} Kronecker delta = 1 if i = j; 0 if i<>j

ε Eddy dissipation rate

κ Von Karman's constant

σ_k Empirical constant in k-ε turbulence model

σ_ε Empirical constant in k- turbulence model

ρ Density (kg/m^3)

μ Laminar viscosity (Ns/m^2)

μ_t Turbulent or eddy viscosity

τ_w Wall shear stress

CHAPTER 1

INTRODUCTION

The refrigeration system serving the refrigerated display cases, cold rooms and numerous other refrigerated fixtures in a modern day supermarket accounts for at least 50% of the electricity bill of the store. The amount of energy which this represents is quite considerable and, with increasing competition in the food retailing sector, provides a suitable target area in which supermarket operators can cut their operating costs.

Until recently, the main focus of researchers has been on the high pressure side of the refrigeration circuit in order to improve the operating efficiency and thus reduce the relatively high running costs. Multiplex parallel compressor packs, evaporative condensers and electronic controls are some of the innovations which have been developed in the last fifteen years in an attempt to reduce the portion of the store's energy bill attributable to refrigeration. However, whilst modifications to the high pressure plant and controls abound, the development of the display cases themselves has remained largely static. This resistance to change is partly due to the demands of the merchandisers who require the refrigerated product to be displayed in the most attractive manner possible in order to optimise their sales. It should not be forgotten however, that different merchandising layout strategies can result in significant variations in the additional energy consumption required to achieve these changes.

It is difficult to understand why refrigerated case design has remained effectively unchanged for the last three or four decades especially when the air flow characteristics of the display fixture directly affect the load on the evaporator. Development of the compressor and condenser plant merely aid the system in dealing with this load more effectively. Clearly, a more methodical approach to the problem would be to reduce the total refrigeration load on the store by improved case design before attempting to manage this load more efficiently.

Retail food stores have different frozen and chilled display strategies. However, frozen food cabinets generally tend to either use closed air systems (cases with glass doors) or the well type case where gravity acts on the cold air minimising infiltration. In these designs, optimising air flow would offer less opportunities for reducing energy consumption by the unit. On the other hand, high temperature multideck refrigerated display cases, when analysed, could account for up to 75 or 80% infiltration losses in the poorest design examples. Infiltration of the store air into the display case is expensive in refrigeration energy as well as causing additional heating requirements in the aisles of the store.

Recently investigations have been carried out on the air flow characteristics of multideck refrigerated display cases using both computational modelling and experimental procedures. Although the correlation between the results of these two methods has been less than satisfactory, this work has shown that firstly it is possible to model display cases using computational fluid dynamics and that secondly there are potential energy savings obtainable by modifying the presently accepted designs.

The aim of this thesis is to model a vertical multideck refrigerated display case using computational fluid dynamics and investigate the effect of introducing various design modifications on the performance of the case. The fluid dynamics and heat transfer characteristics of a display case are surprisingly complicated and some time has been spent on understanding the mechanisms of case operation. This knowledge has then been used to make more educated design decisions rather than relying on laboratory testing driven by intuitive techniques.

There are several reasons for using CFD in this study. First and foremost is that it is a design tool which is dedicated to the investigation of fluid flow and heat transfer, two mechanisms which cannot be neglected in the successful operation of a chilled cabinet. Other analytical techniques would have been possible but these would have involved vastly simplified numerical models and some very coarse assumptions. CFD has the

advantage that reliable and consistent models can be developed whilst still providing the flexibility of incorporating design changes without having to develop new mathematical models.

Another advantage is that CFD allows an extremely small scale evaluation of the fluid properties around the geometry without expensive instrumentation. It can also quantify parameters which may otherwise be difficult to measure such as fluid viscosity or density which, on a microscopic scale, may affect the overall air flow pattern.

It is true that it is expensive for manufacturers to set up an in house CFD capability and that the capital cost can vary enormously depending upon the software license and hardware platform. This can be a prohibitive cost for many companies especially when the return will be unspecified. The initial capital investment is therefore, understandably, the greatest reason for scepticism in the capabilities of CFD modelling. However, this must be weighed against the estimates of cost for case modification and evaluation in a test room. It should be stressed that although a successful model of the display case can be achieved, designs will still require testing in order to satisfy European and International performance standards. It is, however, envisaged that by assessing the significance of various design parameters and having a better understanding of display case operation through CFD, the amount of laboratory time required will be limited to final testing in order to satisfy the relevant standards. This is necessary, in carrying out a CFD analysis and optimisation on a refrigeration system, in order to reduce energy consumption, the overriding consideration must always be that product temperatures are maintained.

This thesis is divided into seven chapters including this brief introduction.
In chapter 2, a review of past work relevant to this study is presented together with some theory behind the fluid dynamics of a display case. In order that the reader may wholly understand this review, a section will also be dedicated to explaining the operation of a vertical multideck display case. The objective of this chapter is to put the present research into perspective and appraise advances in the technology over the past few years.

The design and construction of a suitable test room has formed a large proportion of the present project and this will be presented in chapter 3. In order that this facility can be used for more than merely testing display case operation, much work has gone into ensuring that the test chamber can operate as flexibly as possible whilst still adhering to the requirements of BS 6148:1981 and European Standard EN 441 (1995). These are the British and European test standards for commercial refrigerated cases.

Chapter 4 concentrates on explaining some of the theory behind CFD. It should be pointed out that the aim of this chapter is merely to provide the reader with some understanding of how a CFD code works and the reasons behind some of the modelling decisions and not to carry out an in depth mathematical analysis. The objective of this project, after all, is not to develop innovative CFD models but use a commercially available code as a design tool.

The results of a two dimensional CFD simulation are presented in chapter 5 together with experimental results of validation studies for the model. A comparison is made between these two evaluation techniques for display case performance and conclusions are drawn as to the suitability of CFD for such a study. A two dimensional model is also presented of the display case including the effects of water vapour in the air in an attempt to predict, computationally, the latent refrigeration load. Finally, a three dimensional simulation is described and its applicability examined in modelling what is predominantly a two dimensional flow.

Chapter 6 assesses the performance of several design modifications to the baseline display case using a CFD model. It was envisaged that this process would enable the elimination of designs of little potential and that a better understanding of what makes a display case more energy efficient would be established. Experimental results are also presented from tests carried out incorporating some of the modelled modifications into the case design.

Finally , Chapter 7 summarises the work which has been carried out during the course of this research project and draws final conclusions. These are in terms of the applicability of

the use of CFD in the design process associated with refrigerated display cases and in recommendations for design features which should be considered for cases of the future.

CHAPTER 2

BACKGROUND AND LITERATURE REVIEW

2.1 - INTRODUCTION

During the last 30 years, consumer choice has been transformed by developments in the production, distribution and retailing of food which, along with improvements in the design and equipment in the modern kitchen, have made a major change in our lifestyle.

Although some foods sold from refrigerator cabinets have been available for many years, it was during the 1970's that more products suddenly became available. Then, during the 1980's, numerous technological developments in food production and storage caused the number and variety of products to multiply again. It was not until the early 1990's that the number of chilled food product introductions began to level out.

The basis for the chilled food sector is the availability of chilled storage and display cabinets supported by a product distribution infrastructure. This was stimulated by the advent of self service supermarkets in the UK in the 1950's. The growth of the supermarket sector in the 1960's and throughout the 70's supported the expanding product range of chilled and frozen food. Retail business estimates for the major chilled food categories illustrated a 116% increase in value between 1984 and 1988 with continued growth predicted throughout the 90's.

Foods are chilled or frozen in order to keep them longer and prevent degradation of the product. Food spoilage can be due to one, or a combination of the following causes:

1) Living organisms (e.g. vermin, insects or fungi) feeding on the food and contaminating it.
2) Biochemical activity within the food (e.g. respiration, staling etc.)
3) Physical processes (e.g. spilling or re-crystallisation phenomena in sugar confectionery).

Certain measures such as suitable packaging will stop spillage or insects but other food spoilage processes such as biochemical degradation cannot be contained in this way alone. Successful storage to eliminate or slow down these processes depends on the storage conditions of the food, namely temperature, relative humidity and composition of the store atmosphere.

The rate of biochemical degradation of a food product increases with temperature. This can be expressed mathematically as follows, Ratkowsky et al. (1982):

$$r = b(T - T_{min}) \qquad (2.1)$$

Where r is the growth or spoilage rate, T is the storage temperature, T_{min} is a hypothetical temperature at which the growth rate is zero, and b is a constant. From this formula, it is evident that the lower the temperature of storage, without freezing the products, the slower the rate of spoilage and hence the longer the shelf life.

These changes to the type of food and the way in which is prepared for sale in supermarkets means that there is now a very significant requirement for refrigerated display cabinets on the shop floor supported by efficient high pressure refrigeration plant. The aim of this infrastructure is to preserve the product in the best possible condition whilst merchandising it effectively for customers to buy.

2.2 - EVOLUTION OF SUPERMARKET REFRIGERATION SYSTEMS

When supermarkets began to appear some thirty or so years ago, standard practice was to use the simplest form of refrigeration system consisting of display cases with the compressor and condenser self contained within the base of the case. Adams and Trieb (1985) have examined the evolution from this very simple method to cases with remote condensing units. The main reasons for the shift from self contained to remote high pressure plant seem to have come from a demand for better energy efficiency, more flexibility in system design and ease of maintenance.

Twenty years ago, the majority of refrigeration systems in supermarkets consisted of a remotely located single compressor and condenser for each display case line up. Load matching was achieved by cylinder unloading, hot gas bypass or compressor cycling which was both inefficient and shortened the life of the compressor. However, during the late 1970's and throughout the 1980's the rising cost of fossil fuels and the resulting demand for energy efficiency led to the development of new strategies in refrigeration systems. Although conventional systems do still exist, most of the large supermarket chains now choose to employ state of the art refrigeration systems.

The hub of these modern systems is the multiplex parallel compressor pack. This is a group of equal or different sized compressors operating in unison to refrigerate a major portion of the supermarket's refrigerated cases. Typically, a supermarket will have three compressor packs, each having four to six compressors. The total refrigeration load of the store is then divided between the packs, for example:

- Low temperature cases (e.g. frozen food) with an evaporator temperature of -18/-20°C on pack A.
- Very low temperature (e.g. ice cream) with an evaporator temperature of -26/-28°C supplied by a satellite compressor to pack A.
- Medium temperature (e.g. delicatessen & dairy) with an evaporator temperature of 0/+2°C supplied by pack B.
- High temperature (e.g. produce) with an evaporator temperature of +3/+6°C supplied by pack C.
- Meat satellite with an evaporator temperature of -1/+1°C supplied by a satellite compressor to rack C.

In a compressor pack, the compressors operate at common suction conditions which satisfy the majority of cases supplied by that pack. Sometimes cases of a slightly higher or lower evaporator temperature are also connected to the same pack. In this situation, satellite compressors are used, as mentioned above, which have their own suction manifold but are connected to the pack's common discharge manifold.

The total capacity of the compressor pack can either be divided equally between the machines, or different sized compressors can be used. This latter arrangement is referred to as an unequal parallel system and has the advantage that different compressors can be cycled on and off using a digital stepping sequence in order to more accurately match the required load.

Refrigeration systems with multiplex parallel compressors nearly always use remote air cooled or water cooled condensers for heat rejection. In the USA evaporative condensers are gaining popularity. These consist of bare copper tubes over which water is sprayed against the direction of air flow. This causes the water to evaporate thus cooling the refrigerant gas. The advantage of this design is that the coil can be operated close to the ambient wet bulb temperature, reducing the condenser pressure and therefore the amount of work that has to be done by the compressor. Due to the increased maintenance costs of these systems, however, and the now stringent legislation

to prevent legionella, the evaporatively cooled condenser has failed to gain wide acceptance in the UK.

Off-cycle, electric or hot gas defrost methods can be used with the multiplex refrigeration system. Hot gas defrost involves the circulation of hot refrigerant gas at about 60°C from the compressor discharge manifold through the evaporator. There, the refrigerant first condenses melting the ice formed on the coil, and is then returned to the condenser for circulation to the other display case circuits. Due to the thermally induced stresses which hot gas defrost causes to the evaporator coils some manufacturers now prefer to employ cool gas defrost. With this method the gas is taken from the top of the liquid receiver at about 40°C and circulated around the cases as in hot gas defrost.

As has been previously explained, multiplex parallel refrigeration systems are inherently more efficient than single compressors due to their good load matching characteristics. Furthermore, their centralised location and flexibility mean that further features can be employed to reduce running costs.

It is logical that as the condensing pressure is reduced, the compressor will have to do less work to maintain this pressure in the discharge line. In theory, therefore, the condenser pressure could be reduced in line with a reduction in ambient temperature, as long as a suitable temperature difference is maintained between the refrigerant and the outside air to allow heat rejection. Floating head pressure control allows this option although in reality, certain factors limit the amount by which the condenser pressure can be reduced. One such factor is the operation of the thermostatic expansion valve which is greatly affected by the upstream liquid pressure feeding it. When this pressure is reduced, the ability of the valve to feed refrigerant to the display case is hampered. Also, during low head pressure operation, ambient refrigerant subcooling is limited which can result in possible flashing of the refrigerant in the liquid line.

These problems can be overcome using new types of throttling device. These include electronic expansion valves and balanced port expansion valves both of which allow throttling at low flow rates.

When operating at a reduced condensing pressure, multiplex compressor packs are also able to offer better load matching allowing a more consistent display case temperature. With a conventional system, where the compressor would be working at part load, long off cycle periods could result in unacceptable temperature variations in the display case.

Taking all of the above factors into account, the minimum condensing temperature usually recommended by compressor manufacturers is 21°C.

Ambient subcooling is the cooling of liquid refrigerant below its saturation temperature by heat rejection to the environment. This can be done either in the final passes through the condenser coil or by providing a separate coil dedicated to this task. Subcooling is especially important when floating head pressure is employed.

The amount of ambient subcooling that can be achieved clearly depends very much on the ambient temperature. During operation in high ambient temperatures, subcooling can be limited to as little as 5°C. During periods of low ambient temperatures, the condensing temperature can fall below the desired minimum causing the type of problems described previously. In order to prevent this, a liquid hold back valve is employed at the outlet of the condenser, flooding the final passes of the coil, raising the condenser pressure and also producing additional subcooling. The standard design condition of the ambient subcooling coil is to produce about 10°C of subcooling at ambient design conditions.

Further subcooling of the liquid refrigerant beyond the ambient temperature can be achieved by the use of mechanical methods. In this arrangement, the liquid refrigerant leaves the ambient subcooling coil and enters a further heat exchanger. this coil also acts as an evaporator for a second, smaller refrigeration system thus cooling the liquid refrigerant of the main system. This additional subcooling increases the refrigeration effect of the display case evaporator. This means that less refrigerant has to be pumped around the circuit reducing electricity consumption by the compressor. However, in order for these savings to outweigh the running costs of the subcooling refrigeration system, the secondary refrigeration circuit must operate at a higher suction pressure than the main system. For this reason, mechanical subcooling is normally only applied to low and very low temperature refrigeration systems. The mechanical subcooling compressor can either be part of a high temperature refrigeration circuit or dedicated to subcooling only. Dedicated units normally operate as a satellite on the main compressor pack. Standard practice for mechanically subcooled systems is to provide liquid refrigerant to the expansion valves of low temperature cases at about 5°C.

Another method of enhancing the degree of subcooling is by the use of a separate subcooling coil. This has the advantage of not raising the condenser pressure and also offers greater flexibility in the piping of the refrigeration system.

It is possible for supermarkets to take advantage of the large amounts of heat rejected from their refrigeration systems by reclaiming this heat and using it for space or water heating. During normal operation, the refrigerant is piped directly from the compressor to the condenser. However, when space heating is required, the hot refrigerant gas in the discharge line can be diverted using a three port control valve. It passes through a coil in the store's air handling unit before being passed back to the condenser.

Control of the heat reclaim is usually via a store or water thermostat. This would normally be a two stage control, the first of which would be heat reclaim from the refrigerant, the second, a booster heater battery or immersion heater to bring the supply air or hot water up to the design temperature if required.

One of the disadvantages of heat reclaim is its conflict with floating head pressure control. In order to gain useful heat, the condenser temperature setting is normally of the order of 35°C, requiring the compressor to do more work. There is, therefore a fine balance between reducing the condenser pressure so that the compressor consumes less energy, but also maintaining a high enough condenser pressure to allow effective heat reclaim.

Refrigerant leakage is another problem with multiplex systems. The larger charge, refrigerant line expansion and contraction during hot gas defrost, and the greater number of solder connections and mechanical components all combine to make refrigerant leaks a more likely occurrence on parallel systems.

Whatever the advantages or disadvantages of either system, one thing remains certain. The majority if not all of new supermarkets are now fitted with state of the art multiplex parallel compressor systems.

2.3 - ENERGY STUDIES

Refrigeration and air conditioning accounts for 20% of all the electricity consumption in the UK and its importance is also reflected similarly in other countries.

A study carried out in Texas by Cox et al. (1993) stated that 2.8% of commercial building energy in the US was attributable to food sales. This may seem a small percentage, but, when applied to all of the commercially consumed energy in the US,

represents very significant figures. For instance, grocery stores often consume between two and six times more energy per unit floor area than a typical office building. In the same study, an energy survey was carried out in 93 grocery stores in south central Texas. It was discovered that the total electricity consumption was roughly $100W/m^2$. It was also found that stores built after 1979, on average, consumed 9% less energy per square metre than those built previously. This was attributed to two factors. Firstly, stores built after 1979 were larger and their additional space was used to stock products that did not require refrigeration. Secondly, stores built after this year included a significant number of energy saving measures such as parallel compressors, heat reclaim etc.

Energy savings arising from the introduction of various energy conservation measures have been investigated extensively, again in the United States, by Walker et al. at the Electric Power Research Institute (1990). In their studies, a Safeway supermarket in Menlo Park, California was modified so that it was equipped with both a multiplex parallel compressor arrangement as well as a conventional in line compressor system.

The state-of-the-art multiplex refrigeration system consisted of three packs of unequal, parallel compressors. Two of the packs were also fitted with a satellite machine operating at a different suction pressure than the rest of the pack to which they were piped. Heat rejection was accomplished through the use of an evaporative condenser equipped with separate condensing circuits for each of the three packs. The conventional refrigeration system consisted of 23 individual compressors, each equipped with a water cooled condenser unit for heat rejection.

Testing at the store was carried out over a two and a half year period during which alternate monitoring of the conventional and multiplex system was conducted as well as attempting to isolate the performance of some of the multiplex features such as mechanical and ambient subcooling, floating head pressure etc. Analysis of the energy consumption figures showed that the multiplex system with all of its enhancements achieved a 23.2% reduction in daily energy consumption compared to the conventional system. Most of these savings came from the parallel compressors themselves which accounted for 15.2 of the 23.2 percentage points.

Another feature of the state-of-the-art refrigeration system was its ability to reduce the peak demand of the store thereby saving more money on the annual energy bill. The

store peak demand was taken as occurring at 5pm. The reduction achieved was 34.1 kW which represented a reduction of 29.8% on the demand for the conventional system.

These results proved, quite conclusively, the energy efficiency of a multiplex parallel compressor system and also stimulated a research program to develop a computer model for supermarkets. This was done using the building computer simulation model TRNSYS, a commercially available transient system simulation program with a modular structure. The TRNSYS library contained many of the components needed to simulate a supermarket energy system including the building fabric and HVAC. However, for the refrigeration system model special routines had to be written and modified in order to simulate items such as the compressors, cooling towers, condensers, subcoolers etc.

The computer model was then validated against the test results obtained from the Menlo Park store. The saving in annual energy consumption predicted was approximately 27% compared to 23.2% of the test results. It was also predicted that demand would be reduced by 29% compared to the 29.8% achieved from the metered data. The computer model was then used to simulate supermarkets at six further sites in the US taking into account climatic conditions and regional electricity tariffs to determine simple payback periods for a multiplex refrigeration system along with its various enhancements.

Estimates at 1990 prices, for a 3915m^2 supermarket, such as the one at Menlo Park, showed that there would be a cost premium of $20,000 associated with the unequal parallel system over the conventional one. Other costs taken into account with the calculation of the pay back period were increased maintenance requirements and the use of additional water in the evaporative condenser. The annual maintenance costs were estimated to be $11,500 compared to $8,190 for the conventional system. The additional costs associated with the operation of the evaporative condenser were estimated at approximately $1,500 for mechanical maintenance and $600 for water and sewerage charges.

2.4 - REFRIGERATED DISPLAY CASES

Since the concept of chilled and frozen foods came about, some method has been required by retailers to display the product in an accessible and attractive manner whilst still preserving its low temperature. Basically, there are three types of refrigerated display case in regular use in supermarkets today.

The most common type of display case, certainly for medium temperature applications, is the vertical multideck case as shown in figure 2.1. This design has become popular among merchandisers due to its large display area and ease of access for customers. The principle of operation can best be explained with reference to figure 2.2.

Figure 2.1 - A Typical Vertical Multideck Display Case

Air is forced over an evaporator by means of propeller fans located in the base of the unit. The cooled air then passes up into the back panel of the case which is perforated and allows air to diffuse through over the product. The remainder of the air then passes into the canopy of the case from which it is discharged downwards over the front of the product in the form of an air curtain, forming a barrier between the warm supermarket environment and the chilled display area. Air is then drawn back into the case at a return air grille located at the front of the base unit. The advantage of the air curtain is that a shield is formed to keep the warm air out of the case whilst still allowing a warm hand to penetrate it. The main disadvantage however, is that when a moving stream of air passes through a relatively still environment, some of the ambient air will be entrained into what is effectively a plane jet. The two streams of air will then mix resulting in a mixture of cold and warm humid air which is then drawn back into the case through the return air grille. This adds an energy load to the display case evaporator, not only in the form of additional sensible cooling, but also in defrost load as the humid air condenses on the coil and freezes. The mechanisms

involved in the air curtain and heat and moisture transfer across it will be discussed in more detail in section 2.6.

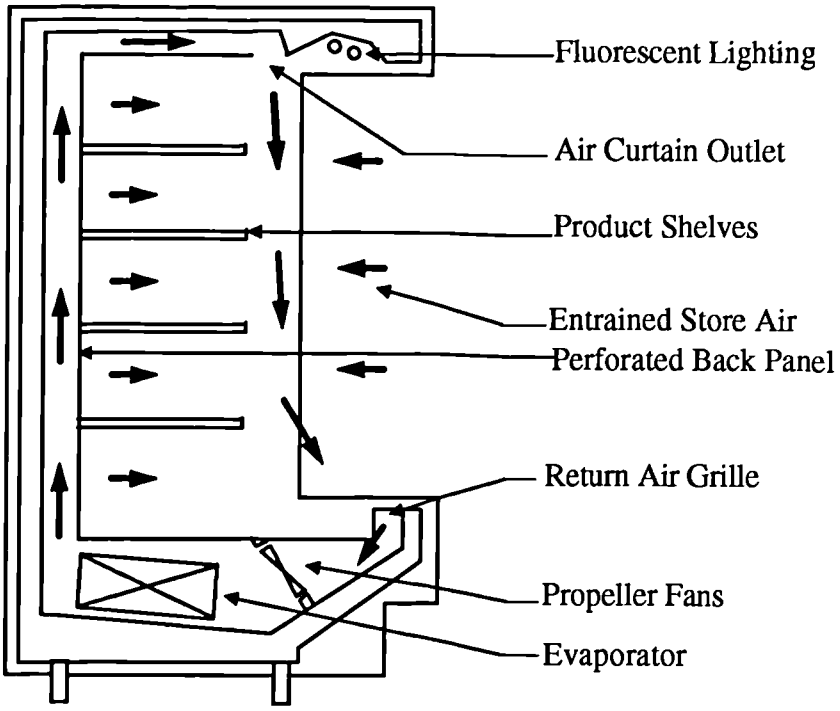

Figure 2.2 - Cross Section Through a Vertical Multideck Display Case

The oldest design of refrigerated case, is the horizontal well type, figure 2.3. This is essentially a vertical case laid on its back. The product is stacked in the case up to the load line and then a curtain of cold air flows across the top of it. However, because of the inherent advantage of this arrangement, namely gravity, the velocity of the air curtain can be reduced, entraining less warm air into the return air grille and reducing cold air spillage into the aisles of the store. Because this case works principally on the difference in density between the curtain and ambient air, it is used principally for frozen food and ice cream displays where the low temperatures mean that this density difference is at its greatest.

The third type of display case is the delicatessen or meat service counter, Figure 2.4. The change in consumers' tastes over the years has led to a requirement for cold meat, cheese, and salads to be served over a counter by a sales assistant. In this way, customers can select exactly what they want and in what quantity as opposed to buying it pre-packaged.

Figure 2.3 - Horizontal Well Type Case with Glass Door Reach-ins Above

Figure 2.4 - A Serveover Delicatessen Case

As will be discussed in more detail in section 2.5 the design of refrigerated display fixtures is usually a compromise between the wishes of the merchandiser and the engineer. In the delicatessen case the design decision is between gravity or forced air circulation and becomes very much a merchandising decision. The gravity design is a

better refrigerator with a low wind chill but a poor merchandiser because it is not possible to incorporate an intermediate shelf which would impede the air circulation. The forced air case is a better merchandiser but can dry out the product on display and consumes up to 77% more energy according to Adams (1992). It is therefore common to see slow moving products wrapped in cling-film to prevent moisture evaporating from their surface.

Means of displaying foodstuffs first appeared in the 1920's and 30's and consisted, rather crudely, of air circulated around the case, paying little attention to air spillage and consistent product temperatures throughout the display area. In 1958, Hussman Refrigeration Co. applied for a patent for a refrigerated display case very similar to those commonly seen today. Its novelty was claimed to be its completely open front as opposed to the high barriers normally seen on previous designs. Following this, several designs appeared changing the size, number and position of the evaporator coil and the position and number of fans. The number of air curtains was another feature subjected to modification with anything from one to four separate air curtains. An idea formulated by several manufacturers including The MaCray Refrigeration company (1963) and Litton Industries (1966) was the use of the underside of the shelves as air curtain outlets, each curtain shielding the product on the shelf below. However, this made the shelves more expensive to produce and also limited the flexibility of the shelf positioning.

A novel variation on the vertical case was patented in 1977 by Emhart Industries Inc. Essentially, a ventilated canopy in the style of conventional designs but without the lower half, it allowed trolleys of milk and other bulky items to be wheeled into the refrigerated space. The product temperature was then maintained by means of an air curtain ejected from the canopy, and returned via a floor grille. This design is still popular today as it allows quick and easy loading of high turnaround products such as milk. An example of this can be seen in figure 2.5.

It is ironic that despite many variations and modifications to the refrigerated display case in the last 35 years, most cases are now extremely simple in their design usually with one air curtain, one evaporator installed in the base and a single row of propeller fans forcing air over the evaporator. In fact, probably the most important modification in this period of time has been to the air curtain outlet. Previously a slot or perforated grille, the air curtain outlet is now normally of a honeycomb design. This is discussed in more detail in section 2.6.

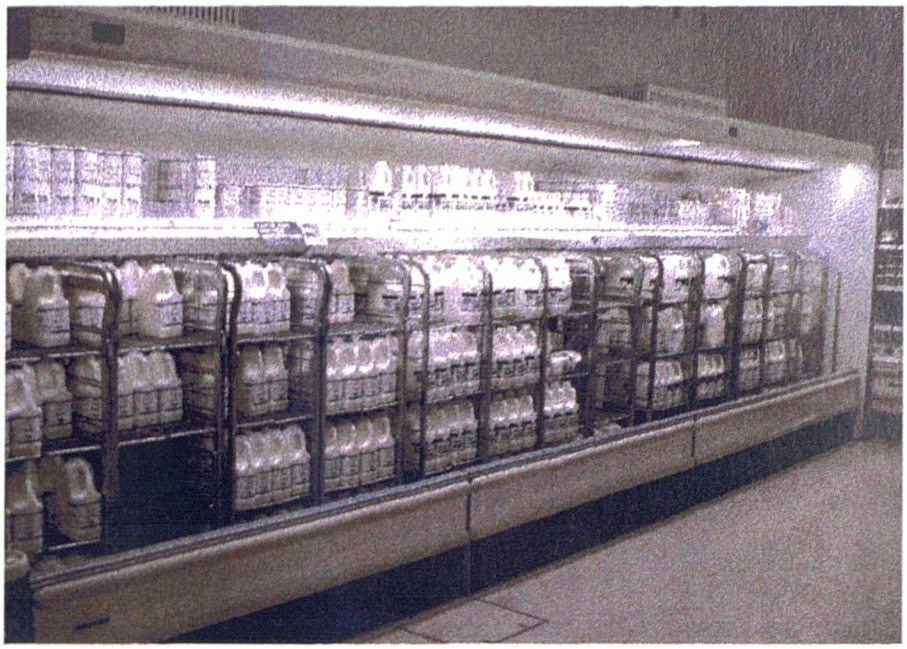

Figure 2.5 - A Typical Wheel-in Dairy Case

Whatever the design of refrigerated display case, four important factors must be considered. Probably the most important criterion that must be adhered to is the product temperatures which must be maintained. In the UK product temperatures are set out in the food safety regulations (1995) and force a legal obligation onto supermarkets to comply with their specifications. From a commercial standpoint, the next two factors cannot be separated due to their dependence on one another. Firstly the product must displayed in such a manner so as to encourage the customer to buy the goods and secondly, it must be done in such a way that the minimum amount of energy is used. This subject is quite complex and is discussed in more detail in section 2.5. The final consideration is that the display cases should not be allowed to influence the indoor climate of the supermarket. The cold air overspill from refrigerated fixtures is widely recognised as a problem adding to the heating load in the winter and causing discomfort in the summer when shoppers are dressed for warm climates. Versagi (1969) recognised this as a problem and examined various ways to combat discomfort in the store as did Adams (1985). Taylor and Adams (1994) also evaluated a method of controlling the environment adjacent to multideck refrigerated cabinets. What these papers have in common, however, is that the methods they suggest do not address the problem of cold air overspill, but of conditioning the store so as to minimise the discomfort felt as a result of this effect.

This seems to be a method of using even more energy to counteract a problem which should be tackled by better case design.

2.5 - MERCHANDISING VERSUS ENERGY CONSUMPTION

As virtually every other part of the refrigeration circuit has evolved over the last 15 years, the standard vertical and horizontal display cases have remained largely unchanged. Their design is very much a compromise between the criteria set by the merchandiser and energy efficient design desired by the engineer.

In order for a large supermarket to make a profit, three factors; price, merchandising and people must be combined. Of these, merchandising and the number of people employed have the greatest effect on profits, the aim being to sell as much produce as possible through good merchandising with the smallest number of employees.

Merchandising is defined as the displaying of products in an attractive manner that will encourage the customers to purchase the products. This very definition is what often leads to conflict between the refrigeration engineer and the merchandiser. It has been mentioned previously that approximately half of a supermarket's fuel bill is accounted for by refrigeration, the general rule being that the best merchandising displays consume the most energy. For example, an open display case consumes twice the amount of electricity as the same case with doors.

An example is given by Adams (1992) in a comparison between two open multideck dairy cases, both with the same display volume and case temperature. At one end of the scale was a cabinet with a 685mm front wall, unlit shelves 610mm deep and a single row of canopy lights which cost $235.54 per linear metre per year to run. At the other extreme is a case with only an 460mm front wall, individually lit 410mm shelves a double row of canopy lights that cost $552.88 per linear metre per year to run. For a 22 metre line-up of these display cases, the latter would cost $6900 per year in additional refrigeration. In monetary terms this is acceptable as long as the second display case can achieve the additional $133,000 worth of annual sales it needs to remain profitable. From a more global perspective, this arrangement is unacceptable because of the additional energy that is being consumed by the case. Energy which is, in effect, wasted.

Energy losses can be reduced by containing the chilled air flow within the cabinet either by the use of glass doors or strips of clear plastic. Although these methods are effective,

some merchandisers are reluctant to install them as they place a barrier between the product and the customer. Statistically, placing clear plastic strips over the opening of the vertical case results in a 40% drop in sales.

One method which has been used in recent years in an attempt to reduce the refrigeration load has been to install night blinds on the cases. This is really a compromise as the blinds are only used during non trading hours and retract completely during the day allowing the customer free access to the case. At night, the blinds cover the case openings entirely, reducing heat gains to the cabinet.

A study carried out by The March Consulting Group (1994) on a Waitrose supermarket in Windsor indicated that retrofitting 60 metres of chilled display cabinet and 34 metres of frozen food cabinets with night blinds would save 25,700 kWh/year worth £1,415 (1992 prices). A simple payback for the investment would be 3.6 years although this time could be halved if the blinds were installed at the time of manufacture rather than being a retrofit item. With 107 Waitrose stores in the UK, annual savings in excess of 2.5 MWh are achievable. It is now common practice for the large supermarket chains to specify night blinds on all chilled and frozen food cases.

2.6 - THEORY OF TURBULENT AIR CURTAINS

As has been illustrated, the most critical factor in the design of a display case is how it interacts with its environment, principally through the medium of the air curtain. Tyler (1960) stated that a good rule of thumb is that the open display case heat load can be divided into fifths with approximately 2/5 coming from radiant sources, 2/5 from diffusion and air change load and 1/5 due to wall conduction and product. This means that in total, 80% of the case refrigeration load is directly affected by the opening and 40% by the air curtain. Calculations carried out in Chapter 5 of this report dispute this division between radiative and infiltration heat gains and show that in fact the refrigeration load affected by the opening is approximately 90% of the total. Nevertheless, the fact remains that the case opening is predominant in determining the refrigeration load and it is therefore appropriate that the fluid dynamics of the air curtain and its effectiveness be examined.

Powlesland (1971) describes air curtains as "an arch of dynamic energy having sufficient momentum to resist the forces working on it and maintain its continuity across the

opening it protects". However, in its simplest form, an air curtain is nothing more than a plane turbulent jet of air with the regions of flow as annotated in figure 2.6.

The plane incompressible turbulent flow of a free jet can be described by the boundary layer equations. The derivation of these equations can be found in several references including Schlichting (1955) and Van (1975). The equations can be solved exactly as shown by Reichardt (1942) and Görtler (1942), although this is restrictive in as far a only uniform velocity and temperature distributions at the outlet can be modelled. Finite difference solutions as explained by Van & Howell (1976) are more flexible.

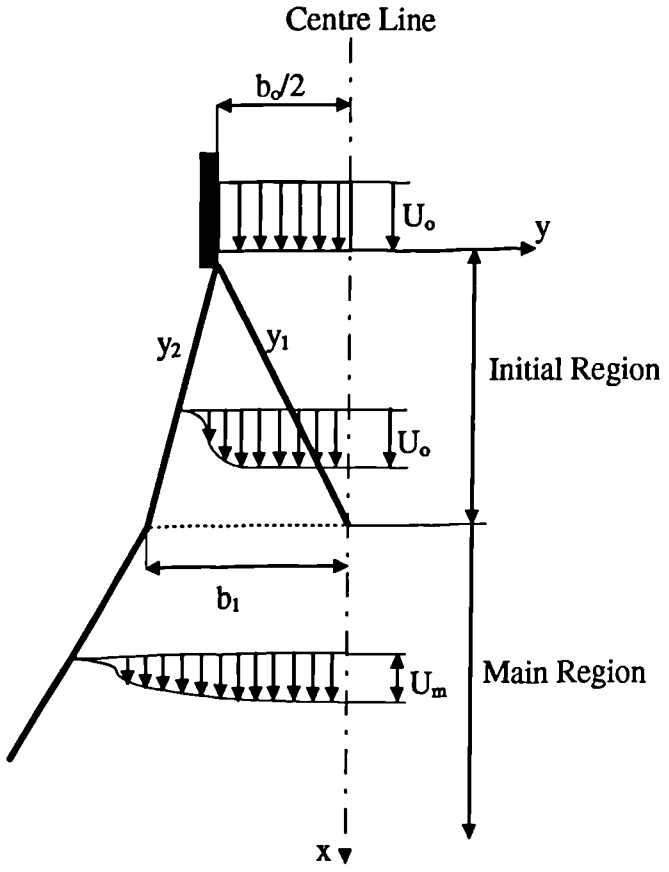

Figure 2.6 - Regions of Flow in a Plane Turbulent Jet

Solution of the boundary layer equations suggests that the flow is generally divided into two regions as depicted in figure 2.6. In the developing or initial region, the centreline velocity remains constant while further downstream in the main region of the jet, the centre line velocity begins to decay. The length of this initial region strongly affects the development and structure of the jet and was investigated by modelling and experimentation by Van (1975) and Van & Howell (1976). They concluded that the

length of the initial region was strongly influenced by the initial turbulence intensity of the jet. The turbulence intensity is a dimensionless ratio of the instantaneous velocity to the mean velocity and as such gives a measure of the quantity of turbulence in the jet.

Given the importance of the initial turbulence intensity on the structure of the air curtain and hence its heat and mass transfer characteristics, several attempts have been made to reduce the degree of turbulence at the air curtain outlet. The feature commonly seen in refrigerated display cases is a honeycomb section located in the air outlet from the canopy. An example of this can be seen in figure 2.7.

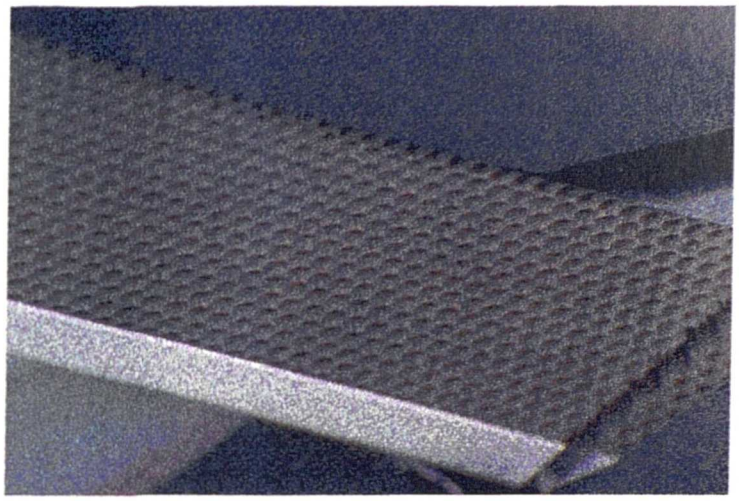

Figure 2.7 - Typical Display Case Honeycomb Section

Honeycombs and perforated screens have been used for many years in order to suppress turbulence in wind and water tunnels. In attempting to reduce the turbulence level in a large water tunnel, Lumley (1964) performed an analysis and experiments comparing a honeycomb to screens. He concluded that for the same reduction achieved using a honeycomb of large length to diameter ratio, four screens would be required of solidity 0.45 with four associated pressure drops. The higher efficiency of the honeycomb was attributed to two effects: a) the annihilation of transverse fluctuations assuming fully developed flow; b) the effect of the mass of the fluid in each cell which must be accelerated to permit the passage of a fluctuation.

Although the use of a honeycomb reduces the level of existing turbulence, it does generate turbulence downstream. This effect was analysed by Lumley & McMahon (1967). They concluded that the turbulence generated by the honeycomb arises from the fully developed flow in the individual cells emerging on the downstream side.

Surprisingly, the degree of downstream turbulence is greater for laminar flows du to the large wake characteristics of laminar cell flow.

An experimental study carried out by Loehrke & Nagib (1976) concluded that the hi frequency fluctuations generated downstream of the honeycomb dissipated r p' l resulting in a net reduction of free stream turbulence. The results also suggested t optimum performance could be achieved by the use of a fine mesh on the downstr side of the honeycomb together with a length to cell diameter ratio equal or greater t ten.

The main criterion for testing the effectiveness of an air curtain is the rate of heat ai d moisture transfer through the air curtain compared to that for the same opening without an air curtain. Hetrsoni (1963), Hetsroni & Hall (1964) and Asker & Berner (1965) reported measurements of heat transfer rates between 60 to 85 percent lower than for the same opening with no air curtain. If the outlet velocity is too high however, there is the chance that the air curtain could actually increase the rate of heat transfer. On the other hand, if the velocity is too low, pressure forces will break the air curtain leaving the bottom portion of the opening unprotected. Therefore, it is obvious that at some optimum outlet velocity, heat transfer will be at a minimum. A further parameter which must be optimised in a successful air curtain design is the deflection modulus. The sealing ability of an air curtain depends on the amount of initial momentum in the jet and the magnitude of the transverse forces which the curtain attempts to seal against. The dimensionless ratio of these forces is known as the deflection modulus and is calculated from the general formula:

$$D_m = \frac{\rho_S b_o U_o^2}{gH^2(\rho_C - \rho_R)} \qquad (2.2)$$

The effects of the initial turbulence intensity, velocity and temperature distribution on the heat transfer characteristics of the air curtain were initially investigated by Howell et al. (1976). They showed that the total heat transfer across an air curtain was directly proportional to the initial velocity and the temperature difference across the curtain. They also showed that latent heat transfer could be a significant proportion (40-50%) of this total.

In attempting to optimise air curtain design for initial velocity and the deflection modulus, Howell & Shibata (1983) concluded that initial turbulence intensity has a moderate effect on the rate of heat transfer through an air curtain and that for each air

curtain there exists a value for the deflection modulus for which heat transfer is at minimum.

These parameters of initial velocity, turbulence intensity and the deflection modulus a therefore all design features of the refrigerated display case air curtain which can l optimised and will be investigated during the course of this research project.

2.7 - CASE / STORE INTERACTION:

The heat and moisture transfer across an air curtain can be quantified using the appropriate energy and momentum balances across the air curtain. These are analysed in detail by Van and Howell (1976), Howell and Shibata (1980 & 1983). Using these relationships, Howell, in two papers (1993), investigated the interaction between refrigerated display cases and their environment.

In the first of these, Howell investigated analytically the effect of store relative humidity on refrigerated display case performance. The procedure was applied to ten types of case with differing curtain thicknesses and heights, discharge velocities and initial turbulence intensities. It was found that the rate of heat transfer across the air curtain was directly proportional to the discharge velocity and curtain height. The heat transfer rate also increased with discharge jet thickness and jet turbulence intensity although the rate of increase did slow significantly at about 130mm jet thickness and also at 7 or 8% turbulence. In all ten types of cases, it was found that higher store relative humidities resulted in a higher total heat transfer. Howell predicted that savings ranging from 5% for glass door reach-in cases to 29% for the multi-deck display cases could be obtained by operating a store at 35% relative humidity rather than the more usual 55%. These figures compared well with the limited amount of experimental data presented by Howell and Adams (1991).

These savings must obviously be weighed against the extra energy cost of reducing the humidity of the store and this additional factor is taken into account in the second of the papers mentioned above. A computer model for the store showed that the increase in the energy required by the air handling unit when operating at 35% rather than 55% relative humidity ranged from 4% to 8% depending on the energy efficiency ratio of the cooling coil. For a store operated at 24°C, 25% relative humidity, the air handling unit might consume about 63,000 kWh more annually than if operated at 55% relative humidity. If there were approximately 60 metres of display cases in the store requiring 9 kW per

metre length, about 103,000 kWh would be saved annually by operation at 25% rela humidity. In addition there would also be savings due to a lower number of defrosts a k less anti-sweat heater operation. However, these figures are merely theoretical a ı was suggested that actual cases be experimentally evaluated operating at diffei ambient humidities. It should also be noted that these simulations were carried out u American weather data and operating parameters which are likely to be different f those experienced in the UK. Therefore, it is suggested that similar research is carr out in this country to determine the net savings achievable by operating supermarket a lower relative humidities.

The flow of heat into and out of a display case was expressed by Howell [1993] and is represented by the equation:

$$Q_{case} = Q_{walls} + Q_{rad} + Q_{sens} + Q_{lat} + de/dt + Q_{lights} + Q_{ASW} + Q_{def}$$

Where:

Q_{case} = The refrigeration or evaporator load on the display case, kW.

Q_{walls} = Heat transfer through the case walls because of the temperature difference between the store and the case, kW.

Q_{rad} = Radiant heat transfer to the display case, kW.

Q_{sens} = Sensible heat transfer by infiltration of ambient air into the case either through the air curtain or due to door opening, kW.

Q_{lat} = Latent heat transfer by infiltration of ambient air into the case either through the air curtain or due to door opening, kW.

de/dt = Energy change in display case due to restocking with product at an initially higher temperature than the case itself, kW.

Q_{lights} = Case lighting load, kW.

Q_{ASW} = Case anti-sweat heater load, kW.

Q_{def} = Case defrost energy load, kW.

Of all of the heat loads on a refrigerated display case, only the term de/dt cannot be changed through the design process since stock must be replenished as it is purchased. The term Q_{walls} is also subject to limitations in the design of the cabinet, as the thickness of the insulation must be optimised against its capital cost. The terms

Q_{lights} and Q_{rad} can be changed through design by moving or eliminating the light which will affect both terms, or by changing the type of heating in the store for example, affecting the radiant element. The four terms Q_{sens}, Q_{lat}, Q_{Asw} and Q_{def} ar related to ambient air infiltration through the curtain. A design feature which has already been shown to be important in section 2.6. The only additional load which may be added to this equation is the heat dissipation from the fans and this will b discussed in Chapter 5.

2.8 - PREVIOUS AIR FLOW STUDIES

Given the ultimate dependence of multideck refrigerated display cases on the air curtain as well as the distribution of air around the case for cooling the product, an investigation into the air flow characteristics of cases is essential before any educated redesign can become reality.

In November 1992, Safeway Stores Plc commissioned a report from Consultants, WS Atkins Engineering Sciences, to try and model the airflow around a multideck chilled food display case. Boundary conditions and case geometries were taken from a working store and applied to a CFD model using the commercial code, STAR-CD. Once a successful model had been established, various modifications were studied such as changing the balance between the back panel and air curtain flow rates as well as subtle geometry changes.

The most significant result obtained from these CFD simulations was that the removal of the air curtain substantially reduced both the net heat gain to the case and the cold air zone in front of the case. Initially there were some doubts as to whether product temperatures could be maintained with this design as warm store air tended to encroach onto the top shelf of the display. This problem was overcome by placing a fairing across the top of the case which directed cold air from the back panel downwards across the product as well as blocking out the warmer air in the region of the fluorescent lights. As a comparison, the sensible net heat flux into the cabinet using the conventional air curtain design was estimated at 532 Watts / metre run of case. With the air curtain removed, small geometry modifications and a reduction in the case air flow rate, this net heat flux would be reduced to 317 Watts / metre run.

Due to the apparent success of this work, Safeway commissioned some experimental work at the Food Refrigeration and Process Engineering Research Centre (FRPERC)

at The University of Bristol in order to try and substantiate the savings shown by th CFD model.

The tests were carried out on a Craig Nicol CD/631 refrigerated dairy cabinet using plastic containers filled with water to reproduce the thermal mass of a fully stock d supermarket case. Product temperatures were measured in Tylose (food substitut) blocks. The tests were carried out in an environmental chamber at ambient conditions of 28.5°C, 20% relative humidity with an air velocity of 0.2 m/s across the face of the cabinet. The tests were carried out twice. Once for the standard case and once for no air curtain and the fairing at the top of the display area.

The mean refrigeration load before and after modification was 3.25 kW and 2.6 kW respectively, a reduction of 20% as compared to 42% shown by the CFD model. Some of this difference could be accounted from the fact that the CFD model simulated only a two dimensional slice and hence neglected any end effects. Furthermore, the two studies were carried out on cases from different manufacturers which may be the predominant cause of the difference between the experimental and simulation results.

2.9 - SUMMARY

This chapter has attempted to provide a background to supermarket refrigeration and refrigerated display cases. The operating principles of the case have been explained together with the theoretical background underpinning these principles. Finally the chapter gives a short summary of recent air flow studies on dairy cases.

The main objective of this research project will be to develop a model for refrigerated display cases and validate this experimentally. From this datum, possible modifications will then be investigated through both CFD modelling and experimentation.

CHAPTER 3

DESIGN OF THE EXPERIMENTAL FACILITY

3.1 - INTRODUCTION

In order to carry out validation tests on the refrigerated display case and compare th results against those from the CFD model, the requirement arose for an experimental test facility. Although, the test standard conditions for display cases will rarely if ever be encountered in a supermarket, the purpose of this type of test is primarily to validate the CFD model in controlled conditions as well as testing the performance of display cases using some benchmarked methods.

The first section of this chapter provides a summary of the British and European Standard testing procedures and test conditions which are employed for the experimental part of this project. The design of the facility is then described including the environmental chamber and its climate control plant. Finally, the design of the refrigeration pack and piping is presented along with the capabilities of the system in terms of flexibility of operation and control.

3.2 - TEST STANDARDS

It is virtually impossible to reproduce exactly the operating conditions experienced by a display case in a supermarket. The turbulence caused by people in the aisle, the opening of doors, the haphazard stacking of the product and warm hands penetrating the air curtain are all random events which cannot be reproduced accurately. Therefore, it was proposed that tests be carried out according to the conditions laid down in the relevant British and European standards. General test conditions for commercial refrigerated display cabinets are laid out in BS6148:part 2:1981. This British Standard has recently been superseded by the European Standard EN 441. This standard is largely the same as its predecessor except for the addition of test room climate class 6 which specifies a dry bulb temperature of 27°C with a relative humidity of 70%. A summary of the requirements is as follows:

Air Movement: With the display cabinet switched off, the air velocity at any point along line A-A′ shown in Figure 3.1 shall be 0.2 ±0.1 m/s.

Radiant Heat: Walls and ceiling of rooms intended for the testing of display cabinets should be painted in light coloured semi-gloss paint. The surface temperatures of the walls and ceiling shall be maintained within ± 2°C of the air temperature measured at the same level. Fluorescent lighting corresponding to 600 Lux ± 100 Lux measured at a height of 1 metre above the floor shall be installed and shall be on continuously during test periods.

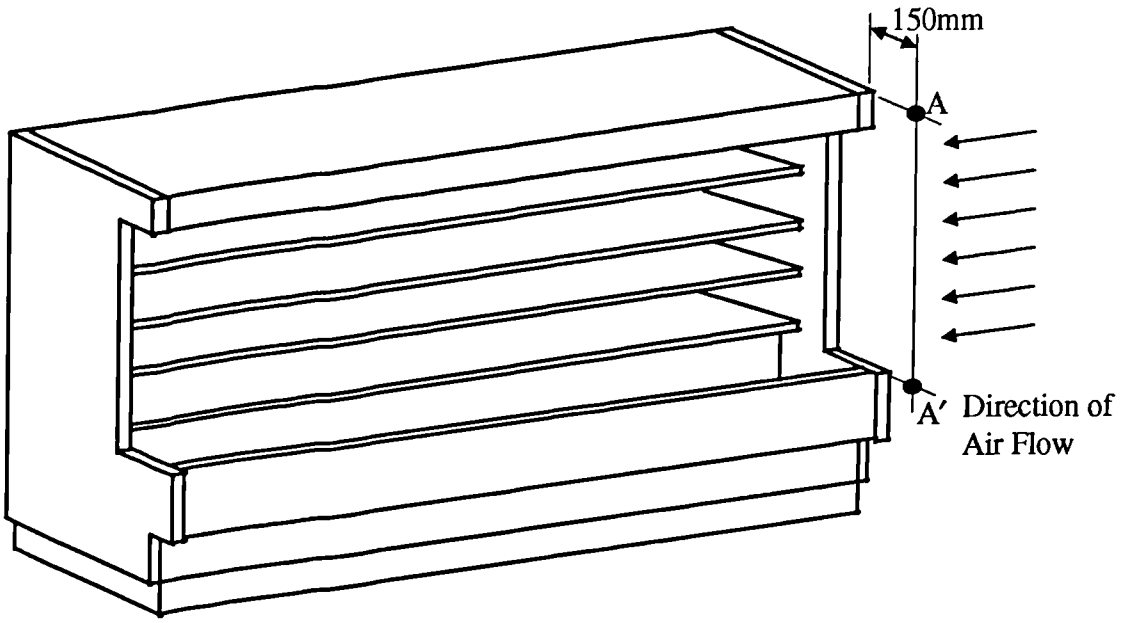

Figure 3.1 - Air Velocity Measuring Point for a Vertical Multideck Case

Temperature Gradient: Vertical temperature gradient shall not exceed 2°C/metre and there shall not be a difference of more than 6°C between the temperature measured at the floor and the ceiling levels.

Climate Measuring Point: The point of measurement for ambient temperature and relative humidity shall be approximately midway along the length of the cabinet and in accordance with Figure 3.2.

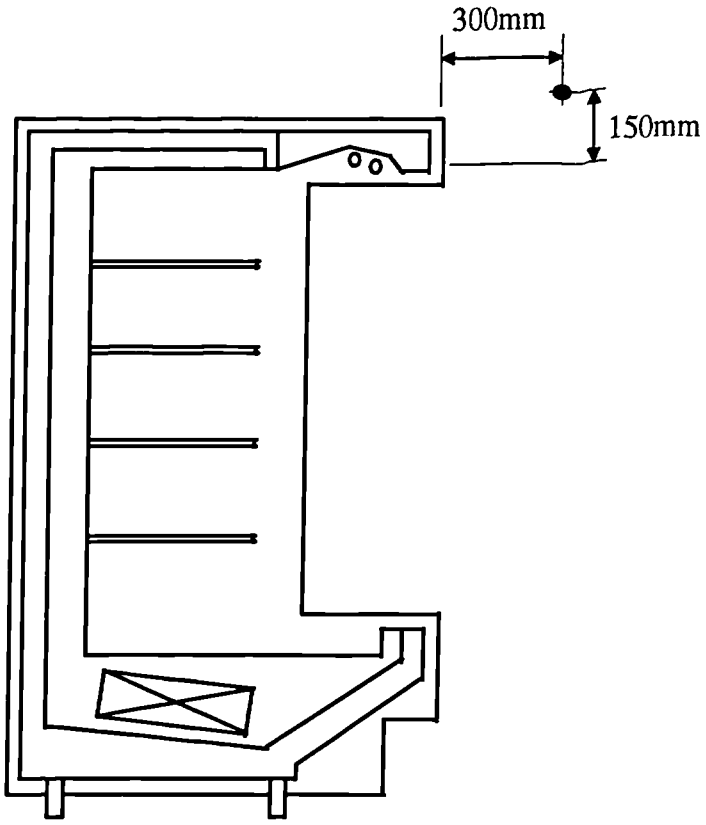

Figure 3.2 - Climate Measuring Point for Vertical Multideck Cases

Test Room Standard Climates: Cabinets should be tested to one of the standard climate classes as given the Table 3.1

Table 3.1 - Test Room Climate Classes

Test Room Climate Class	Dry Bulb Temperature (°C)	Relative Humidity (%)
1	16	80
2	22	65
3	25	60
4	30	55
5	40	40
6	27	70

Tolerances:	Temperature ± 1°C
	Relative Humidity ± 5 units
Accuracy of measurements:	Temperature ± 0.5°C
	Illumination Flux ± 100 lux
	Pressure ± 2 Pa
	Relative Humidity ± 3 units
	Energy Consumption ± 2%

3.3 - ENVIRONMENTAL CHAMBER & AIR HANDLING SYSTEM

In order to achieve uniform test conditions as specified in the test standard a custom built facility is required. This comprises an insulated room served by an air handling system complete with a heating coil, a cooling coil, and a humidifier. A general schematic of the arrangement is shown in figure 3.3.

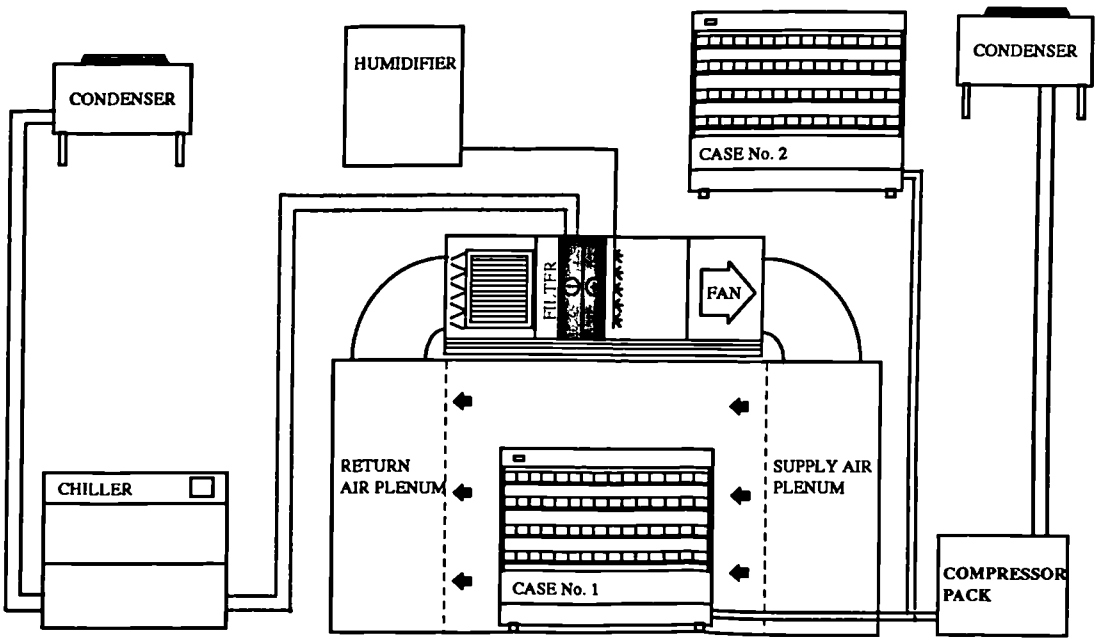

Figure 3.3 - General Arrangement of Test Facility

3.3.1 - ENVIRONMENTAL CHAMBER

The environmental test chamber is a self contained unit positioned within a laboratory (see figure 3.4). It is constructed from 100mm thick modular cold room panels. It has

a sliding door in one of the long walls which is large enough to allow a 2.5 metre display case to be positioned inside. The overall internal dimensions of the chamber are 7 metres long, 3.5 metres wide and 3 metres high, large enough so that the airflow around and out of the cabinet will not be restricted by the walls of the chamber. A double glazed window is also positioned in one of the walls allowing inspection without penetrating the controlled environment.

One metre at each end of the chamber is partitioned off to create supply and return air plenums. The supply air plenum wall is constructed from a bank of opposed blade dampers (figure 3.5) allowing the velocity profile across the chamber to be adjusted as required. The return air plenum is constructed from panel filters (figure 3.6) which create a pressure drop and thus a uniform face velocity. Lighting is provided by means of two 6 foot twin fluorescent tube luminaires fixed to the ceiling and giving a lighting level of between 500 and 550 lux measured one metre above the floor.

3.3.2 - AIR HANDLING SYSTEM

The climate in the environmental chamber is maintained by means of an air handling unit positioned on a purpose built support and located on the roof of the structure. The unit comprises a mixing box, a filter, a chilled water cooling coil, an electric heater battery, a humidifier housing and a centrifugal fan. A schematic diagram of the unit is shown in figure 3.7. Technical specifications of the air handling unit and ancillary items of plant can be found in appendix A.

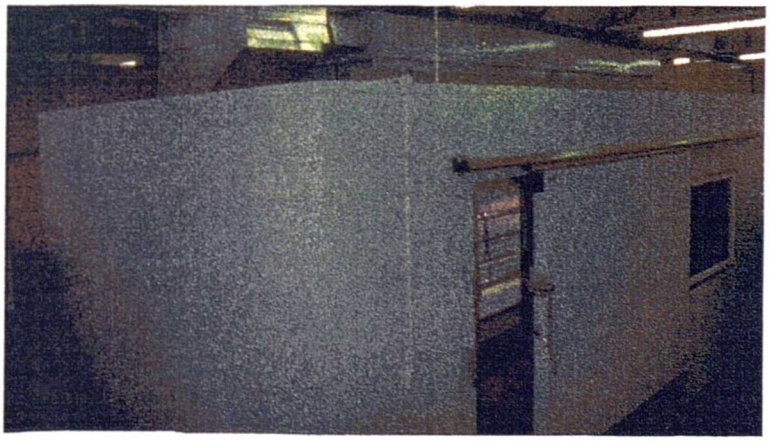

Figure 3.4 - Environmental Chamber

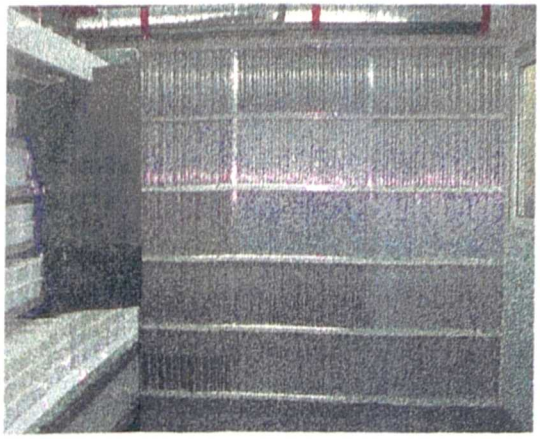

Figure 3.5 - Supply Side Plenum Wall

Figure 3.6 - Return Air Plenum Wall

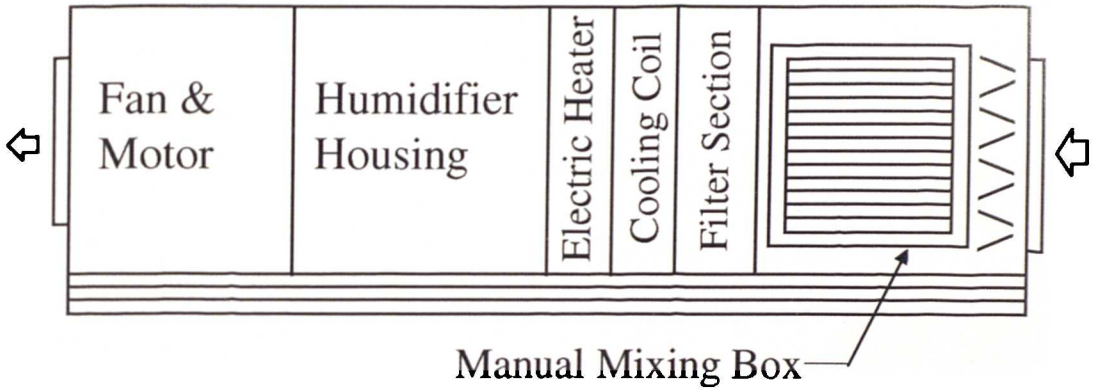

Figure 3.7 - Schematic Diagram of Air Handling Unit

3.3.3 - CHILLER

The cooling coil of the air handling unit is supplied with chilled water from a 9.9kW chiller. The compressor is a semi-hermetic machine and the evaporator is of the shell and tube configuration.

Capacity control is achieved by means of a hot gas bypass valve which is inserted between the compressor discharge line and the inlet to the evaporator at the outlet side of the expansion valve. When the system is operating at full capacity this valve remains closed. However, if the load on the evaporator decreases and the evaporator temperature falls below its set point, the discharge gas pressure then overcomes the valve spring pressure and some hot gas mixes with the liquid discharged from the expansion valve. This raises the evaporator temperature and pressure and thus closes

the hot gas bypass valve. The cycle is repeated every time a decrease in capacity results in a decrease in the evaporator temperature below the set point.

A pump, located within the chiller housing, circulates chilled water around the cooling coil. The water flow through the coil is regulated by means of a three port motorized diverting valve.

3.3.4 - HUMIDIFIER

Humidification of the supply air is accomplished by the provision of a steam humidifier which supplies steam through a distribution pipe located in the humidifier section of the air handling unit. The humidifier is of the electrode boiler type and has a capacity of 8 Litres/hour. Proportional control is achieved through an in-built control board and a humidity sensor in the supply duct after the fan.

3.3.5 - ELECTRICAL SUPPLY AND CONTROL SYSTEM

Electrical supply to the climate control air handling system is provided from a central distribution board with each item of plant having a separate isolator.

As mentioned in the foregoing sections, the chiller and humidifier are supplied with their own autonomous control systems and as such require only an electrical supply from the main panel.

The heating and cooling coils are controlled from a proportional heating and cooling controller within the main panel. Control temperatures are set to create a dead band where neither heating or cooling is required. In addition proportional bands are set independently for heating and cooling. For the cooling coil, a 0-10 Volt output signal from the controller operates the three port motorized valve at the coil. For the electric heating coil, a 0-10 Volt output signal controls the electrical supply to the coil via a thyristor control module.

A control schematic for the air handling system can be seen in figure 3.8.

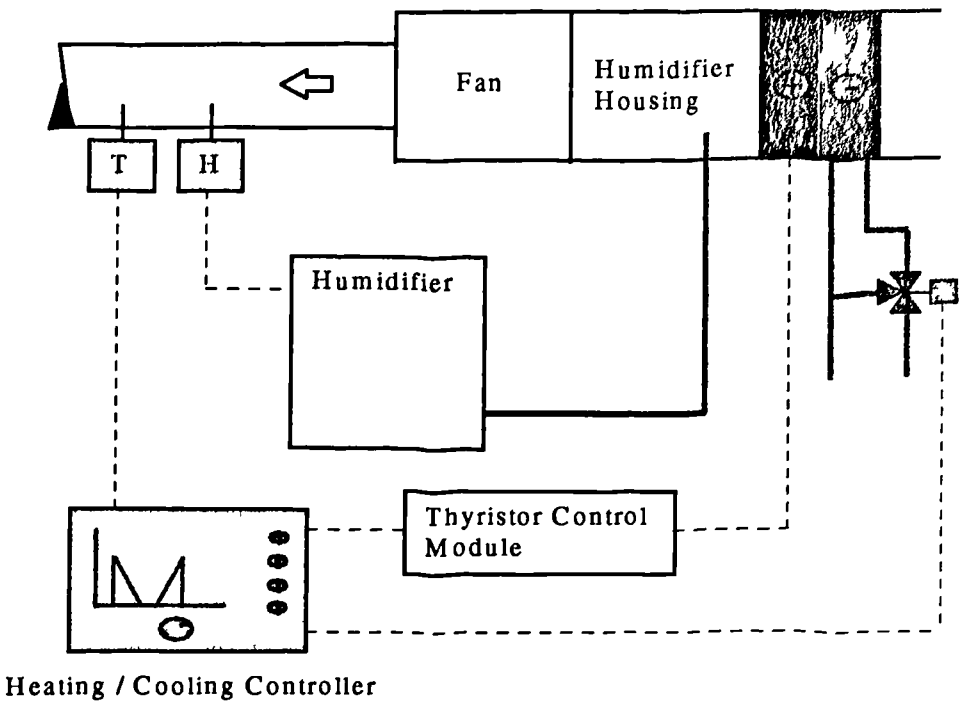

Figure 3.8 - Control Schematic for Air Handling System

3.4 - REFRIGERATION PACK

A schematic layout of the refrigeration pack design is shown in figure 3.9. The main objective in designing the refrigeration circuit to drive the display case on test was to reproduce as closely as possible the type of system which is in use in many supermarkets. The design also allows the flexibility of testing different combinations of defrost type, different expansion valves and compressor and condenser fan control strategies. The refrigerant used is R22.

3.4.1 - THE COMPRESSOR PACK

The compressor pack comprises three semi-hermetic machines which are mounted on a framework as shown in figure 3.10.

The three compressors are of different sizes with motor ratings and cooling capacities as given in table 3.2. The cooling capacities given are approximate for evaporating and condensing temperatures of -8°C and 40°C respectively.

The compressors are located on anti-vibration mountings. Any movement of the machines is isolated from the pipework by flexible connectors.

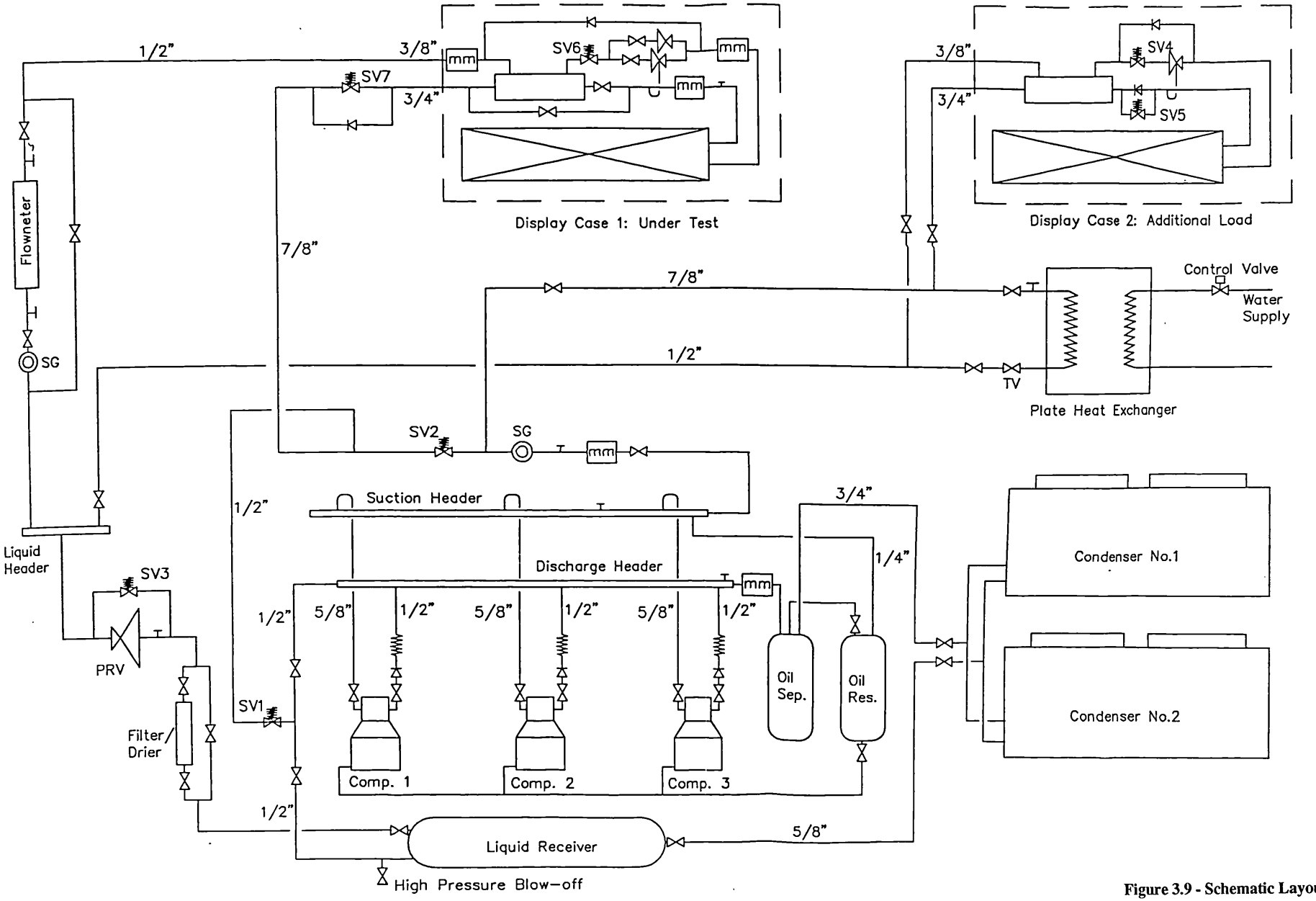

Figure 3.9 - Schematic Layout of Refrigeration Pipework

The oil return system comprises a 3.5 litre oil separator and a 7.5 litre oil reservoir in the discharge line and these are mounted adjacent to the compressors. The oil separator is also provided with a heater in order to prevent liquid flooding back to it when the system is switched off.

An 18 litre liquid receiver is mounted underneath the compressor pack with tappings for liquid return from the condensers, liquid supply to the case, cool gas for defrost and a high pressure blow off.

Table 3.2 - Schedule of Compressor Sizes

	Motor Rating (kW)	Cooling Capacity (kW)
Compressor 1	0.55	2.6
Compressor 2	0.74	2.8
Compressor 3	1.10	3.3

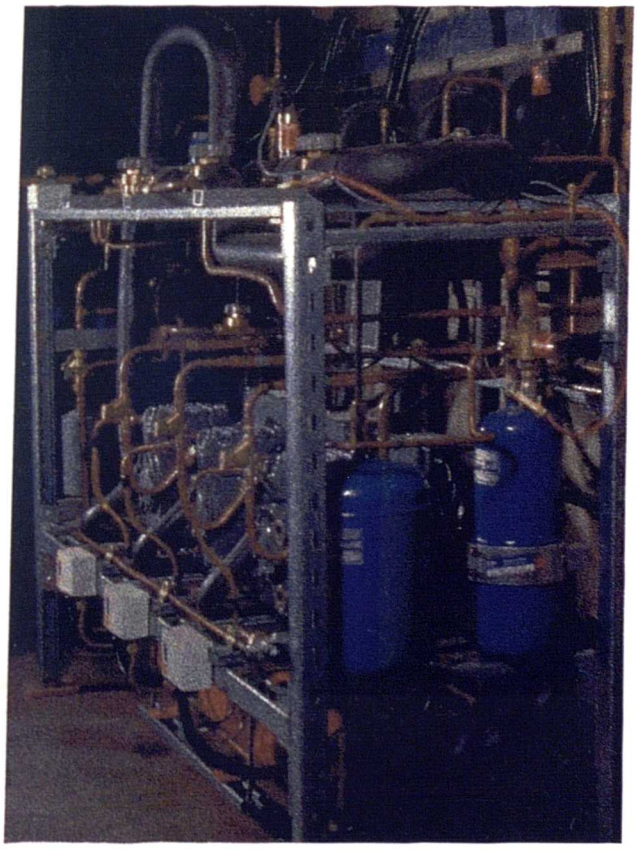

Figure 3.10 - Compressor Pack

3.4.2 - CONDENSERS

Two twin fan air cooled condensers are mounted at high level above the compressor pack. Location at this height prevents excessive head loss from the condensers to the display case which may result in liquid flashing to gas in the liquid line. The condensers are shown in figure 3.11.

The two condensers are piped in parallel with each fan being switched independently. This gives a five stage control of the condensing pressure, i.e.

Stage 1 - All fans off
Stage 2 - One fan on
Stage 3 - Two fans on
Stage 4 - Three fans on
Stage 5 - All four fans on

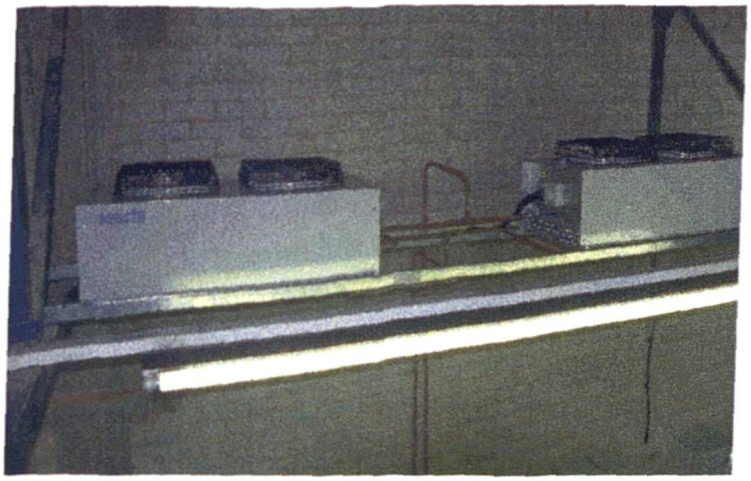

Figure 3.11 - Air Cooled Condensers

3.4.3 - REFRIGERATED DISPLAY CASES

The refrigeration system shown in figure 3.9 serves two display cases.

Case no. 1 is the display case under test in the environmental chamber. This is a 2.5 metre refrigerated dairy case from a large U.K. manufacturer. This particular model is commonplace in today's supermarkets and with minor modification provides the basis of the fresh meat case by the same manufacturer.

The case is standard except for the following modifications:

- A bypass has been added around the liquid / suction heat exchanger. This is to enable future tests on the effect of the heat exchanger on the performance of the refrigeration cycle to be carried out.
- The case incorporates both an electronic and a thermostatic expansion valve with the option to switch between the two. Tests on the different valves will also be the subject of future research.
- Pressure and temperature probes have been fitted to the case before and after the expansion valve to establish the refrigeration cycle on a pressure-enthalpy diagram.
- The standard sheet metal cover on top of the evaporator has been replaced by a perspex cover. This is to enable frost formation on the coil to be monitored visually as well as through the data logging system.

In order to give a thermal mass to the case, the shelves are stacked with one litre plastic containers filled with water. In the case of the containers which are used to measure product temperatures, these packages are filled with a polyacrylic gel and are intended to simulate better the thermodynamics of a food product.

Case temperature is controlled between 0°C and 1°C. This requires an evaporating temperature of approximately -7°C. A graph showing how the various case temperatures change with time in an actual store can be seen on figure 3.12.

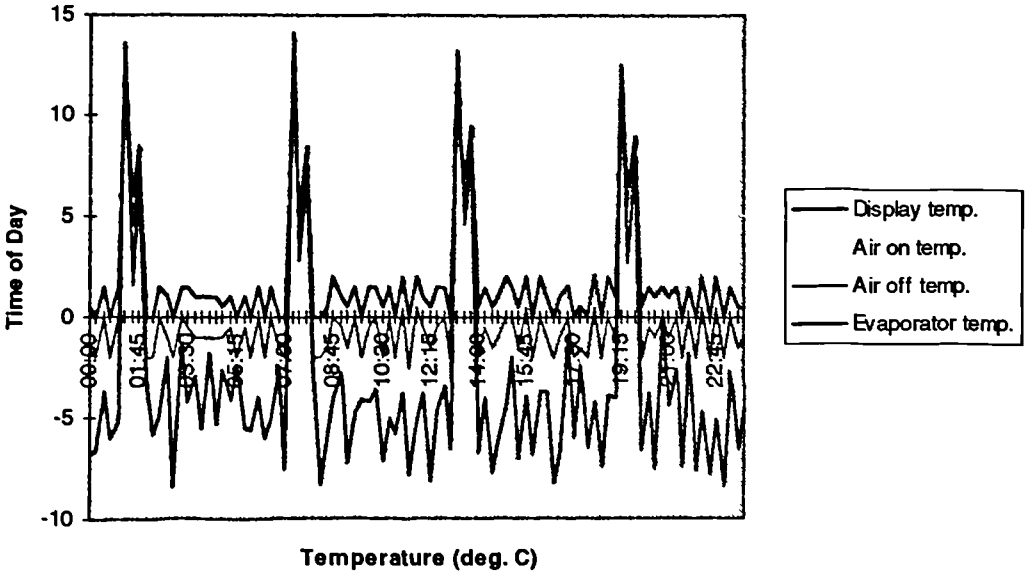

Figure 3.12 - Graph Showing Change in Case Temperature with Time

This data was taken from a similar dairy case in an actual supermarket in Airdrie, Scotland and clearly shows the variation in case temperatures throughout a typical working day. The temperatures shown are the evaporator temperature as well as the air on and air off of the evaporator. The display temperature is a weighted average of these latter two temperatures and is generally accepted as being the case temperature which is displayed on an LCD on the canopy of the refrigerated case. The four timed defrosts in each day are clearly indicated by the peaks which occur every six hours starting at approximately 1.30 am. It can also be seen that evaporator temperatures tend to fluctuate to quite a degree due to the control provided by the thermostatic expansion valve. These fluctuations are translated onto the air temperatures to a lesser degree such that the case temperature is maintained between 0°C and 2°C.

In the test facility, the second display case is a standard 2.5 metre refrigerated dairy case by another U.K. manufacturer which is located outside the test chamber. The purpose of this case is twofold. Firstly, it provides an additional load on the compressor pack which means that better control can be achieved by reducing compressor cycling. Secondly, this case, together with a plate heat exchanger, acts as a re-evaporator during a gas defrost of the case on test.

3.4.4 - DEFROST STRATEGY

Electric and off-cycle defrosts of the evaporator can be accomplished by having the compressor pack piped directly to the display case under test. However, for a gas defrost, the gas condenses in the evaporator and cannot be returned to the suction manifold of the compressor pack without causing damage to the compressors. The condensed gas must therefore be re-evaporated so that it takes the form of a saturated gas at the suction side of the compressor. This is achieved by the provision of the second display case and the plate heat exchanger which not only act as re-evaporators for gas defrost, but also as additional loads on the pack.

In figure 3.9, under normal operation, solenoid valves SV2, 3, 4, 5, 6 & 7 are open and SV1 is closed. Refrigerant flows from the discharge manifold, through the oil recovery equipment to the condensers and then to the liquid receiver. Liquid refrigerant is then supplied from the receiver to the evaporators of the two display cases before returning to the suction manifold of the compressor pack.

Upon initiation of a hot gas defrost, solenoid valve SV1 opens, SV2, 3 & 6 close, while SV4, 5 & 7 remain open. Saturated gas then flows from the discharge header

of the pack to case no. 1 through the suction line. The gas condenses in the evaporator and the heat generated in the process is used to melt the ice on the coil. The liquid exiting the evaporator bypasses the expansion valve on its return to the liquid header via the liquid line. The pressure reducing valve controlled by SV3 ensures that the liquid line supplying case no. 2 and the plate heat exchanger are at a lower pressure than the liquid returning from case no. 1. and so there is a tendency for this liquid to flow to case no. 2 which is refrigerating as normal. The liquid is then re-evaporated in case no. 2 and the heat exchanger before returning to the suction manifold of the compressor pack.

3.4.5 - CONTROL SYSTEM

The system employed to control the refrigeration circuit is a commercially available control system manufactured by Elm Ltd. and is used in many supermarkets. It comprises a central control module serving the compressors, condensers and solenoid valves and case controllers on each display case. A user interface for the setting of global parameters such as defrost timing is provided in the form of a keypad and liquid crystal display (LCD) screen, this module being called a "Supervisor". Settings for the case and pack controllers such as type of defrost, number and size of compressors, number of condensers etc. are made using a hand held service unit which plugs into the respective control board. A schematic diagram showing the location of the control components and their connections is shown in figure 3.13.

The compressor control strategy works purely on the suction pressure of the compressor pack. The setting up of the control requires the selection of three parameters, the target suction pressure, a pressure differential and a time delay. When the measured suction pressure is more than the value of the differential above or below the target pressure, the controller starts to count off time. If the preset time delay is reached and the suction pressure has returned to within its deadband, the controller does nothing. However, if after the time delay, the suction pressure is still outwith the target band, the next compressor is switched on in order to assist with the load. As the load reduces and the suction pressure falls off, a similar delay is employed to switch the compressor stages off. These delays prevent the controller from responding to short term changes in suction pressure which could be detrimental to the compressors and produce an unstable control system.

The condenser fans are controlled in a similar manner to the compressor but working on the discharge pressure with a target, a differential and a time delay. In the case of the condenser fans, however, a further control option can be selected. This is done by specifying pressures at which each fan will switch on or off. Although this method is more precise, more experience is required to set the control system up as a target pressure and a differential must be specified for each of the condenser fans.

Control of defrost is achieved through the defrost relay board which switches the required solenoid valves (as described above) in response to the initiation of a defrost cycle. Defrosts are carried out on a time basis although this can be overridden and other defrost strategies introduced.

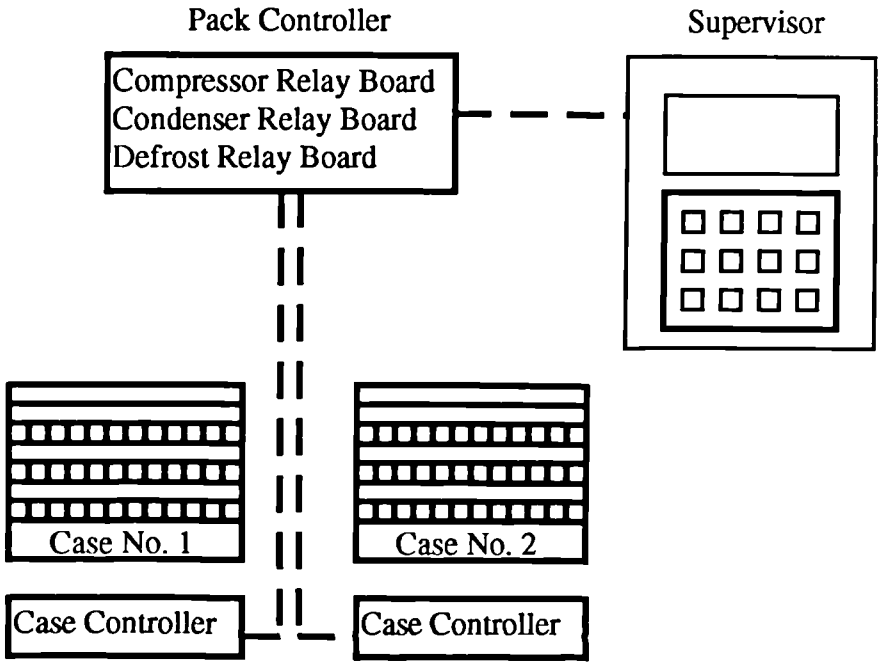

Figure 3.13 - Schematic Diagram of Elm Control System

Due to the flexibility that was required in the refrigeration system, a further control system was designed into the electrical panel whereby the compressors and condenser fans could be controlled from a PC. This means that different control strategies can be investigated for these items of plant by designing and implementing control algorithms through the computer.

3.5 - MEASUREMENT AND DATA LOGGING EQUIPMENT

In order to monitor the display case and assess its performance, measurements must be taken to compare its temperature maintaining capabilities and cooling load against a benchmark. This is done by means of many measurements taken automatically through a data logger and stored on a computer.

3.5.1 - MASS FLOW METER

The energy efficiency of a display case is determined by the load that it places on the refrigeration circuit to which it is connected. In order to calculate this load, the enthalpies before and after the evaporator need to be measured as well as the mass flow rate of refrigerant circulating around the case.

Turbine flow meters are susceptible to errors caused by factors such as velocity profile, bearing wear, cavitation, foreign material, entrained gas, meter orientation, viscosity, temperature pressure and density. Due to these factors a method was needed to measure the mass flow rate than a simple turbine flow meter. For this reason, a coriolis mass flow meter was chosen. Although these meters are also subject to inaccuracies arising from the presence of gas in the liquid refrigerant (Hawken et al., 1985) suitable precautions were taken to ensure that this did not occur. These measures included mounting the condensers at high level in order to avoid loss of pressure head and the installation of sight glasses before and after the meter so that the state of the refrigerant could be monitored.

Coriolis forces are present in any system when a mass moves towards or away from an axis of oscillation. The meter consists of a thin tube which is vibrated at its natural frequency as the fluid passes through it. The momentum of the flowing fluid causes a deviance in the motion of the tube from that which would be expected of a tube with no flow through it. These coriolis forces which are generated are then directly proportional to the mass flow rate. The forces generated are extremely small and superimposed on the fundamental component of the measuring tube. The total motion of the tube is picked up by inductive sensors and through signal processing is presented as a mass flow on an LCD display as well as being logged on a computer.

The signal logged is a voltage which is stored by the computer. In order to convert these voltages to a flow rate a calibration exercise was carried out on the flow meter measuring voltage signals for several mass flow rates. The results of this procedure

are illustrated in figure 3.14 which shows a graph of mass flow rate plotted against voltage, the resulting linear equation and a correlation coefficient in terms of R .

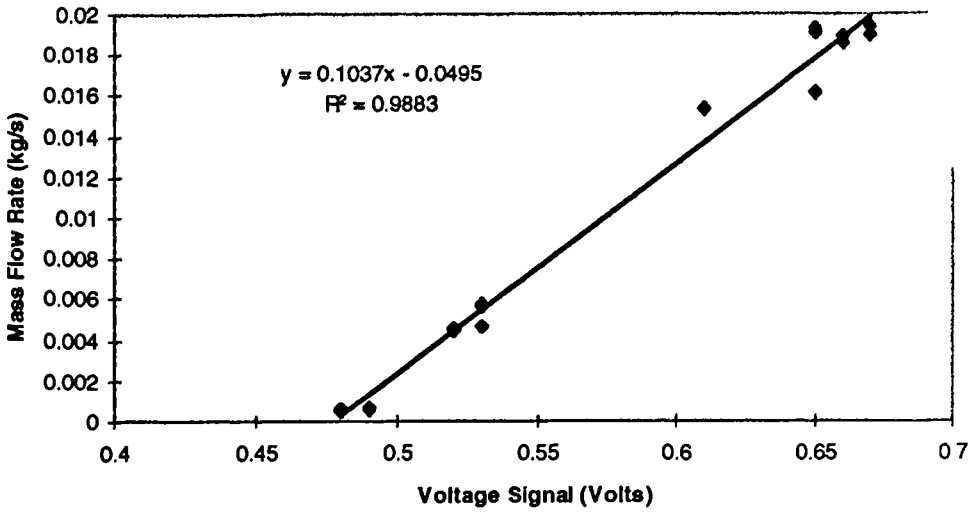

Figure 3.14 - Calibration Graph for the Mass Flow Meter

The sensitive nature of the mass flow meter measuring principle means that it must be installed according to the manufacturers instructions in order to maintain accuracy. The self diagnostic facility of the meter includes the calculation of a so-called installation factor. This factor indicates whether the meter has been correctly installed in the pipeline. The installation factor for the meter in the liquid line was calculated to be 6 which compares to the manufacturer's recommendation of a maximum factor of 35 when the measuring tube is full of water.

There are significant difficulties of calibrating the flow meter using refrigerant due to it's low boiling point. A calibration check was therefore made by running water through the meter and comparing the measured value of the total mass with the mass of water collected over the period of a few minutes. The results of this calibration are given in table 3.3.

Table 3.3 - Flow Meter Calibration Data

	Mass Measured on Flow Meter	Mass of Water Collected	Percentage Error
Calibration 1	6.844 kg	6.840 kg	0.06 %
Calibration 2	7.325 kg	7.180 kg	2.02 %
Calibration 3	6.846 kg	6.870 kg	0.35 %

3.5.2 - POWER METERS

In order to monitor the power consumption of the compressor pack, a power meter was installed in the supply to each machine. Each meter has a selector switch and an LCD display for the display of voltage, current, indicated and reactive power, power factor and total power consumed. In addition, the parameters of current, electricity demand and total power consumed are logged on the computer via an analogue output.

3.5.3 - PRESSURE TRANSDUCERS

Five pressure transducers are installed in the refrigerant pipework in order to monitor compressor suction and discharge pressures, pressures before and after the expansion valve and at exit from the evaporator. The transducers are installed in measurement modules which are essentially blocks of brass with tappings for a pressure transducer and a thermocouple. The modules in the suction and discharge lines also have a tapping for the additional pressure transducers required by the Elm control system. These measurement modules were silver soldered into the pipeline and their locations are indicated on figure 3.9. A photograph showing one of the measurement modules is shown in figure 3.15.

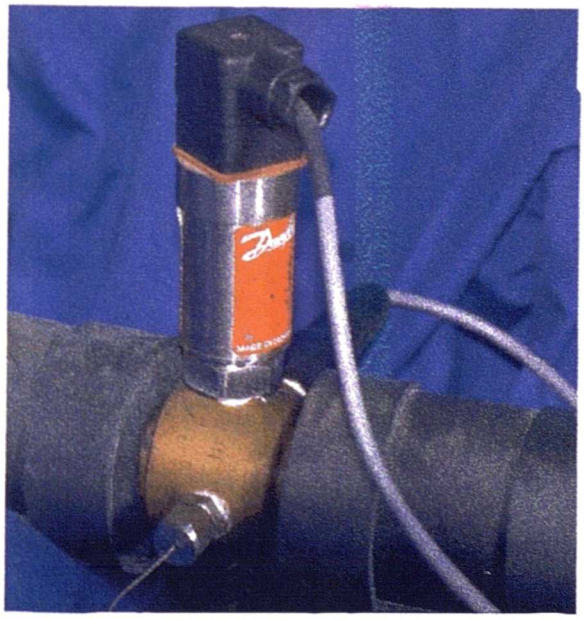

Figure 3.15 - Pressure / Temperature Measurement Module

The pressure transducers produce a 0-10 Volt d.c. output which had to be calibrated to give a reading of pressure. This procedure was carried out on a deadweight pressure gauge tester, measuring the voltage output for a series of known pressures. Graphs of voltage against pressure were drawn as shown in figures 3.16 (a) to (c). An equation giving the best straight line fit through the points was then derived and used in the data logging program to enable the automatic recording of the pressures. Due to further requirements outside of the current research, the transducers were calibrated using the imperial units of pounds force per square inch. These values were later converted to bar in the file of logged values.

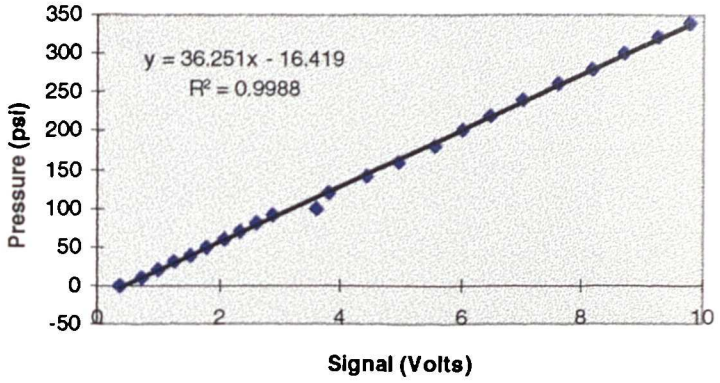

Figure 3.16(a) - Calibration Curve for Pressure Transducer at Inlet to Expansion Valve.

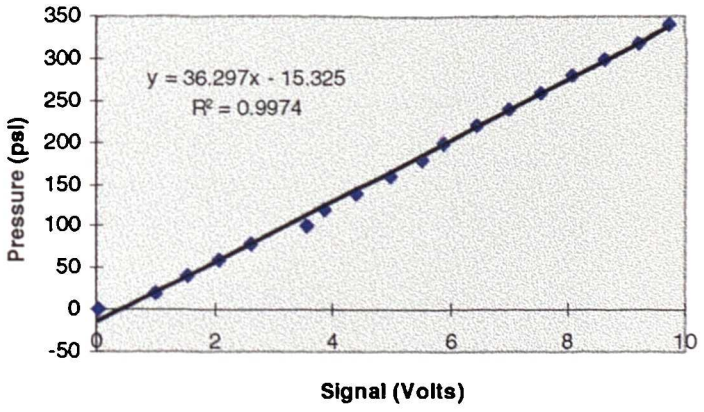

Figure 3.16(b) - Calibration Curve for Pressure Transducer at Evaporator Inlet

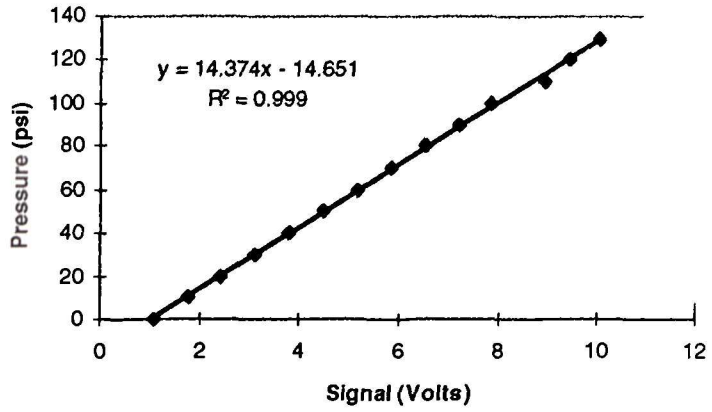

Figure 3.16(c) - Calibration Curve for Pressure Transducer at Evaporator Outlet

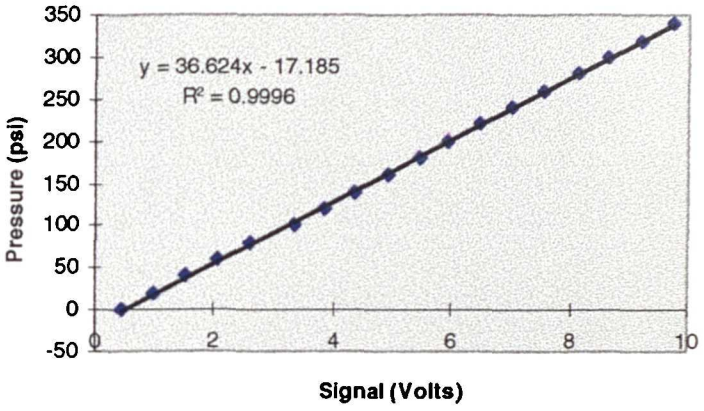

Figure 3.16(d) - Calibration Curve for Discharge Pressure Transducer

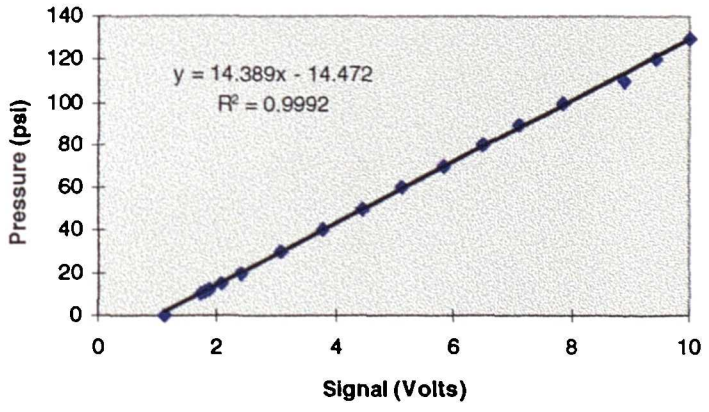

Figure 3.16(e) - Calibration Curve for Suction Pressure Transducer

3.5.4 - TEMPERATURE MEASUREMENT

Measurement of temperatures was achieved by the use of thermocouples. Refrigerant temperatures were measured with the use of K-Type thermocouples inserted into tappings in the measurement module described in section 3.5.3.

All other temperatures, for instance product and air temperatures were measur d using welded tip T-Type thermocouples with a temperature range of -50 to 200°C.

All thermocouples were pre-calibrated on delivery but were rechecked against the known benchmark temperatures of boiling water and a mixture of ice and water. All were found to be within the tolerances specified by the manufacturer.

3.5.5 - CLIMATE MONITORING

The temperature and relative humidity within the environmental chamber are monitored by the use of sensors positioned as described in figure 3.2. Each sensor produces an analogue signal which is calibrated and logged on the computer.

The temperature sensor is of the platinum resistor type manufactured to BS1904 class B with a 4-20mA output. Its range is 0-50°C with an accuracy of ±0.5°C. The humidity sensor also has a 4-20mA output with a range of 0 to 100% RH. Its accuracy is ± 3% over the range of 10 to 90% RH. Its accuracy outside this range was not specified.

The signal logged is a voltage which is stored by the computer. In order to convert these voltages to temperatures and humidities a calibration exercise was carried out on the sensors measuring voltage signals for several readings. The results of this procedure are illustrated in figure 6.17 and 6.18 which show a graphs of temperature and humidity plotted against voltage, the resulting linear equations and correlation coefficients in terms of R^2.

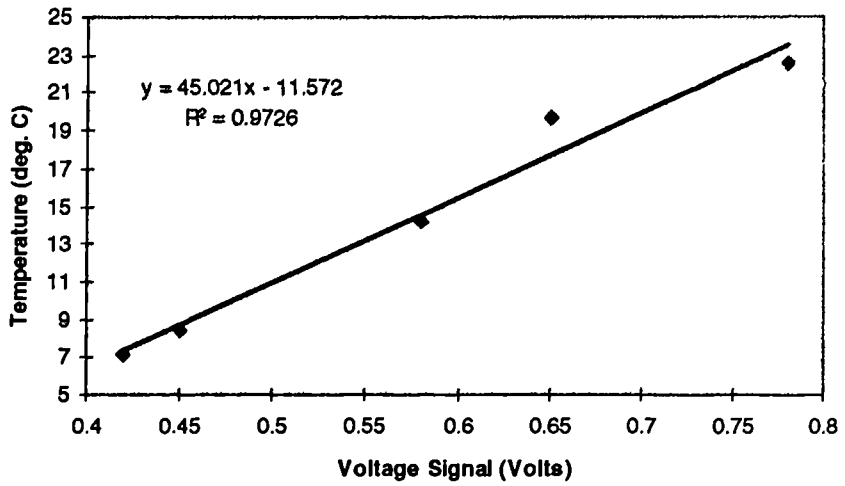

Figure 3.17 - Calibration Graph for Temperature Sensor

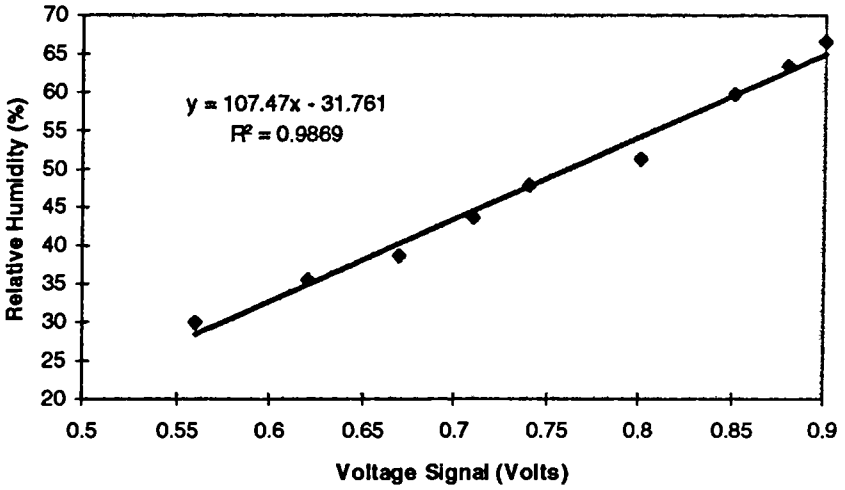

Figure 3.18 - Calibration Graph for Humidity Sensor

3.5.6 - DATA LOGGING EQUIPMENT

As mentioned previously, refrigerant pressures and temperatures, climatic conditions in the test chamber and temperatures around the display case are all logged on a computer system. The data acquisition hardware is located external to the computer and communicated with it through an RS232 cable.

The system selected consisted of modules which could be added to, to expand the system up to 1000 channels. Modules could be selected with 8 or 16 channels and mixed and matched to give analogue and digital inputs and outputs. Ranges could also be selected individually for each channel.

As mentioned in section 3.4.5, an option of the refrigeration control system was that a PC could be used to switch compressors and condenser fans. This meant that the computer software had to be capable of producing digital output for the control functions. The software selected is Labtech Control. This is fully compatible with the data acquisition hardware and allows a mix of up to 2000 analogue and digital channels. The control functions allow PID loop auto tuning and the facility to create mimic displays, and alarm logging.

3.5.7 - POSITIONING ROBOT

In order to ensure that measurements are taken consistently and avoid duplication of expensive measuring instruments such as air flow meters, a three axis positioning robot has been installed within the environmental chamber. The robot is shown in figure 3.19.

Tests on the accuracy and repeatability of the positioning robot showed that measurements within ± 1mm were possible with a similar repeatability of location.

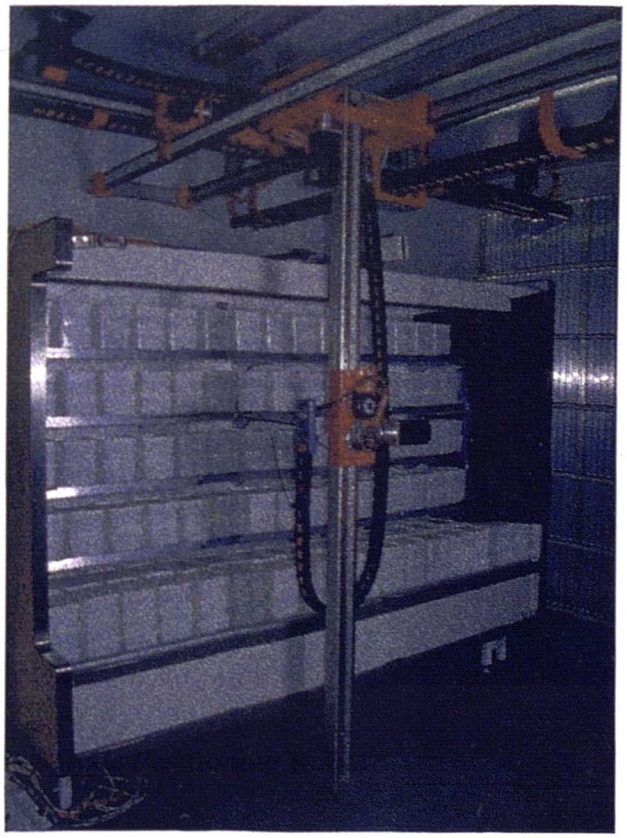

Figure 3.19 - Three Axis Positioning Robot

3.6 - COMMISSIONING DATA

In order to ensure compliance of the test facility with the conditions and tolerances set down in the British and European standards, tests were carried out on the temperature and humidity of the chamber over a period of time as well as on the cross flow velocities measured at the front of the case. Figure 3.20 illustrates the variation of temperature and humidity over the period of approximately one hour. This shows that the conditions within the chamber measured at the point indicated in figure 3.2 are within the tolerances laid down in the test standards.

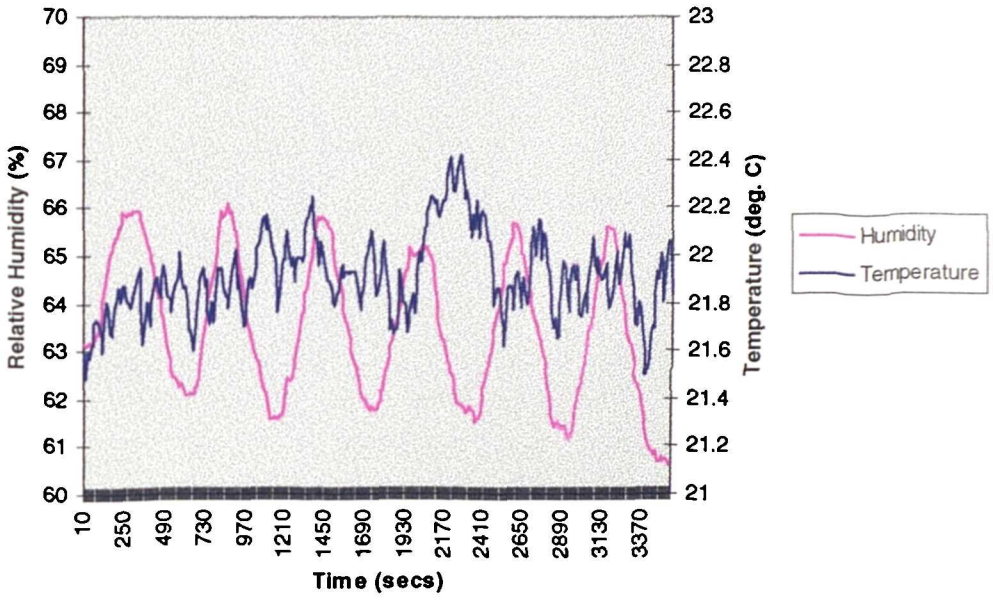

Figure 3.20 - *Variation of Environmental Chamber Conditions with Time*

The cross flow velocity of ambient air was measured along the plane indicated in figure 3.1. It was found that the velocities varied between 0.04 m/s at the top of the case and 0.19 m/s at the level of the return air grille. Some difficulty was experienced in ensuring a uniform cross flow which was due to the construction of the supply plenum wall. At the low velocities measured, however, this is not thought to have been detrimental to the results since all of the case modifications were tested against the same ambient conditions.

3.7 - CHAPTER SUMMARY

This chapter has described the British and European Standard requirements for the testing of refrigerated display cases for performance assessment. A detailed

explanation has also been given of the experimental facility which h been constructed at Brunel University as a significant part of this project and will not ɔ l y be used for the present research but also for future work. Commissioning data ha been provided indicating how well, the facility adheres to the requirements of the t standard.

In Chapters 5 and 6 experimental results obtained using the test facility are present ¹. These results are used to validate the CFD model.

CHAPTER 4

INTRODUCTION TO COMPUTATIONAL FLUID DYNAMICS

4.1 - INTRODUCTION

The CFD code used during the majority of this research was FLUENT v. 4.3 for tl PC. FLUENT is a finite volume based general purpose CFD package capable of modelling fluid flow, heat transfer and chemical reactions.

Any CFD code consists of three parts as shown in figure 4.1, a pre-processor, a solver and a post-processor.

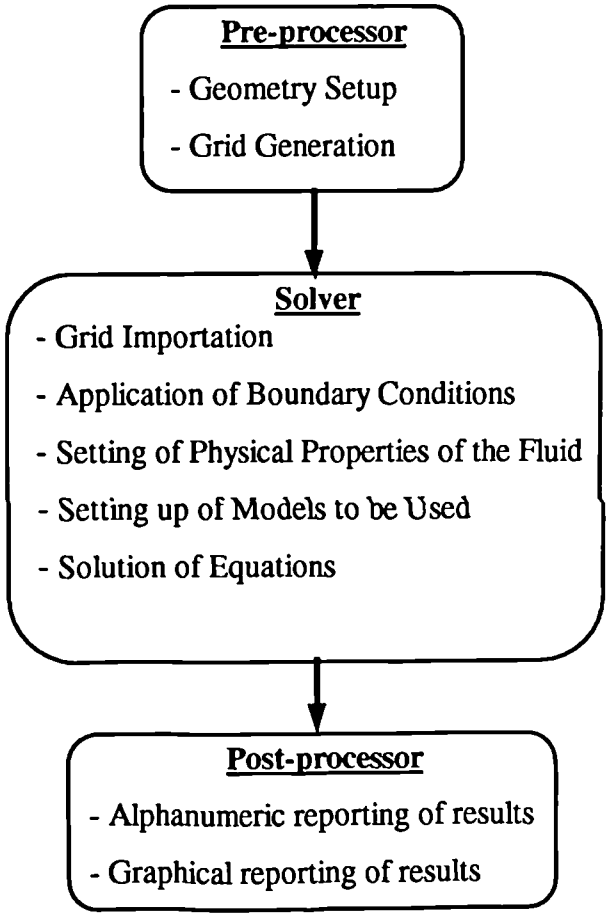

Figure 4.1 - Typical Structure of CFD Software

FLUENT combines the solver and the post-processor into one piece of software which is also capable of generating simple cartesian grids. However, for more complicated geometries and the generation of body fitted meshes a pre-processor ,called PreBFC is used. The merits and drawbacks of each type of grid will be discussed later in this chapter.

Although software varies between manufacturers in terms of grid generation, post-processing capabilities and the front end of the solver, all codes are based on the governing equations of fluid flow. This chapter aims to give an insight into the theory behind computational fluid dynamics and relate this to how the model was created within FLUENT. Some of the models used will also be explained and their impact on predicting an accurate solution assessed.

4.2 - GOVERNING EQUATIONS

Computational fluid dynamics is a technique which has been around for many years, in fact, long before there existed the computer hardware capable of solving practical problems.

The aim in CFD is to predict fluid motions using a computational grid and applying mass, momentum and energy balances across each grid cell. The solution of the problem is an iterative process making adjustments to the cell values at each iteration until a converged solution is reached for all of the governing equations. For a non reacting, single-phase flow, this means predicting the pressure (p), Temperature (T), Density (ρ) and three velocity components (u, v and w) at each grid cell at each moment in time. For these six unknowns, six equations are required. These equations are known as the Navier-Stokes equations and comprise the following:

A continuity equation representing the conservation of mass:

$$\frac{\partial \rho}{\partial t} + \frac{\partial}{\partial x_i}(\rho u_i) = S_m \qquad (4.1)$$

Three momentum equations to calculate the x, y and z momentum of the form:

$$\frac{\partial}{\partial t}(\rho u_i) + \frac{\partial}{\partial x_i}(\rho u_i u_j) = -\frac{\partial p}{\partial x_i} + \frac{\partial}{\partial x_j}\left(\mu \frac{\partial u_i}{\partial x_j}\right) + g_i \rho \qquad (4.2)$$

And an energy equation:

$$\frac{\partial}{\partial t}(\rho h) + \frac{\partial}{\partial x_i}(\rho u_i h) = \frac{\partial}{\partial x_i}\left(k \frac{\partial T}{\partial x_i}\right) + S_h \qquad (4.3)$$

In addition, the equation of state is also solved:

$$\rho = \frac{p}{RT} \qquad (4.4)$$

The Navier Stokes equations are a general set of equations describing all types of flow. Although their direct solution is a subject of interest in academic research, they are a set of simultaneous, non linear, partial differential equations and consequently they are extremely difficult to solve for flows of practical interest. For instance, by calculating the smallest eddy in a turbulent flow with a Reynold's number of 10^4, the number of grid cells required would be of the order of 10^8 and would be a supercomputer application. For a typical aircraft model, a Reynold's number of 10^8 can be expected, requiring 10^{16} grid cells. Engineers, however, are seldom concerned with such small scale integration. It is usually of more interest to look at the overall pattern of the flow and hence the Navier-Stokes equations can be simplified and the number of grid cells reduced.

When analysing turbulent flow, the small scale, apparently random nature of the velocity fluctuations is superimposed on the mainstream velocity of the fluid as shown in figure 4.2.

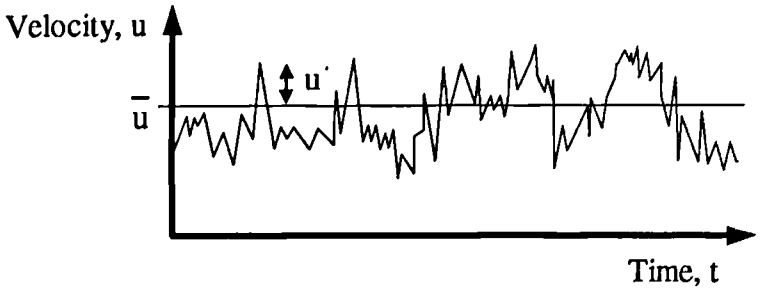

Figure 4.2 - Small Scale Velocity Fluctuations Associated with Turbulent Flow

When describing turbulent flow it is often convenient to express each of the velocity components as the sum of a mean and a fluctuating part, i.e.:

$$u = \bar{u} + u' \tag{4.5}$$

$$v = \bar{v} + v' \tag{4.6}$$

$$w = \bar{w} + w' \tag{4.7}$$

Where the barred characters, are the mean velocities at a point in space defined by x, y, z co-ordinates and averaged over a time step t which is large compared to the small scale velocity fluctuations. They are defined by the equation:

$$\overline{u_i} = \lim_{t \to \infty} \frac{1}{\Delta t} \int_t^{t+\Delta t} u_i(t)dt \tag{4.8}$$

Generally, for engineering problems, knowing every minute detail of the flow is of little consequence and it is of more interest to look at the path of the mean flow in a time averaged form. This would be similar to taking a long exposure photograph of the flow field and thus gain a time averaged view of the flow. By equating each velocity component to a mean and fluctuating part, Reynolds (1874) modified the classical governing equations into a time averaged form. However, the averaging process introduces some unknown turbulence correlations. These are known as the Reynolds stresses and represent the rate at which momentum is transported or diffused by turbulent fluctuations. They are, in their full form:

$$-\rho\overline{u'^2}, \quad -\rho\overline{v'^2}, \quad -\rho\overline{w'^2} \qquad \text{Normal Stresses}$$

$$-\rho\overline{u'v'}, \quad -\rho\overline{v'w'}, \quad -\rho\overline{u'w'} \qquad \text{Shear Stresses}$$

The original Navier-Stokes equations form a closed set of simultaneous equation . The unknown Reynolds stresses, introduced by the averaging procedure make the equations unsolvable. This presents a closure problem which can be solved by turbulence modelling.

4.3 - MODELS OF TURBULENCE

For any forced convection problem, the Reynolds number is deemed to be a good indication of whether the flow is laminar or turbulent. The physical significance of the Reynolds number is that it provides a measure of the relative magnitude of the inertial forces, associated with the acceleration or deceleration of a fluid element, to the viscous forces occurring within the flow. In this dimensionless ratio, ρu^2D^2 can be taken as a representative measure of the inertia forces and μuD as a representative measure of the viscous forces. Therefore:

$$Re = \frac{\text{inertia forces}}{\text{viscous forces}} = \frac{\rho u^2 D^2}{\mu u D} = \frac{\rho u D}{\mu} \qquad (4.9)$$

In general, Reynolds numbers below 2000 suggest laminar flow and above 4000 denote a fully turbulent flow. In between these two values, the flow is said to be of a transitional nature. In a display case application, calculation of the Reynolds number at the air curtain outlet with the honeycomb section, yields a value of approximately 300 thus indicating that the flow is laminar. However, further downstream in the air curtain where the velocity is maintained but the length scale increases, as well as in the back panel where higher velocities exist, the Reynolds number will rise to a value of approximately 5000. This means that the flow, although laminar in some areas, becomes just about turbulent in others and thus a turbulence model is needed in order to more accurately describe these regions.

A turbulence model consists of a set of differential equations which allow for the determination of the Reynolds stresses and hence allow the time averaged governing equations to be solved. The assumption made by any turbulence model is that turbulent fluctuations exist and are superimposed on the mean flow. The limitation which this leads to is that in regions of the domain where the flow is laminar, the accuracy of the model can be compromised. In order to describe how each model deals with this, it is first necessary to explain the strategies adopted by the different models.

The Reynolds stresses can be determined by one of two approaches. The first is to relate the unknown terms to the mean velocity or some other knowable quantity. This is termed an eddy viscosity model. Secondly, by constructing differential transport equations for the Reynolds stresses, the equations may be solved in a similar manner to the Navier-Stokes equations. Turbulence models of this type are referred to as Reynolds stress transport models.

4.3.1 - EDDY VISCOSITY MODELS

The hypothesis upon which eddy viscosity turbulence models are based is that of Boussinesq (1877). This was built on an analogy with laminar flows where the stresses are exactly proportional to the velocity gradients or rates of strain, the proportionality coefficient being the laminar viscosity of the fluid. For turbulent flows, Boussinesq proposed that the Reynolds stresses may be modelled as being proportional to the mean rates of strain with the proportionality coefficient being the turbulent or eddy viscosity. Therefore, the turbulent viscosity unlike its laminar equivalent, expresses the nature of the flow and not of the fluid. This may be expressed mathematically as:

$$-\rho\overline{u_i'u_j'} = \mu_t\left(\frac{\partial u_i}{\partial x_j}+\frac{\partial u_j}{\partial x_i}\right)-\rho\frac{2}{3}\delta_{ij}k \qquad (4.10)$$

where μ_t is the kinematic eddy viscosity, k is the turbulent kinetic energy and δ_{ij} is the Kronecker delta meaning that the second term on the right hand side of the

equation only appears when i = j. Using this analogy, the eddy viscosity is calculated from the turbulence model and is then, in turn, used to calculate the Reynolds stresses.

The model for determining the eddy viscosity can be very simple, for example setting a constant value at the start of the problem or relating it to the velocity scale for various types of shear layers. However, although simple to implement and computationally robust, these "zero equation" models are unsuited to complex recirculating flows and cannot account for historical effects in convective or diffusive flows.

By far the most common turbulence model used today is the two equation k-epsilon (or k-ε) attributed to Launder and Spalding (1974). In this model, the eddy viscosity is evaluated from the solution of two differential equations, one for the turbulent kinetic energy, k, and the second for the rate of dissipation of the turbulent kinetic energy, ε. The complete k-ε model equations are as follows:

$$\mu_t = \rho C_\mu \frac{k^2}{\varepsilon} \tag{4.11}$$

$$\frac{\partial}{\partial t}(\rho k) + \frac{\partial}{\partial x_i}(\rho u_i k) = \frac{\partial}{\partial x_i}\left(\frac{\mu_t}{\sigma_k}\frac{\partial k}{\partial x_i}\right) + G_k + G_b - \rho\varepsilon \tag{4.12}$$

$$\frac{\partial}{\partial t}(\rho \varepsilon) + \frac{\partial}{\partial x_i}(\rho u_i \varepsilon) = \frac{\partial}{\partial x_i}\left(\frac{\mu_t}{\sigma_\varepsilon}\frac{\partial \varepsilon}{\partial x_i}\right) + C_{1\varepsilon}\frac{\varepsilon}{k}\left(G_k + (1 - C_{3\varepsilon})G_b\right) - C_{2\varepsilon}\rho\frac{\varepsilon^2}{k} \tag{4.13}$$

The model equations contain five coefficients. C_{1_ε} , C_{2_ε} and C_{3_ε} are empirical constants, σ_k and σ_ε are Prandtl numbers governing the turbulent diffusion of k and ε. The rate of production of turbulent kinetic energy by shear is denoted by G_k and is only present in compressible flow. G_b is the generation of turbulence due to buoyancy. The most commonly used values for the coefficients are:

$C_\mu = 0.09,\ C_{1_\varepsilon} = 1.44,\ C_{2_\varepsilon} = 1.92, C_{3_\varepsilon} = 0, \sigma_k = 1.0, \sigma_\varepsilon = 1.3$

In recent years, the k-ε turbulence model has received wide acceptance for predicting a wide range of turbulent flows. However, the semi-empirical prediction of the eddy viscosity means that the turbulence is assumed to be isotropic i.e. the turbulent viscosity is equal in all directions. This means that the k-ε model in its standard form is not well suited for predicting highly non isotropic turbulence as encountered in swirling flows, separation regions, buoyancy, compressibility and adverse pressure gradients. Nevertheless, because it is so widely used, many modifications have been made to its standard form in an attempt to improve its performance. Examples of these modifications include Launder et al's (1975) for curvature and rotation, Hanjalic & Launder's (1981) for pressure gradients, Rodi's (1979) for buoyancy and Mcguirk & Rodi's (1977) for axi-symmetry.

FLUENT incorporates a modified version of the k-ε model called the RNG or Renormalised Group Theory k-ε model. Retaining the two equation framework used by its predecessor, the RNG model uses more of a mathematical foundation to turbulence transport modelling as opposed to the semi-empirical approach described above. The RNG k-ε model differs from the standard k-ε model in several important ways.

- Constants and functions in the RNG model are evaluated by the theory and not by empiricism and the model is therefore widely applicable without modification.
- Low-Reynolds effects are included in the RNG theory allowing laminar-like behaviour to be predicted.
- New terms appear in the dissipation rate transport equation for the treatment of separated and stagnation flows.
- Compressibility effects on turbulence are included.

This means that the model provides a more general basis for deriving predictions of fluid flow, yielding improved predictions of near wall flows, flow separation, low Reynolds number flows and detailed wake flow.

4.3.2 - REYNOLDS STRESS TRANSPORT MODELS

In Reynolds stress transport models, the eddy viscosity concept is abandoned and the unknown Reynolds stresses are obtained directly from the solution of the differential transport equations in which they are the dependent variables. In two dimensional flows, four equations are solved. In three dimensional flows, six equations are solved. An additional equation for ε is also solved in each case.

The Reynolds stress transport equation introduces new unknown correlations related to the production and dissipation of turbulence. These are calculated from several analogies and assumptions in terms of known quantities and using empirically derived coefficients in order to close the equations.

Reynolds stress transport models represent the state of the art in turbulence modelling and are destined to remain so for some considerable time to come. Although less stable and having a penalty in terms of solution time, they are becoming increasingly popular because they provide a more accurate representation of turbulence as well as being valid over a wider range of flows.

The principal disadvantage lies in their complexity. In three dimensional flows for example, they involve the solution of seven differential transport equations compared to only two for the k-ε model. Therefore, they may be of limited use in situations where the flow is influenced by factors other than turbulence such as heat transfer or chemical reaction. Computationally, they are less stable than the eddy viscosity models particularly when higher order discretisation schemes are employed.

4.3.3 ASSESSMENT OF A SUITABLE TURBULENCE MODEL

As with many parameters in CFD modelling, the general rule is that the higher the accuracy that is required, the longer will be the calculation time to arrive at a converged solution. If laminar flow were to be assumed and a turbulence model neglected, less equations are required to be solved and a solution is arrived at relatively quickly. If a simple two equation model with empirical constants is used such as the k-ε model the calculation time is extended slightly. When the model constants need to be calculated as in the RNG k-ε model, calculation time is extended further and instabilities on the convergence process begin to be introduced. A Reynolds stress turbulence model extends calculation time to a quite lengthy process and instabilities are such that a converged solution using one of the lower order models is usually required as an initial starting point to prevent divergence.

As mentioned in section 4.3 above, calculation of the Reynolds number at various points in the display case flow domain indicates that the problem is laminar but there are regions where transitional flow between laminar and turbulent is encountered and these are largely in the areas of most importance such as the air curtain.

Turbulence is a phenomenon of great complexity and an accurate method of describing it mathematically has been sought after for many years. The difficulty comes in finding a model which can describe the range of length and time scales encountered in many engineering flows. It is clear that each of the models has its advantages and disadvantages and many users have their own particular favourites. Therefore, the only true test of a particular model lies in the comparison with experimental results. In Chapter Five, such a comparison is made of results obtained using each of the models available in FLUENT.

4.3.4 - WALL TREATMENT FOR TURBULENT FLOWS

Wall functions are empirical relationships which are used at the near wall grid cell to predict the velocity within the near wall boundary layer. This means that instead of attempting to predict the entire turbulent boundary layer using many grid cells in this

region, the problem can be simplified and the near wall grid point can be placed relatively far from the wall. Placing this cell in the log region of the turbulent boundary layer reduces the number of grid cells and with it, the computer effort required for turbulent flow simulations.

Under equilibrium conditions, FLUENT uses the standard log-law wall function:

$$\frac{u}{u_\tau} = \frac{1}{\kappa}\ln(Ey^+) \tag{4.14}$$

where: $$u_\tau = \sqrt{t_w/\rho} \tag{4.15}$$

u is the fluid velocity at a point in the log-law layer, κ is von-Karman's constant, E is an empirical constant set by default to 9.8 for a smooth wall, and y^+ is the dimensionless distance from the wall.

$$y^+ = \frac{\rho u_\tau y}{\mu} \tag{4.16}$$

When, in turbulent flows, $y^+ > 11.225$, FLUENT applies equation 4.14. When y^+ falls below this value, the centre of the near wall cell lies in the viscous sublayer of the turbulent boundary layer. In this region, the wall function no longer applies and the wall shear stress is then calculated from the formula:

$$\tau_w = \mu\frac{\partial u}{\partial n}\bigg|_{wall} \approx \mu\frac{\Delta u}{\Delta n} \tag{4.17}$$

where u is the velocity component parallel to the wall and n is the coordinate normal to the wall. Δu and Δn are determined using the values stored in the computational cell adjacent to the wall.

4.4 - EFFECTS OF BUOYANCY

Due to the temperature difference between the case air and its surroundings, the air curtain can be considered as being negatively buoyant and account must be taken of

the gravitational acceleration, g, as an additional physical quantity. The significance of the body forces due to gravity can assessed by evaluation of the Froude number. This dimensionless ratio provides a measure of the inertia forces to the gravitational forces occurring within the flow. In the Froude number, $\rho g D^3$ can be taken as a representative gravitational force and $\rho u^2 D^2$ as a representative measure of the inertia forces. Therefore:

$$Fr = \frac{\text{Inertia forces}}{\text{Gravitational forces}} \quad \frac{\rho u^2 D^2}{\rho g D^3} = \frac{u^2}{gD} \tag{4.18}$$

When this ratio is equal to zero, the flow can be said to be purely buoyant and when equal to infinity, inertia forces dominate and the source is said to be a jet. In the model of a refrigerated display case, the lowest temperature occurs at the bottom of the back panel. However, this is also the region of highest velocity and the above ratio can be evaluated at approximately 10. In the region of the air curtain, much reduced velocities are experienced and here the Froude number falls to a value of 1.6. Further downstream of the air curtain outlet, lower velocities and larger length scales result in lower values of the Froude number of the order of 1×10^{-3}. This analysis demonstrates the significance of the buoyancy contribution on the flow pattern and this must therefore be considered in the CFD model.

The most straightforward and accurate method of accounting for buoyancy in FLUENT is to make the density dependent on temperature by a piecewise linear approximation. This involves giving the code several values of temperature and the corresponding densities. Similarly, other properties of the fluid may also vary with temperature. Fluid properties which vary by more than 10% over the temperature range 250 to 300K have been assumed to be significant. The values used to specify the buoyant fluid are shown in table 4.1. The specific heat capacity of moist air varies across the domain and is dependent on both temperature and humidity. Averaging the value between the store air and the case air yields a value of Cp = 1.01 kJ/kg.

Table 4.1 - Temperature Dependent Properties of the Buoyant Fluid			
Temperature (K)	Density (kg/m^3)	Viscosity (kg/ms)	Conductivity (W/mK)
250	1.412	1.599×10^{-5}	2.227×10
275	1.284	1.725×10^{-5}	2.428×10^{2}
300	1.177	1.846×10^{-5}	2.624×10^{2}

Having established the significance of buoyancy using the Froude number, it is applicable that this influence should be demonstrated. Figure 4.3 shows the display case modelled assuming that the density is dependent on temperature and that a gravitational force is present in negative y-direction therefore taking the buoyancy contribution into account. In this diagram, the velocity vectors are colour coded with the fluid temperature in order to simultaneously indicate the values of the two quantities. It can be seen how the air curtain is deflected towards the shelves forming a quite distinctive flow pattern. Figure 4.4 shows the results of a similar model where temperature has been calculated but the density remains constant. In this case, the gravitational force remains but the air curtain is projected on a path more perpendicular to the outlet.

This example not only demonstrates the significance of buoyancy but also the capability within CFD to model situations which could not be experienced in reality, i.e. making density independent of temperature.

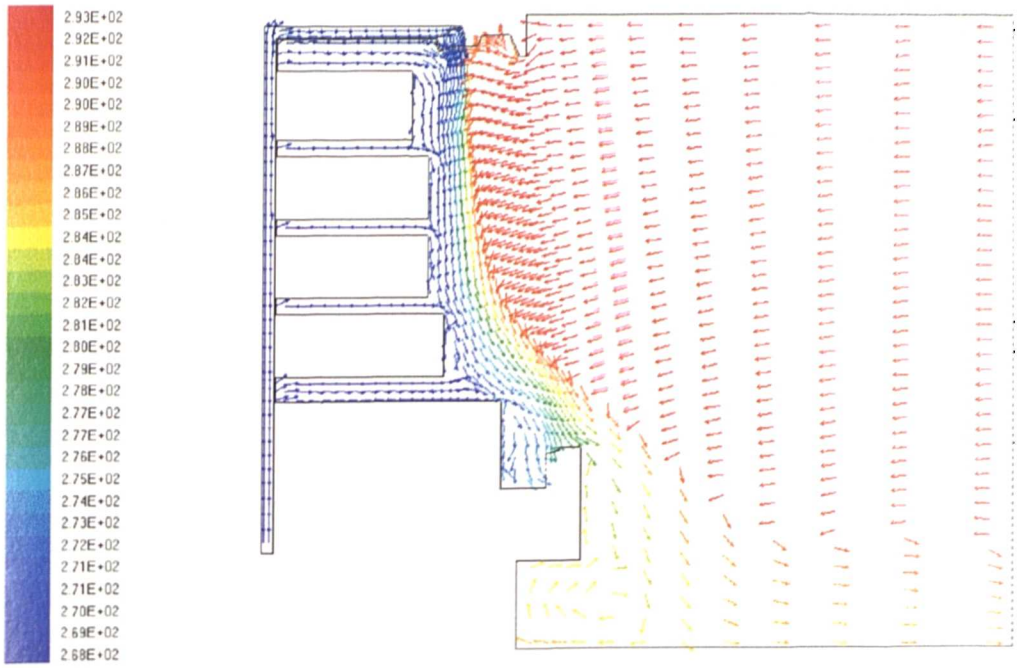

Figure 4.3 - Case Modelled with Density Dependent on Temperature

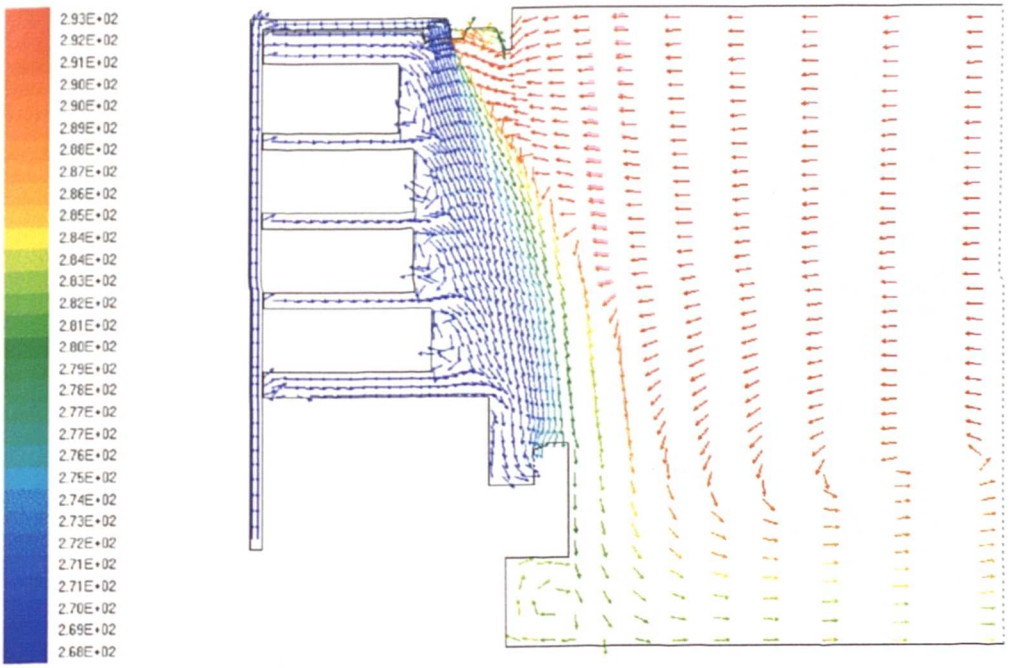

Figure 4.4 - Case Modelled with Constant Density

4.5 - POROUS MEDIA MODELLING

Experimental work on the performance characteristics of honeycombs has shown that the honeycomb section at the air curtain outlet can have a significant effect on the structure and propagation of the air curtain. Therefore, the honeycomb must be modelled to complete an accurate prediction of the development and path of the air curtain.

To model the small scale geometry of the honeycomb section within the overall large scale model of the display case would require an impractically large number of cells. Therefore, the problem must be reduced to a simulation of the action of the honeycomb on the flow. In FLUENT, this simplification can be achieved by modelling the honeycomb as a tube bank using the code's porous media model. In essence, this is nothing more than an added momentum sink in the momentum equations applied across the porous region. This general momentum sink is given by:

$$\frac{\mu}{\alpha} v + C_2\left(\tfrac{1}{2}\rho v|v|\right) \tag{4.19}$$

Where α and C_2 are empirical inputs of permeability (m^2) and inertial resistance factor (m^{-1}) in each component direction respectively. This equation gives a pressure drop over the porous region which is in proportion to the fluid velocity in the cell. However, when modelling a tube bank or a perforated plate, the dependence of pressure drop on the dynamic head pressure becomes predominant and the permeability term can sometimes be eliminated. Then, the pressure drop per unit thickness of the porous media becomes:

$$\frac{\partial p}{\partial x_i} = C_2\left(\tfrac{1}{2}\rho u_i|u_i|\right) \tag{4.20}$$

The velocities in this equation are not true velocities as they are based on 100% open area. Therefore, a correction needs to be made to the inertial loss coefficient to account for this.

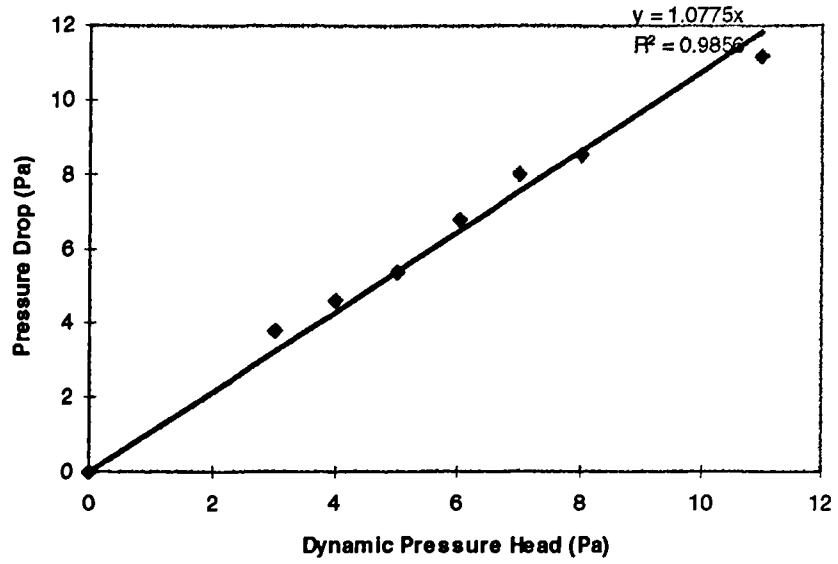

Figure 4.5 - Honeycomb Pressure Drop against Dynamic Pressure Head

The empirically derived results for the pressure drop versus dynamic head are shown in figure 4.5. From this, it can be seen that the pressure drop is 1.08 times the dynamic pressure head. Based on an open area of 91%, The loss factor K_L is defined as:

$$\Delta p = K_L\left(\tfrac{1}{2}\rho v_{91\%\ open}^2\right) \tag{4.21}$$

and therefore K_L is equal to 1.08 based on the actual fluid velocity through 91% open area. To calculate an appropriate value of C_2, corrections must be made to the velocity for 100% open and then converted into dynamic head loss per unit thickness of the porous region. K_L' is based on 100% open area where:

$$\Delta p = K_L'\left(\tfrac{1}{2}\rho v_{100\%\ open}^2\right) \tag{4.22}$$

If the flow rate is the same then

$$v_{91\%\ open}^2 = \frac{100}{91} \times v_{100\%\_open} \tag{4.23}$$

$$\therefore K_L' = K_L \times \frac{v^2_{91\%\ open}}{v^2_{100\%\ open}} = 1.078x\left(\frac{1}{0.91}\right)^2 = 1.302 \qquad (4.24)$$

The adjusted loss factor, therefore, has a value of 1.302 and the loss coefficient per unit thickness,

$$C_2 = \frac{K_L'}{\text{Thickness}} = \frac{1.302}{0.015} = 86.8 \ \ m^{-1} \qquad (4.25)$$

When the porous medium is non isotropic as in the case of a tube bank, the inertial loss factor must be calculated in each of the three co-ordinate directions. In the case of the honeycomb, no flow will occur in the i or k directions and hence the inertial resistance factor is made large relative to the value for the j direction. The effect of this is to align the flow perpendicular to the face of the outlet.

To give more flexibility in the grid, the perforations in the back panel of the case were also made up of porous cells. This meant that the amount of air flowing through them was not governed by the size of the outlet hole but on the pressure drop across the panel. A summary of the parameters used in the modelling of the porous media is given in table 4.2.

Table 4.2 - Model Constants for the Porous Media

	Permeability, α		Resistance Factor, C_2	
	i-direction	j-direction	i-direction	j-direction
Honeycomb Section	1.0×10^{-6}	5.0×10^{9}	1.0×10^{5}	1.0×10^{2}
Perforated Back Panel	5.0×10^{9}	1.0×10^{-6}	1.0×10^{4}	1.0×10^{4}

The use of porous media for the modelling of a honeycomb section has been tested and validated against experimental result, Patel (1996). The investigations carried out demonstrated that this methodology provided a good representative model for a

honeycomb, predicting air velocities, in most cases, to within 12% of experimental measurements.

4.6 - GEOMETRY AND GRID

In using CFD to model engineering problems, it is the exception rather than the rule to represent the geometry exactly. Only where seemingly insignificant geometry features are likely to affect the overall flow (such as at supersonic velocities) are they modelled as close to reality as possible. The main limitation is that the smaller the scale of the geometry features that are modelled, the larger the number of grid cells that are required to capture flow patterns around them. The number of grid cells directly affects the solution time and the stability of the solution. This number should, therefore, be kept to the minimum number required to accurately calculate the overall flow pattern. If the effect of smaller geometrical features on the flow is not known, they can be modelled separately at a higher resolution to determine their significance. A decision can then be made on whether they should be included in the system level model.

Simplifying the geometry, also means that features which are not of interest do not have to be modelled. This leads to a faster, more stable and more accurate solution provided that the correct boundary conditions are applied. For instance, for the purposes of the current research project, the design of the fans and the evaporator will remain unchanged since the main scope of the work is to concentrate on the air flow patterns within the refrigerated space. To model the fan and the evaporator would have required a fan model and a further porous media with a specified heat flux to represent the evaporator. Therefore, the problem has been simplified by measuring velocities and temperatures at the base of the back panel and using these experimental values as inputs to the model.

The geometry of the model for the refrigerated dairy case was constructed using measurements taken from the actual case under test in the laboratory. The geometry outline is shown in figure 4.6. It was felt that some of the geometrical features could

not be adequately represented by an orthogonal grid and therefore, a 7482 cell body fitted grid was applied to the geometry. This is shown in figure 4.7.

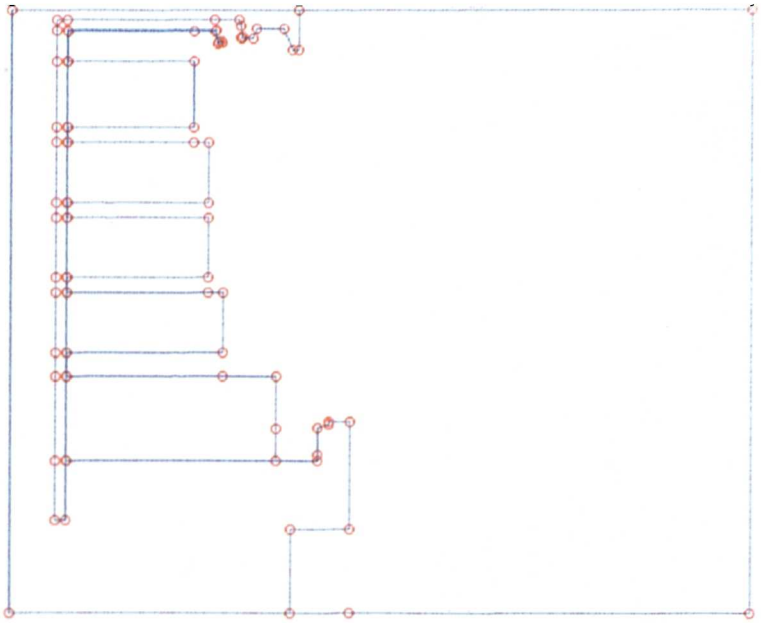

Figure 4.6 - Geometry Outline for Two Dimensional CFD Model

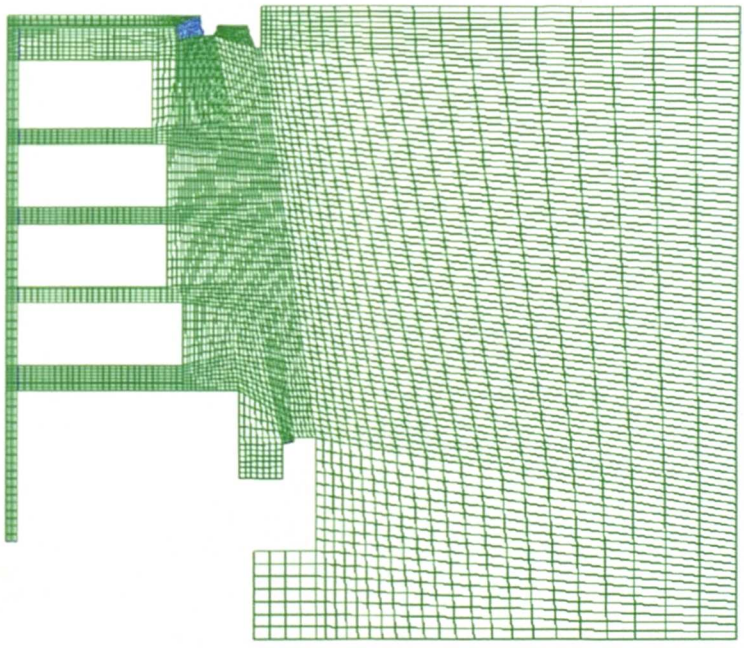

Figure 4.7 - Computational Grid for Two Dimensional CFD Model

Determining whether the constructed grid contains a sufficient number of cells to accurately solve the flow field is a critical step in the modelling of any CFD related problem. For any model there is an optimum number of grid cells defining a grid density which solves the flow field to an acceptable degree of accuracy. Increasing the number of cells beyond this maximum only serves to increase the calculation time and is of little benefit as the required accuracy has been achieved. A grid dependency check was carried out by applying several different grid densities to the geometry shown in figure 4.6. The performance of each grid was assessed against a relevant parameter, in this case the net sensible heat gain into the calculation domain. This parameter was selected because it is pertinent to the overall objective of the project, namely the investigation of case performance and energy consumption. A graph showing the calculated net sensible heat transfer plotted against the number of grid cells is shown in figure 4.8.

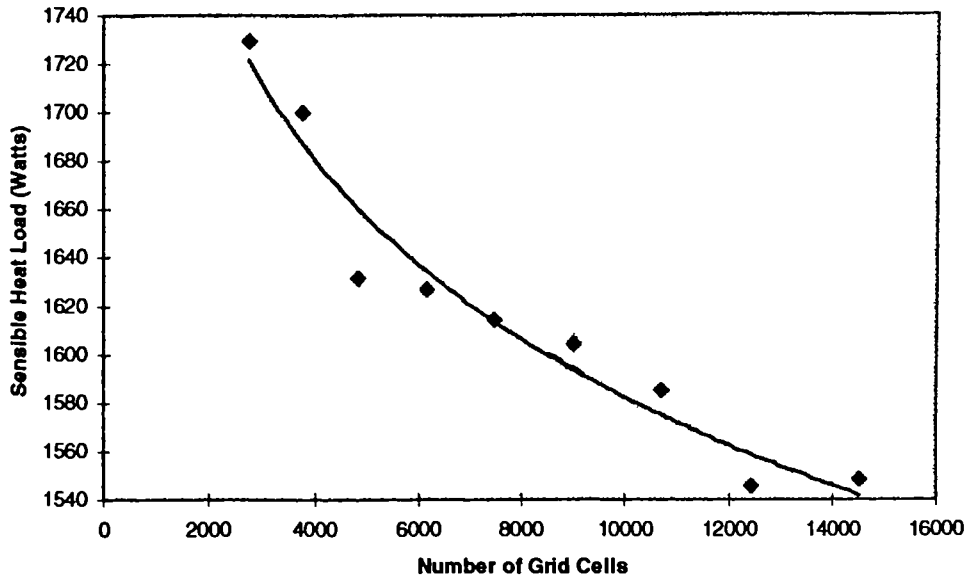

Figure 4.8 - Graph of Sensible Heat Load Against Number of Grid Cells

Superimposed on the calculated points is a trendline showing the exponential decrease of the predicted sensible load with the increase in the number of cells. It is apparent that as the number of grid cells approaches 14,000 the sensible load has levelled out at approximately 1550 Watts. The grid shown in figure 4.5 with 7482 cells has a calculated sensible load of 1615 Watts. This corresponds to a 4% error

from the most accurate, grid independent solution with just over half of the number of cells required to reach that most accurate solution. Therefore, the proposed grid can be described as the optimum for this problem, achieving a relatively fast solution time without sacrificing accuracy.

4.7 - SOLUTION PROCEDURE

As described in section 4.2, the governing equations for fluid flow are a set of simultaneous equations which must be solved over the domain by an iterative process. This is done by supplying the code with an initial guess of density, temperature, pressure and velocities. The solver then re-calculates these values for each grid cell applying the mass, momentum and energy balances.

Until the conservation equations are satisfied, the degree of imbalance is reported in the form of a residual. At the end of each of these iterative steps, a residual is reported which is the total imbalance summed over all of the cells in the domain. When the residuals reach a predetermined level, a balance of the conservation equations has been achieved to an acceptable degree of accuracy and the problem is said to have converged.

4.8 - BOUNDARY CONDITIONS

Although the geometry and a suitable calculation grid are of importance in a CFD problem, it is generally recognised that it is the boundary conditions that have the greatest influence on the accuracy of the result.

Boundary conditions are the parameters known about the flow. They are supplied to the model as a fixed or known flow condition. The model of the refrigerated display case is assumed to be a steady state problem and therefore the boundary conditions will remain constant throughout the solution process. In reality, the display case is not a steady state problem. A build up of frost on the evaporator will change both the air off temperature and the back panel velocity in between defrosts. However, the

simulation of frost build up on the coil would be an unnecessary complication at the initial stages of design. It is sufficient to assume a clear coil and thus, maximum air flow rate. After the model has been validated, the effect of frost build up can be investigated by applying appropriate boundary conditions obtained from experimental measurements.

The boundary conditions for the two dimensional case model relate to air temperatures and velocities, wall temperatures and turbulence quantities. For the baseline case they are as shown in tables 4.3(a) and (b). These were obtained by carrying out measurements on an actual display case tested in the environmental chamber.

Table 4.3(a) - Temperature Boundary Conditions for Baseline Model

	Temperature (K)
Walls inside case (W1)	273
Walls outside case (W2)	283
Floor and ceiling of store (W3)	293
Inlet at base of back panel (I1)	268
Horizontal Return Air Grille (I2)	281.5
Vertical Return Air Grille (I3)	293
Open Boundary on Right of Domain (I4)	277.5

Table 4.3(b) - Flow Boundary Conditions for Baseline Model

	u-velocity (m/s)	v-velocity (m/s)	Static Pressure (Pa)	Turbulence Quantities: Turb. Intensity, Characteristic length
I1	-	2.7	-	10%, 0.04m
I2	-	0.8	-	10%, 0.04m
I3	Fixed Pressure		0	10%, 2.0m
I4	1.0	-	-	10%, 0.04m

4.9 - SUMMARY

Having established a geometry from physical measurements, applied a suitable grid to the problem and applied appropriate boundary conditions, the model is now in a position to be solved. This chapter has given an overview of CFD models and methodology in order to inform the reader of the modelling options available and their implications. Clearly, the test of any computer model lies in its solution a d comparison to measured quantities. This next logical step is presented in Chapter 5 where the results from this comparison are then used to select a suitable turbulence model.

CHAPTER 5

CFD MODEL SET-UP AND VALIDATION

5.1 - INTRODUCTION

In Chapter 4 consideration was given to some of the theory behind CFD and how this was used to decide which mathematical model(s) would be used in the simulation of a refrigerated display case. Despite this analysis, it is sometimes appropriate to assess certain criteria experimentally trying different models to find the most accurate for the particular application. This is necessary because although the performance of different turbulence models or solution methods has been well documented for various flow types, each application is quite specific in the demands it makes of the code. In any computer model, simplifications must also be made and experimental validation is one way of ensuring confidence in the assumptions which have been made.

The objective of this chapter is to present a preliminary two dimensional CFD model and then to validate this against experimentally derived results. In Chapter 3 the experimental facility constructed for the purposes of this research project was described. In section 5.3 the experimental procedure followed during the course of the validation will be explained. Following a comparison of results from the CFD model and the experiments, a baseline model will be established and its accuracy assessed. In section 5.8 the results of a three-dimensional model will be presented.

5.2 - MODELLING STRATEGY

The general purpose nature of many CFD codes means that it is necessary to select a combination of mathematical models in order to fully describe the problem. It is not usually of relevance and sometimes impossible to solve for every detail of the flow and as a consequence it is common practice to simplify the problem. The type and

degree of this simplification depends very much on what aspect of the flow is of interest and may be in terms of grid size, cell concentration or models used.

The geometry, grid, boundary conditions and physical constants for the fluid which were used in the baseline display case were specified in Chapter 4. It was also shown that the flow is buoyant and this was taken into consideration in all CFD simulations by making density dependent on temperature and specifying a gravitational acceleration in the negative y-direction of 9.81 m/s^2.

In modelling a refrigerated display case, the resultant parameter of most interest is the cooling load on the evaporator, and hence the selection of models for heat transfer is of paramount importance. As described in section 2.7, heat transfer from the ambient environment into the display case occurs in several ways:

- Conduction through the walls, Q_{wall}.
- Sensible heat transfer due to air infiltration across the air curtain, Q_{sens}.
- Latent heat transfer due to air infiltration across the air curtain, Q_{lat}.
- Radiant heat transfer across the case opening, Q_{rad}.

Each of these contributions to the cooling load can be considered using CFD. For each model, however, boundary conditions are required. Boundary conditions describe what is known about the flow and therefore they are the single most important factors affecting the accuracy of a solution.

The aim of this project is to model, to within an acceptable degree of accuracy, the airflow around the display case and how this affects the load on the evaporator. Conduction through the walls of the case is not greatly influenced by the pattern of airflow and is neglected in the present study. Heat transfer by radiation, although occurring through the case opening, is also unaffected by air flow and hence neglected. Sensible and latent heat transfer are, however, directly influenced by turbulent mixing in the air curtain and must be considered.

Sensible and latent heat transfer components are both directly proportional to th mass flow rate of air across the case opening. Therefore, for a certain mass flow rate of ambient air across the air curtain it is feasible to assume that the sensible and latent components can be expressed as a ratio of the combined total. Modelling for moisture as a species and its difficulties will be described in section 5.7 but in order to reduce the number of boundary conditions and computational time, sensible heat transfer only was considered in the majority of simulations. Because of the relationship between the mass flow rate of air across the air curtain and the sensible and latent heat transfer components, it was assumed that latent load could then be expressed as being proportional to the sensible load.

5.3 - EXPERIMENTAL PROCEDURE

All of the experimental work for this research project was carried out in the custom built experimental facility in the Department of Mechanical Engineering at Brunel University, which has been described in Chapter 3 of this report.

In order to achieve steady state test conditions, the refrigerated case was run overnight to bring the water filled product packages down to an equilibrium temperature. Prior to all tests, a gas defrost of the evaporator was carried out to ensure that it was clear of frost. A one hour period was allowed from the initiation of the defrost to allow case temperature to recover. Figure 5.1 shows the case and product temperatures over the period of one hour in order to justify this methodology. The graph shows the variation over time of the air temperature in the honeycomb and three product temperatures at different positions in the case, the positions are chosen at random for the present analysis. The rise in the honeycomb air temperature clearly indicates the time when the defrost has been initiated and its fall denotes termination of the cycle. The product temperatures are largely unaffected by the defrost and hence, the case can be said to be in a state of steady operation one hour after initiation of the defrost cycle.

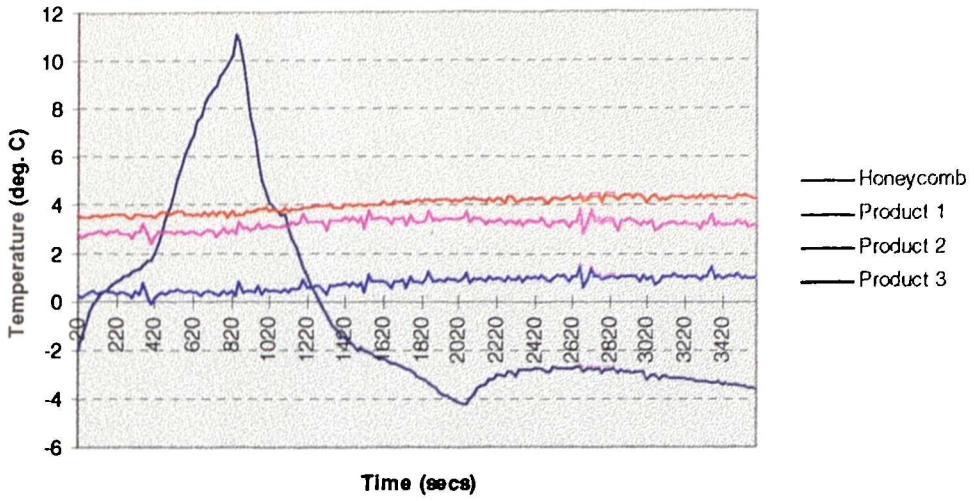

Figure 5.1 - Variation of Temperature During and After a Defrost Cycle

The validation of the CFD model was carried out in three stages. Initially, a comparison of velocity profiles was made in order to assess the accuracy of the prediction of the flow field. Temperature profiles were then evaluated as the prediction of the temperature field directly influences the heat transfer across the curtain. Finally an evaluation of the cooling load on the display case was carried out and compared with both theoretical and experimental results.

The velocity and temperature profiles were measured using the three axis positioning robot in order to locate the probes at points corresponding to grid cell centres on the CFD model. In this way, velocity and temperature profiles were taken at the front of each shelf as shown in figure 5.2. Measurements were taken using a constant temperature velocity probe. A certain amount of instability was observed in the readings which could have been for one or a combination of two reasons. The first reason could be the effect of turbulence causing fluctuating velocity readings similar to those shown in figure 4.2. However, the velocity probe used had a slow response time and would have tended to dampen any high frequency oscillations. The second effect could have been a certain amount of inherent unsteadiness in the flow. This is possible even given steady state boundary conditions and can be equated to the

vortex shedding which occurs downstream of a cylinder placed in a flow with a steady upstream velocity.

In an attempt to show mean velocities, ten readings were taken at each position and the average calculated. Figure 5.3 shows the minimum, maximum and mean velocity readings at each measuring location for the top shelf profile. Each of the other three shelves showed similar variations in the measurements.

The cooling capacity of the evaporator was calculated using the enthalpy difference across the coil and the mass flow rate of refrigerant to the case on test. Making an assumption that the expansion of the refrigerant was isenthalpic, the enthalpy of the refrigerant entering the evaporator, h_{in}, was calculated as being saturated liquid at a temperature immediately prior to the expansion valve. The enthalpy of the gas leaving the evaporator, h_{out}, was calculated from measurements of the temperature and pressure of the refrigerant in the suction line performing a linear interpolation from the property tables for R22. All of these parameters were logged every ten seconds over a one hour period in order to establish the cooling load on the evaporator. This is described in more detail in section 5.6 with a graph of cooling load versus time shown in figure 5.18.

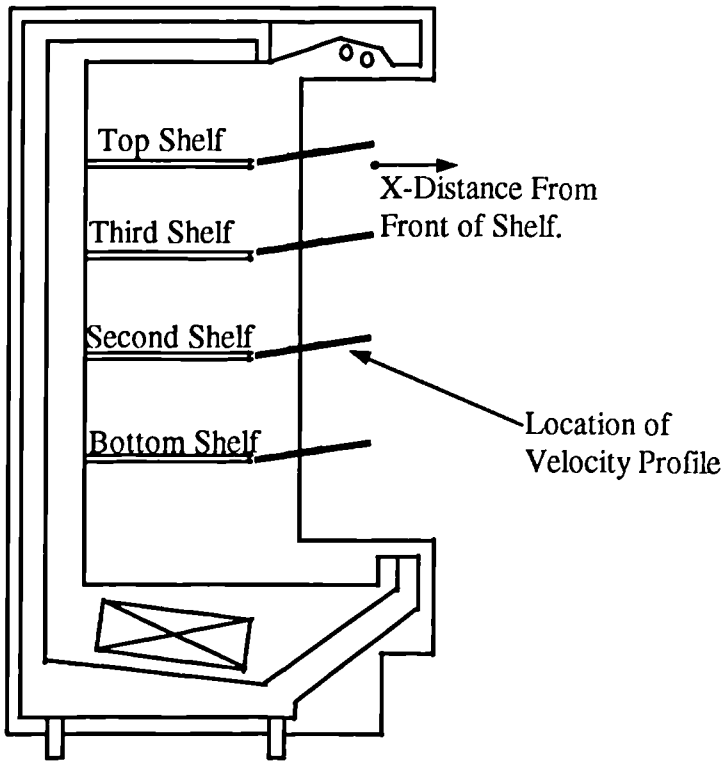

Figure 5.2 - Location of Velocity Profiles in Front of Shelves

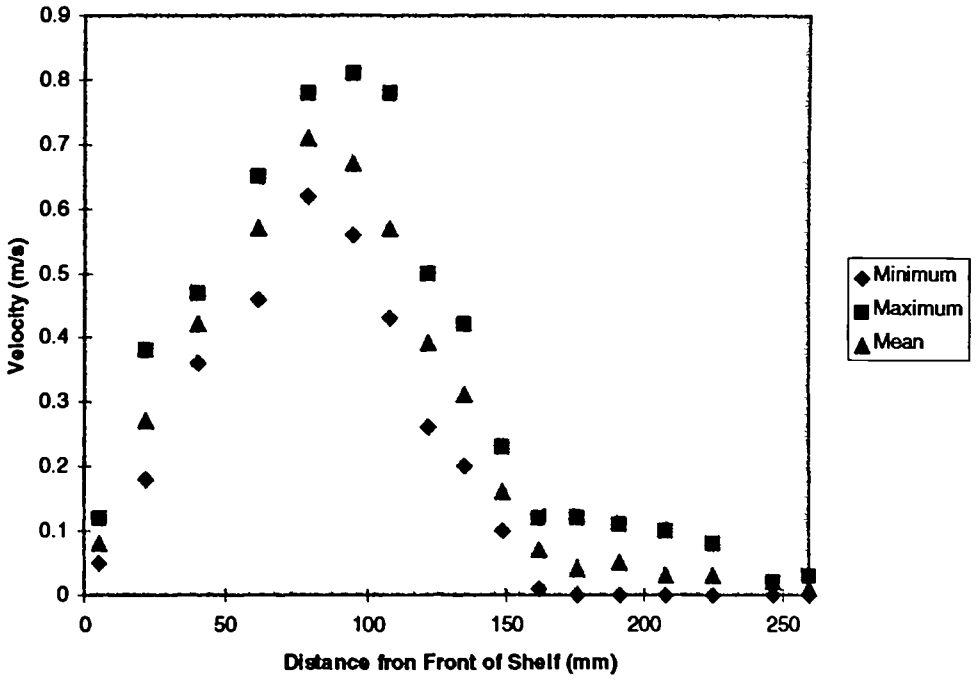

Figure 5.3 - Minimum, Maximum and Mean Velocity Readings for the Profile Adjacent to the Top Shelf.

5.4 - COMPARISON OF VELOCITY PROFILES

In order to establish a reliable baseline CFD model for the refrigerated display case, it was first necessary to decide on a suitable turbulence model, if any, for the particular application. The main criteria which had to be fulfilled by the model were:

1) - It had to be suitable for low Reynolds number flows.

2) - It had to be able to cope with buoyant flows.

3) - It had to be able to cope with separation regions etc. in complicated geometries.

As explained in Chapter 4, FLUENT incorporates three turbulence models with the additional option of neglecting turbulence and assuming laminar flow. The models available are k-ε, Renormalised Group Theory k-ε (RNG) and Reynolds Stress Model (RSM). The nature of the problem, incorporating all of the above flow phenomena made it necessary to compare the results obtained using each turbulence model with measured velocity profiles taken across the air curtain. Figures 5.4 to 5.7 show velocity profiles at each shelf for each of the modelling options compared with experimentally measured results. Error bars showing a ± 10% error on the experimental measurements are included in order to give an indication of the accuracy of the CFD predictions.

In figure 5.4 it can be seen that at the top shelf, the laminar model is by far the best predictor of the velocity profile. This is to be expected due to the small length scale in this region resulting from the air curtain outlet and honeycomb equating to a low Reynolds number. Both k-ε models performed well on the outside of the curtain. The RSM however, failed to predict the velocity profile with any accuracy.

At the third shelf shown in figure 5.5, the laminar model still predicted the peak velocity well but became less accurate on the outside of the air curtain. The fact that all three of the turbulence models predicted this velocity gradient much better than the laminar option tends to suggest that the flow may be more turbulent in this region. With reference to figure 2.6, accepted theory for turbulent jets suggests that an initial region of the jet exists prior to deterioration of the structure of the jet

further downstream. As the air curtain develops downstream of the outlet, the centreline velocity decays and the pattern of the air flow spreads. It then follows that small eddies in the flow cascade into larger ones increasing the length scale and resulting in a higher Reynolds number. It seems, therefore, that the flow is becoming more turbulent. Of the three turbulence models considered, the RNG model provided the best prediction of the velocity profile at the third shelf.

At the second shelf (figure 5.6), the laminar model again failed to capture the spreading due to turbulent mixing although this was expected. The RNG model seemed to provide the best prediction of the peak velocity whilst the RSM and standard k-ε provided good predictions at the outside of the curtain.

As shown in figure 5.7, none of the turbulence models predicted the velocity profile at the bottom shelf in the area next to the shelf with any accuracy. On the outside of the curtain, however, which is of most relevance, all of the turbulence models predicted the velocity gradient satisfactorily with the RNG model producing results closest to the experimental profiles.

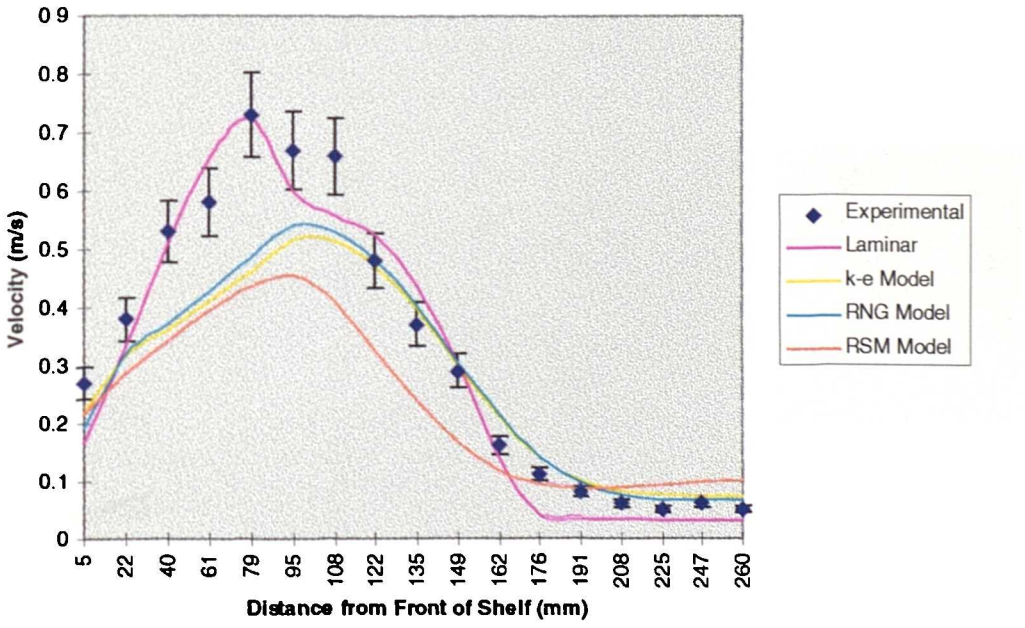

Figure 5.4 - Comparison of Velocity Profiles at Top Shelf

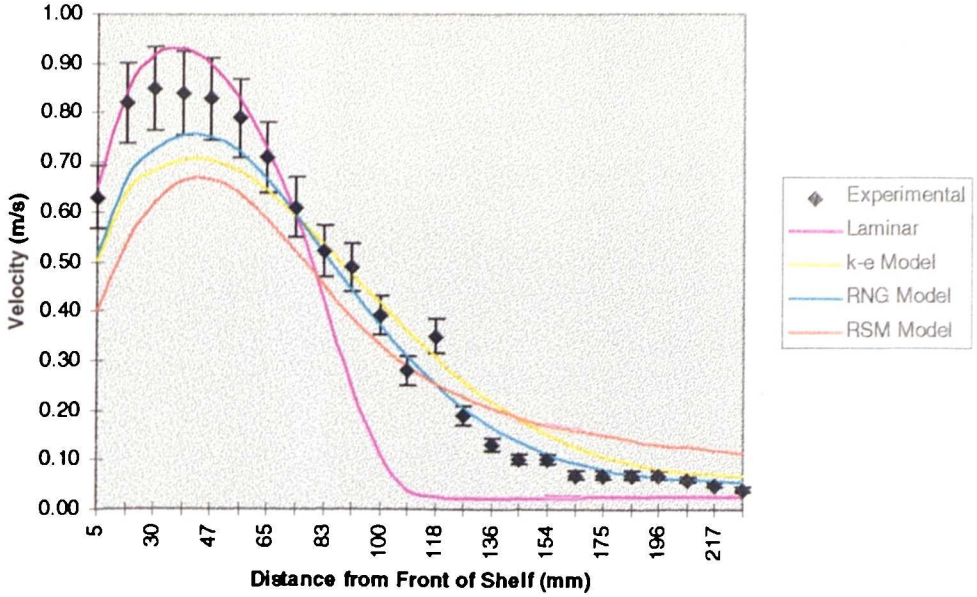

Figure 5.5 - Comparison of Velocity Profiles at Third Shelf

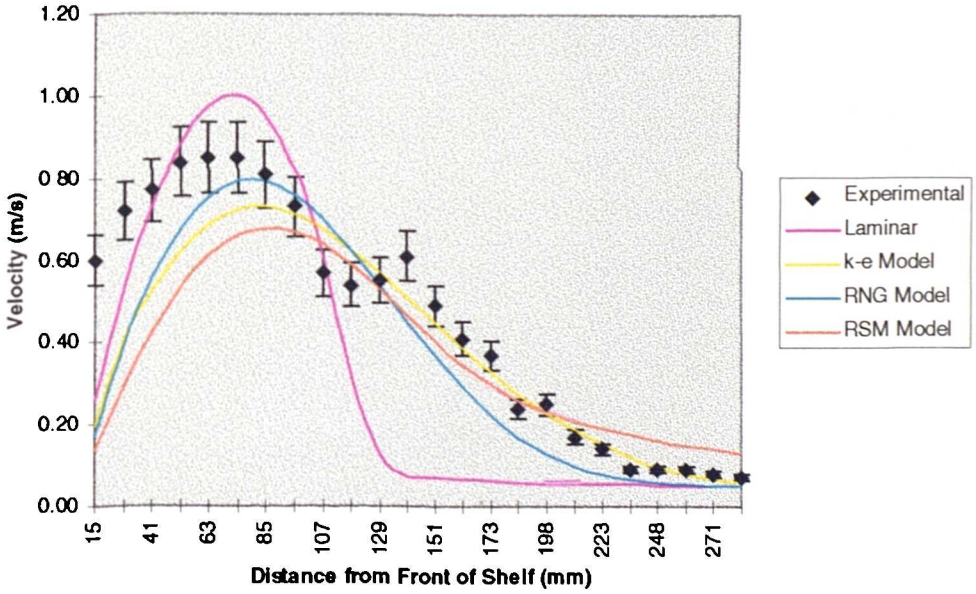

Figure 5.6 - Comparison of Velocity Profiles at Second Shelf

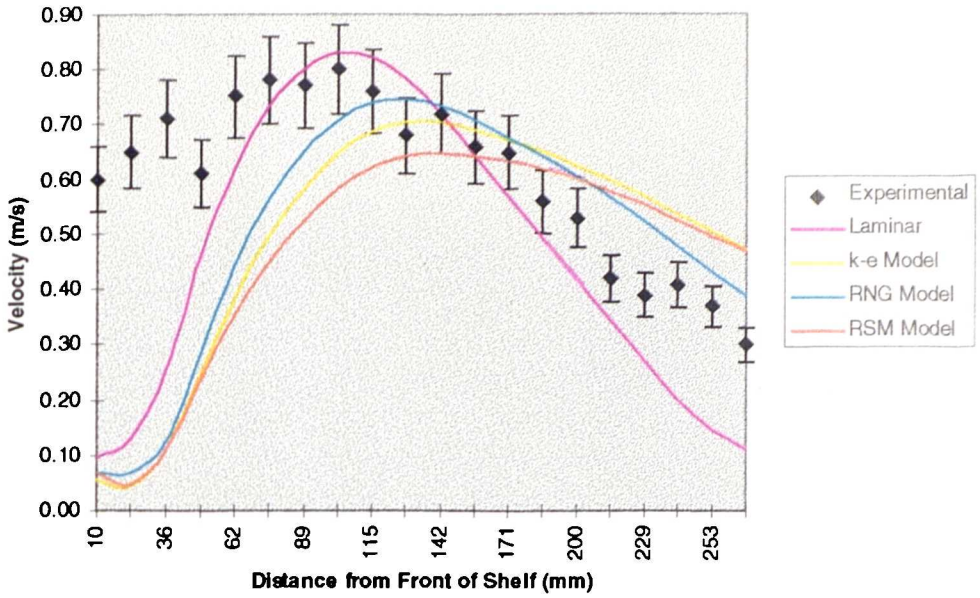

Figure 5.7 - Comparison of Velocity Profiles at Bottom Shelf

In all of the profiles at the front of the shelves, it can be seen that each of the turbulence models give a good representation of the flow pattern on the outside of the air curtain. This is due to the increase in free stream turbulence which occurs as the jet develops downstream of the air outlet. This phenomenon can be seen with reference to figure 5.8 which shows the contours of turbulent kinetic energy. Near to the air curtain outlet, there is very little turbulence. However, as the curtain develops, contours indicating an increase in turbulence intensity begin to appear on the outside of the curtain. Because there is very little in this region to provide an obstruction to the flow and hence regions of separation are limited, it is likely that turbulence in this region may be close to being isotropic. The mathematical nature of the lower order turbulence models such as the k-ε model assumes that turbulence is isotropic and therefore provides an explanation as to the high order of accuracy in predicting velocities in this region.

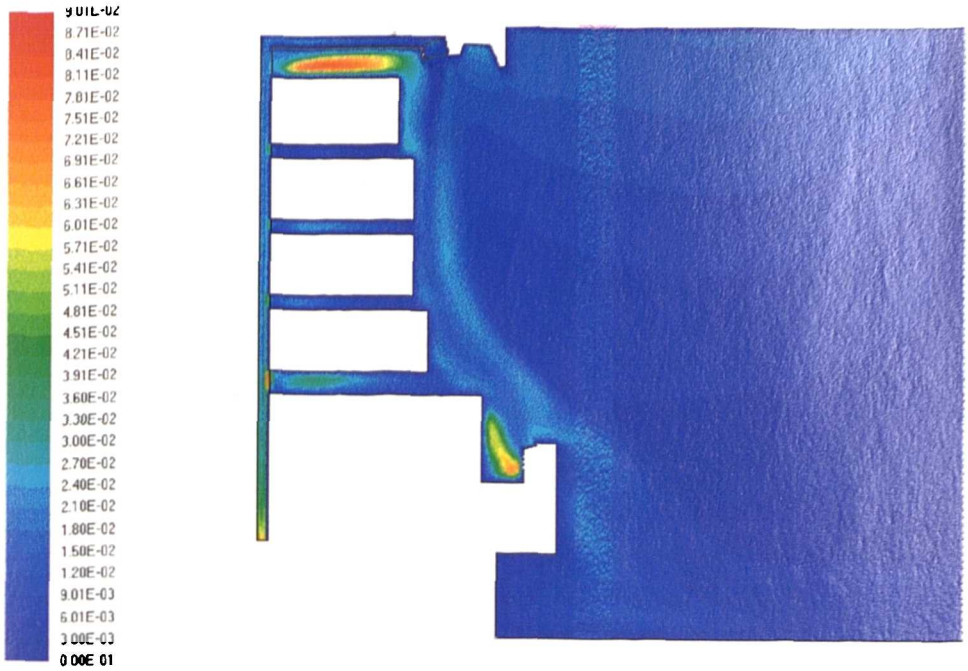

Figure 5.8 - Contours of Turbulent Kinetic Energy for Baseline Case

Far less accurate is the prediction of the flow field on the inside of the air curtain adjacent to the front of the shelves. This may be due to one, or a combination of several factors.

The first consideration is the grid density on the inside of the curtain where relatively complex flows are taking place. However, the grid dependency analysis carried out in chapter 4 shows that the heat transfer into the case is largely independent of the grid at 7482 cells. This means that even if the grid density is the reason for the discrepancy in the results next to the shelves, the lack of resolution in this region does not affect the overall outcome which is to examine the case cooling load.

The location of the near wall grid cell also influences the way that the code treats wall effects and boundary layers as described in section 4.3.4. The proximity of the near wall grid cell to the surface and hence the validity of the wall function used is described by the dimensionless value, y^+. Calculated values of y^+ lie in the range from 12 to 20 at the front of the shelves. This means that the boundary layer is treated using the standard log law function as described by equation 4.14. More importantly, the values of y^+ are very much lower than 500. This means that the near wall grid

cells are sufficiently small that they lie in the surface boundary layer as they should and not in the fully turbulent region of the flow.

A reasonably coarse assumption has been made in the model in representing the product as a large block with no contribution to the case cooling load. In actual fact, for the experiment, the product on the shelves of the case is made up of numerous water filled containers with air gaps in between. Therefore, not only is there a certain amount of flow from the back panel through the product, but product temperatures measured and which are above the indicated case temperature suggest that there is a small load contribution from the packages. A dependency test was carried out using the CFD code to represent the product as two dimensional porous media. Difficulties with the grid generation meant that the products could not be modelled using the porous media model. As a compromise, the products were represented as solids with a pressure boundary on the front of the packages above the shelf. This had the effect of allowing air to be entrained from the product into the air curtain. Although using this method yielded predictions closer to the experimental profiles near to the bottom shelf, the other profiles were somewhat worse.

Another assumption made was that the product extended all the way from the front of the shelf to the back panel when in reality there was a gap between the product and the back panel. A modification was therefore made to the model to assess the significance of this simplification. Figures 5.9 and 5.10 show a comparison between the velocity profiles for the baseline case and the case with the smaller product on the second and the bottom shelves.

It can be seen that there is an increase in the velocities nearer to the shelf which would bring them more into line with those measured experimentally. A comparison between the two flow fields can also be seen in figure 5.11 with velocity vectors colour coded with a temperature scale. Although there are differences in the flow around the product, the overall pattern remains largely unaffected and in fact the predicted sensible heat transfer into the case only changes by less than 2%. Given

these results, it was decided to use the simple representation of the product in order to simplify the geometry and reduce the number of grid cells.

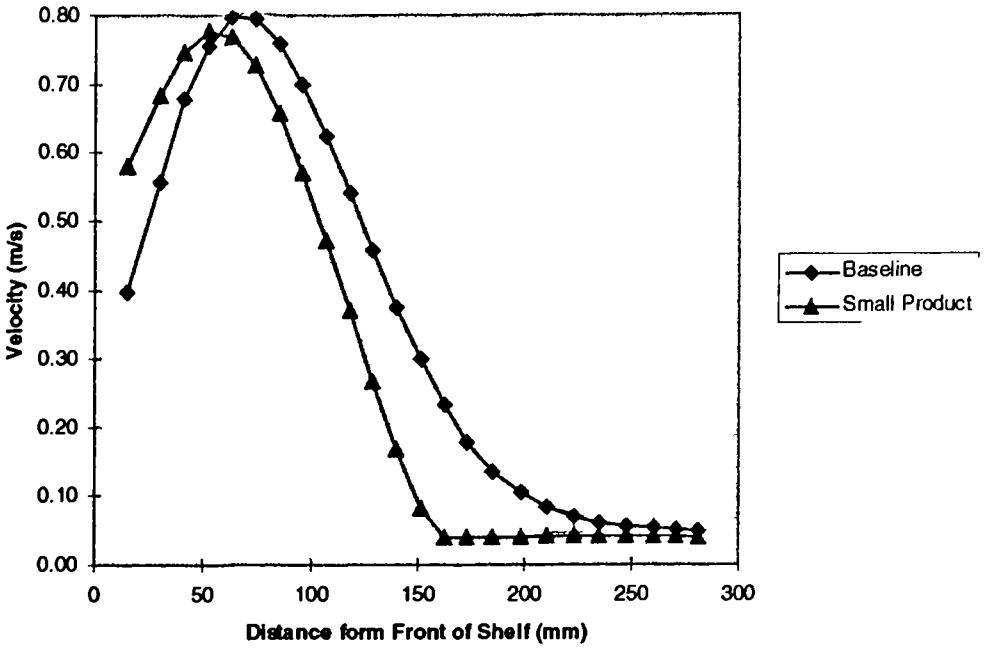

Figure 5.9 - Comparison of Velocity Profiles for Baseline and Modified Product at the Second Shelf

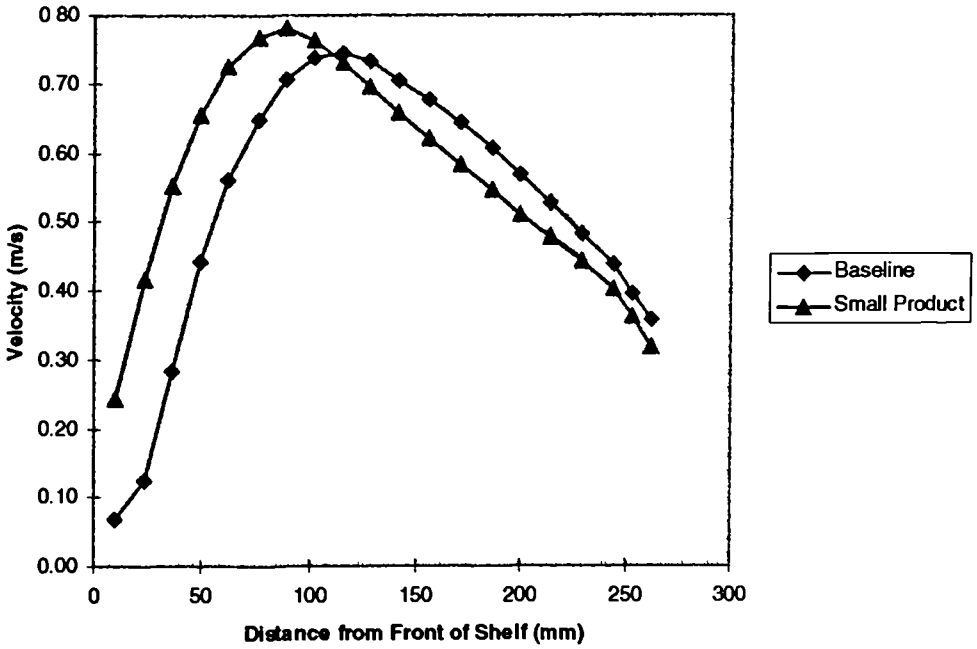

Figure 5.10 - Comparison of Velocity Profiles for Baseline and Modified Product at the Bottom Shelf

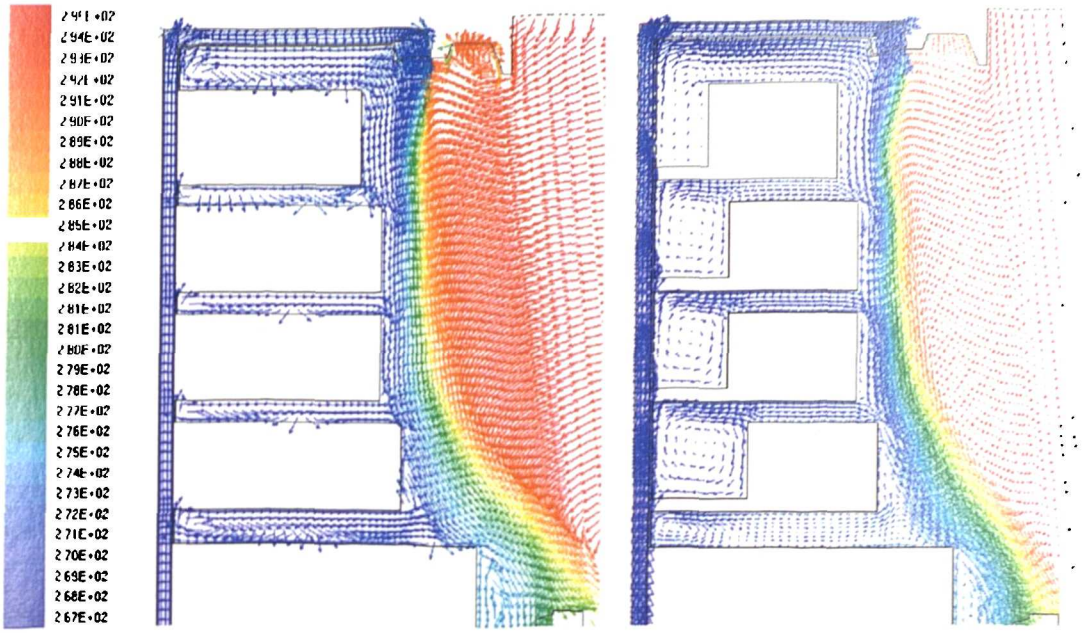

Figure 5.11 - Comparison of Flow Fields for Baseline and Modified Product

The velocity vector plots illustrated in figure 5.11 clearly shows the entrainment of the air from the store. It can be seen that at about the position level with the top of the top shelf, the initial region of the air curtain comes to an end and the jet begins to spread and mix with the entrained air. This is shown by the change in colour across the air curtain as a temperature gradient begins to form. Progressing downstream of the air curtain outlet, the region of mixing on the outside of the curtain gradually widens until the air at the return air grille is at approximately 8°C

Due to the transitional nature of the flow from laminar near the air curtain outlet to a low Reynolds number turbulent flow further downstream, a versatile turbulence model was required. It has been demonstrated that the laminar model is only applicable in the region of the air curtain outlet where it clearly outperformed the turbulent options. The k-ε model has difficulty coping with transitional flows and is also best applied for simple geometries where the turbulence is nearer isotropic. For this specific application, the RSM model also had difficulty dealing with near laminar

flows. On the evidence of the above tests, the most appropriate turbulence model for this particular application was the RNG k-ε model.

5.5 - COMPARISON OF TEMPERATURES

Comparisons were also made of the temperature profiles for each turbulence model against temperatures measured on the actual display case. These temperature profile comparisons are shown in figures 5.12 to 5.15 with ± 2°C error bars in order to give an indication of the accuracy of the CFD predictions.

It can be seen in all the temperature profiles that modelling the flow as being laminar means that a sharp temperature gradient exists along the entire length of the curtain with very little diffusion taking place. This is due to the lack of turbulent mixing that is assumed in laminar flows. All of the turbulence models and the experimental results indicate that there is a large amount of turbulent diffusion in the air curtain. This is especially apparent further downstream as the temperature gradient becomes flatter.

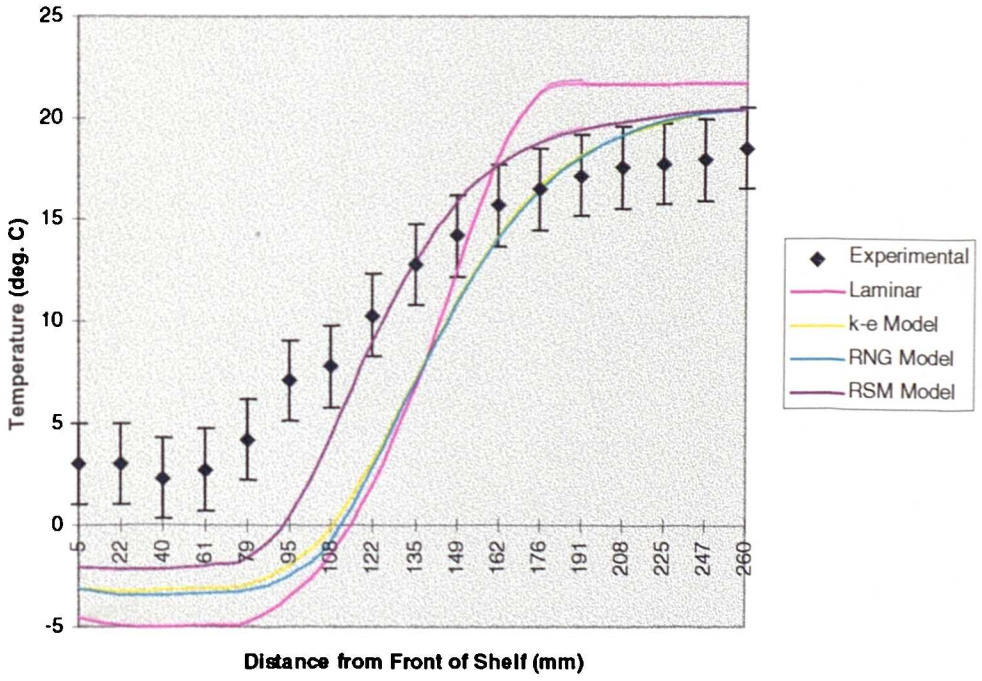

Figure 5.12 - Comparison of Temperature Profiles at Top Shelf

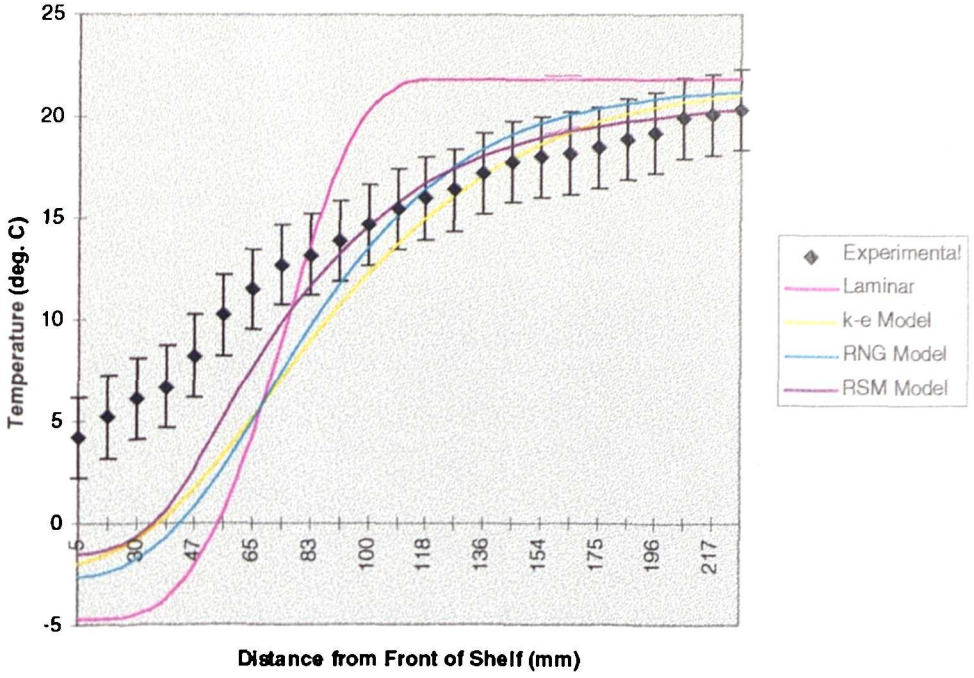

Figure 5.13 - Comparison of Temperature Profiles at Third Shelf

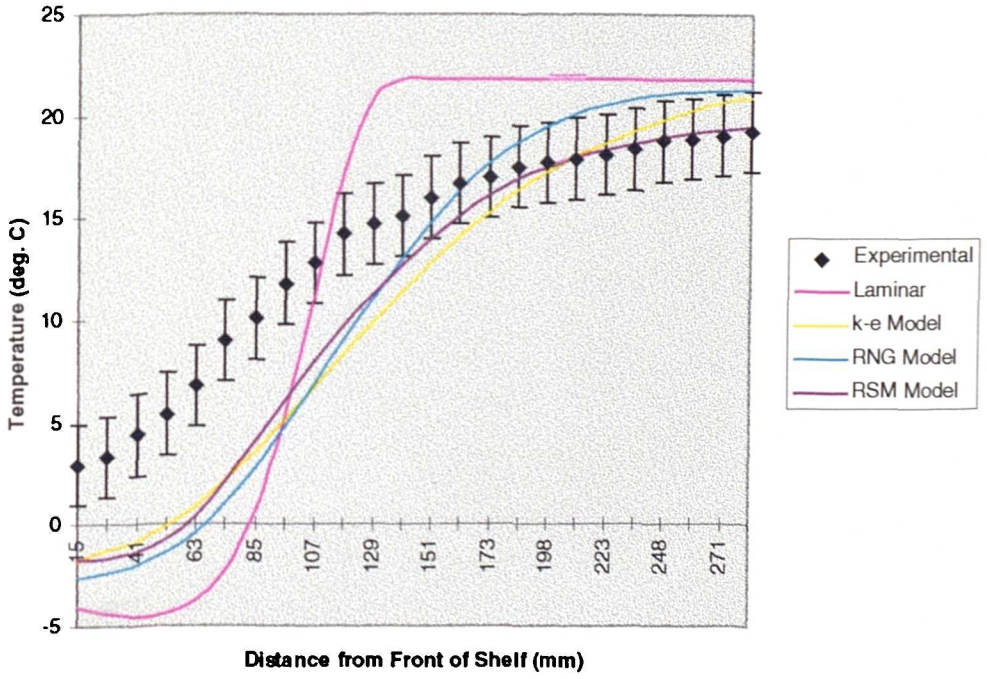

Figure 5.14 - Comparison of Temperature Profiles at Second Shelf

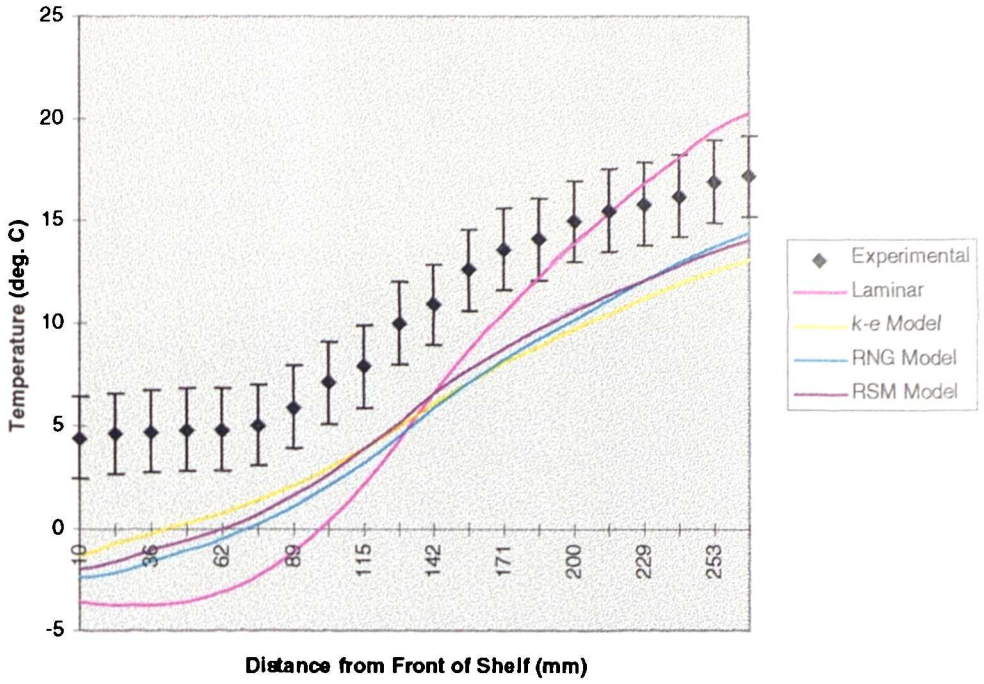

Figure 5.15 - Comparison of Temperature Profiles at Bottom Shelf

Figure 5.12 shows that at the top shelf, the k-ε and the RNG models follow virtually the same profile which is markedly different from that predicted assuming laminar flow. The RSM model falls somewhere in between these two extremes and could probably be said to be the closest to the experimental results.

At the second and third shelves up (figures 5.13 and 5.14), the temperature profiles for all three of the turbulence models follow a much more similar path to one another and all show agreement within 2°C of the experimental profile on the outside of the curtain. On the inside of the curtain, the predictions are generally up to 5°C lower than the measurements. At this point, the laminar modelling assumption will be discounted because of its inability to predict the spreading of the air curtain due to turbulent mixing.

Figure 5.15 shows that all three of the models predict a similar temperature profile and there is therefore, little to distinguish between them. The predicted profiles also

show good agreement with measurements in terms of the shape of the profile although the former are generally 5°C lower throughout the profile.

It is interesting to note that the region where the majority of the discrepancies occur is on the inside of the air curtain in the same area where the errors in velocities were observed. Therefore, it could be argued that the same factors were significant in the temperature field as in the velocity field. In order to validate this assumption, a comparison was made, similar to that carried out in section 5.4, to examine the effect of the size of the product. Figures 5.16 and 5.17 show the temperature profiles taken at the bottom and the second shelves and compares the two models at these locations.

There is some improvement in the model with the smaller product in terms of the temperatures modelled on the actual display case. It is therefore surmised that this is the most likely reason for the discrepancies between the baseline CFD model and the experimental measurements.

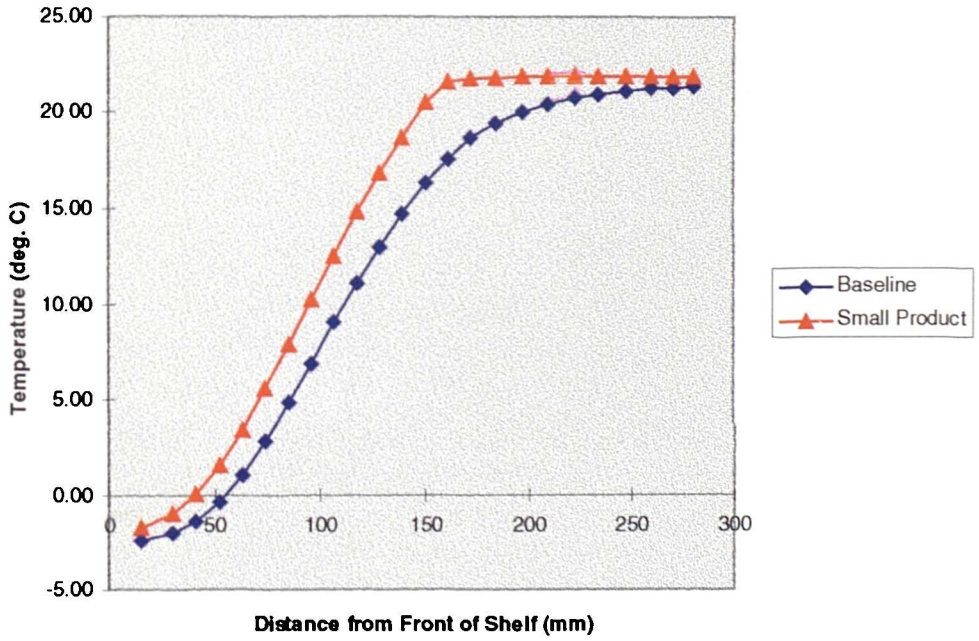

Figure 5.16 - Comparison of Temperature Profiles for Baseline and Modified Product at the Second Shelf

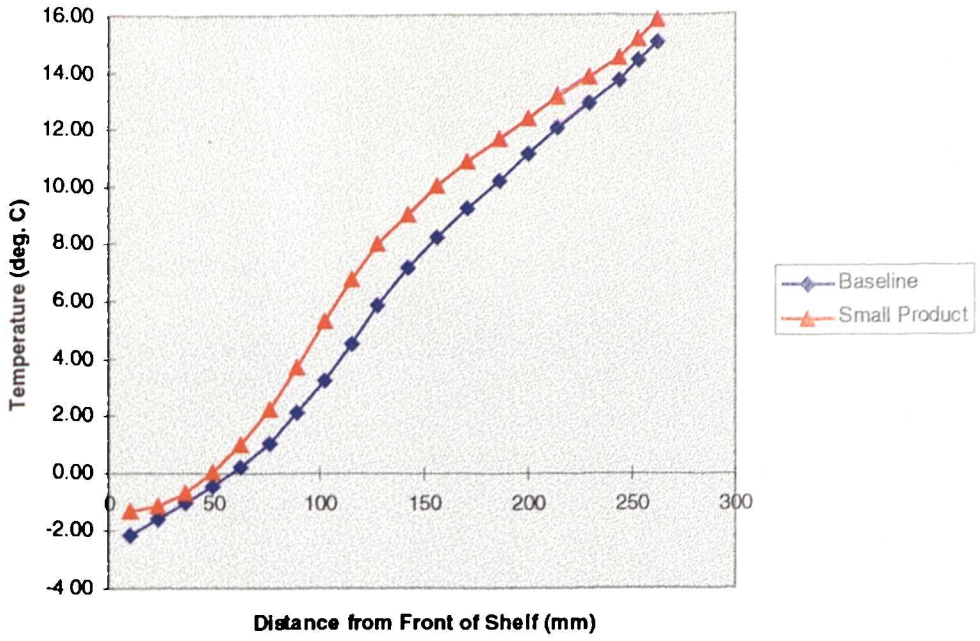

Figure 5.17 - Comparison of Temperature Profiles for Baseline and Modified Product at the Bottom Shelf

5.6 - COMPARISON OF COOLING LOAD

As explained in the preceding sections, reasonable correlation was shown between the CFD model and the experimentally measured profiles. However, the final test was to assess the model's ability to predict the refrigeration load.

An equation for the total cooling load on the display case was given in Chapter 2. If certain assumptions are made, however, this equation may be simplified. For example, when assessing the steady state performance of the case, defrosts are not taken into account and the load required to recover from a defrost may be disregarded. Similarly, if the product temperatures are allowed to reach a steady state, there will be no load associated with bringing them down to temperature. The refrigeration load from ancillary items such as lights and anti-sweat heaters may also be discounted by switching them off for the duration of the test. Making these assumptions as well as adding the load from the fans to the equation which was omitted by Howell (1993), the refrigeration load on the display case can be simplified as follows:

$$Q_{case} = Q_{walls} + Q_{rad} + Q_{scns} + Q_{lat} + Q_{fans}$$

This equation describes the most significant refrigeration loads on the case and it these which will be considered in the following analysis.

The total refrigeration load on the evaporator was determined experimentally over four, separate, one hour measuring periods as described in section 5.3. The variation in load over such a period can be seen in figure 5.18. The total load, Q_{case}, averaged over the four periods was calculated as being 3412 Watts. This compares to a total load of 3443 Watts quoted by the case manufacturer for the same case.

In order to assess the degree of accuracy of the CFD model's prediction of sensible heat transfer, it was first necessary to calculate the contributions from the walls, radiation, latent gain and fans. These were determined theoretically and can be found in Appendix B. They are also summarised in table 5.1 below together with their percentage contributions to a total case load of 3412 Watts.

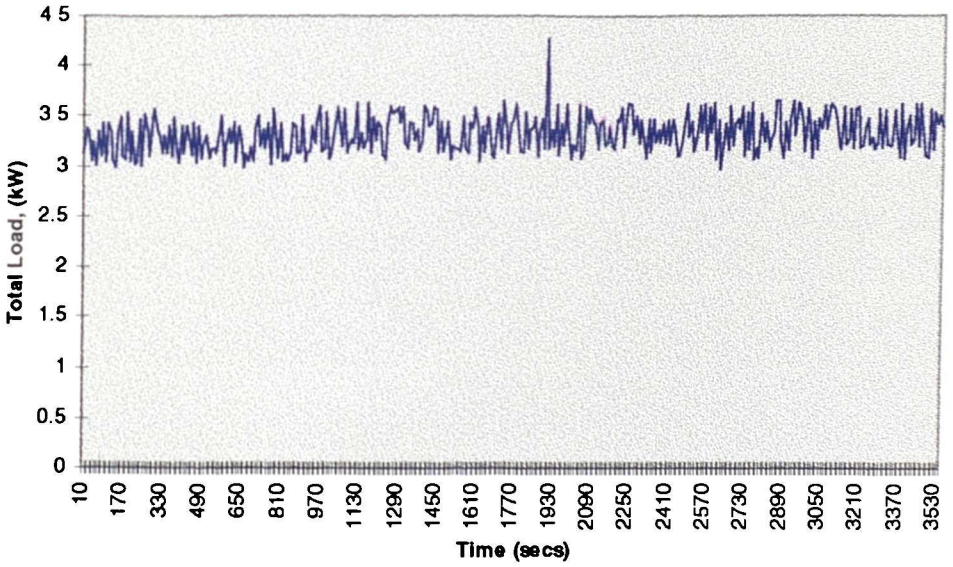

Figure 5.18 - Graph of Total Refrigeration Load vs. Time

Table 5.1 - Theoretical Contributions to Case Refrigeration Load		
	Load (Watts)	Percentage Contribution
Q_{walls}	164	4.8 %
Q_{rad}	313	9.2 %
Q_{lat}	1179	34.6 %
Q_{fans}	84	2.5 %

The above calculations indicate that the sensible cooling load on the case should be in the order of 1672 Watts or 51.1 % of the total.

The CFD prediction of the sensible load was found by summing the heat transfer entering and leaving the calculation domain. The two dimensional model assumes a unit depth of the computational domain equal to 1 metre and therefore the result was corrected with a multiplier of 2.45 metres equivalent to the width of the case opening. The total sensible heat transfer predicted by the model was 1575 Watts, therefore having a 6 % variance from that predicted in the calculations.

5.7 - CALCULATION OF HUMIDITY

As demonstrated in section 5.6, the latent heat transfer into the case contributes a major portion to the total refrigeration load. Using the CFD code's capability for the modelling of species, moisture was introduced into the air at each of the inlet boundary conditions. One limitation was that it was not possible to model any surface condensation with the standard code although generally this was not thought to be a significant factor.

Boundary conditions were measured using a Rotronic temperature and humidity probe at the bottom of the back panel, at the return air grille and in the environment in which the case was tested. Mass fractions of moisture content were then calculated from the psychrometric chart.

The results from this simulation are shown in figures 5.19 and 5.20 colour coding the velocity vectors with a vapour mass fraction and a temperature respectively.

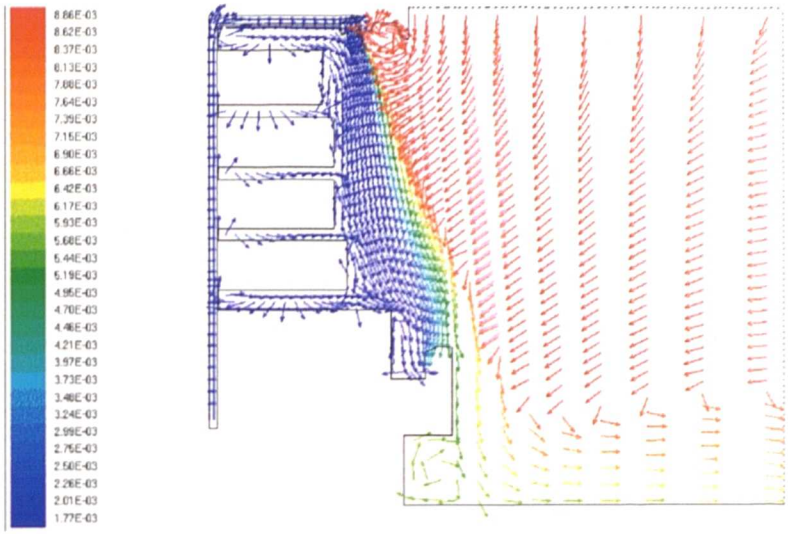

Figure 5.19 - Velocity Vectors Colour Coded with Vapour Mass Fraction

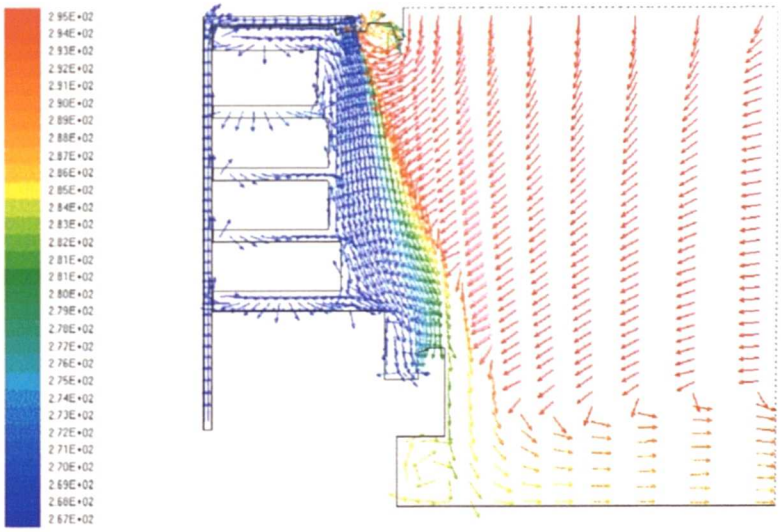

Figure 5.20- Velocity Vectors Colour Coded with Temperature

It can be seen that the contours of the mass fraction coincide with the temperature contours to a large extent. Equating the net mass transfer of moisture into the domain yields a value of 1.05 kg/h compared to experimental results which point to a value of 1.5 kg/h.

Although this result indicates an error of almost 30%, it must be remembered that some rather coarse assumptions have made in the CFD model. The lack of a surface condensation model in effect means that the water vapour was being modelled as nothing more than a non-reacting species. This would equate to the simulation of smoke which is a non-reacting particulate in the air flow.

As far as the standard code is concerned, the modelling of condensation is not possible. This would require a user defined Fortran routine which would equate the temperature and humidity of the air to a dew point and thereby make a prediction of the condensation of water vapour from the air.

In order to further analyse these results and the reasons for any discrepancies, a comparison of the temperatures and humidities at various points around the case is shown in figure 5.21. At each point indicated by the red dot, the figures in red represent the CFD predictions and the figures in blue indicate the experimental values. In general, there is reasonably good agreement between the CFD model and the measurements taken on the actual case. Again, the main regions of error occurred close to the shelf fronts. In these areas, the model predicted humidities more than 10% below those measured. *In fact, if the temperatures are also taken into account* and the moisture content is calculated, the errors are in excess of 30%. It is thought that this is due to the effect of surface condensation occurring on the actual case, locally increasing the humidity close to the shelf fronts. No surface condensation is modelled within the CFD code which is clearly quite important at least in the prediction of moisture mass fraction close to walls.

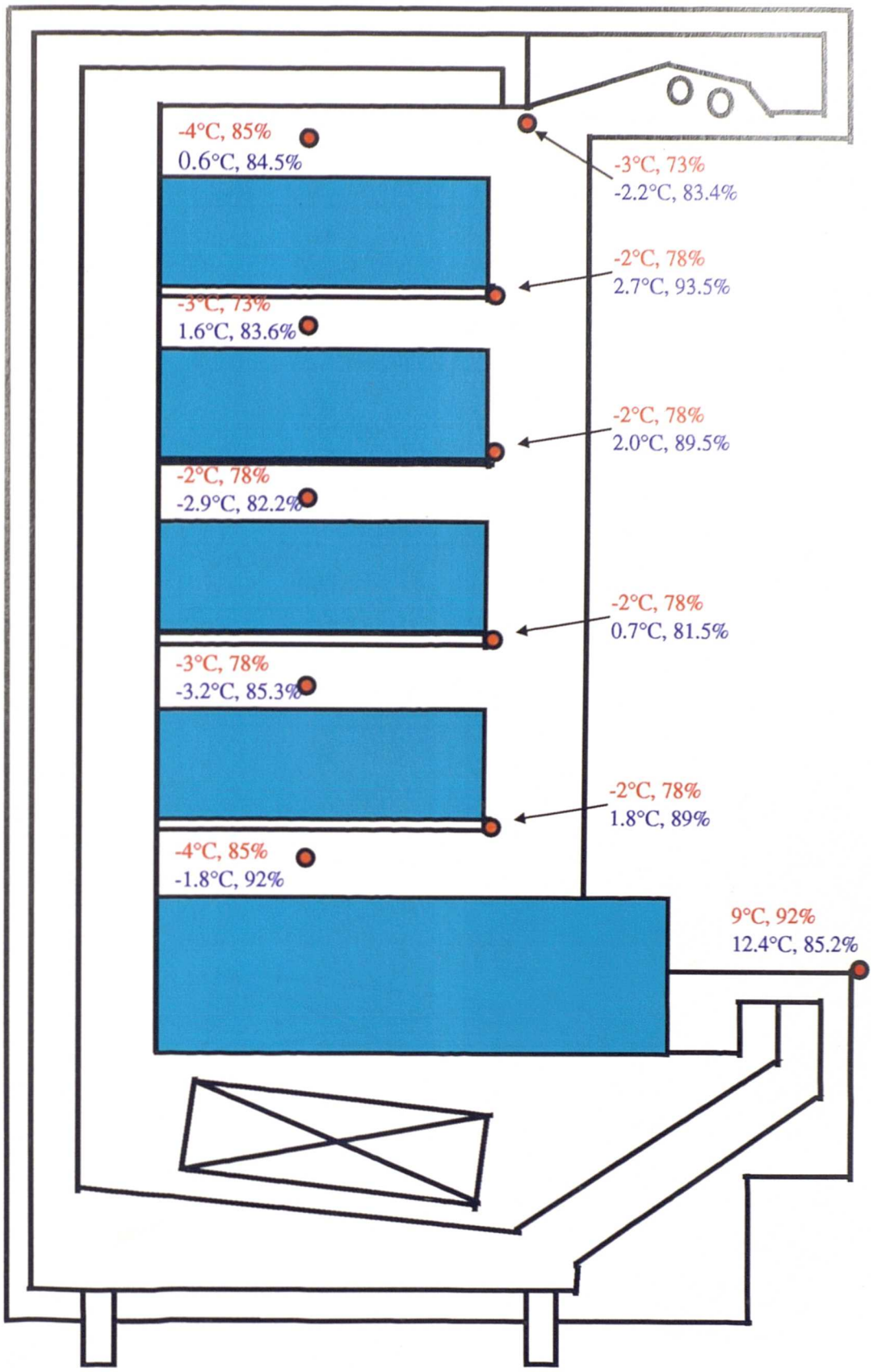

Figure 5.21 - Comparison of Temperatures & Humidities Around The Case

5.8 - THREE DIMENSIONAL MODEL

Up until this point the main assumption made in setting up the computational model is that the flow is predominantly two dimensional and therefore can be simplified into two dimensions. In considering this, two factors must be taken into consideration. First, is the effect that the end walls have on the air flow within the display cas and whether this is significant enough to warrant modelling in three dimensions. Second, is the effect of the requirements of the testing standard which specifies that there should be a movement of air across the front of the case with a velocity of 0.2 m/s.

A three dimensional model of the display case was therefore constructed in order to support the assumption of a predominantly two dimensional flow. This was carried out on a workstation using FLO*VENT*®, another commercially available finite volume CFD code using similar principles to those employed by FLUENT but calculated over a cartesian mesh. Ordinarily, it would have been possible to model only half of the display case and use a symmetry plane half way along its length. With a crossflow across the front of the case, however, the model had no plane of symmetry and therefore it was necessary to model the entire display case.

The results of a three dimensional model without air flow across the front of the case are shown in figure 5.22. The data is presented in two ways. Temperature contours on a plane 50mm from the floor are shown to indicate the pattern of the air overspill from the case. In addition to these contours, particle tracks are shown which originate from the air curtain outlet.

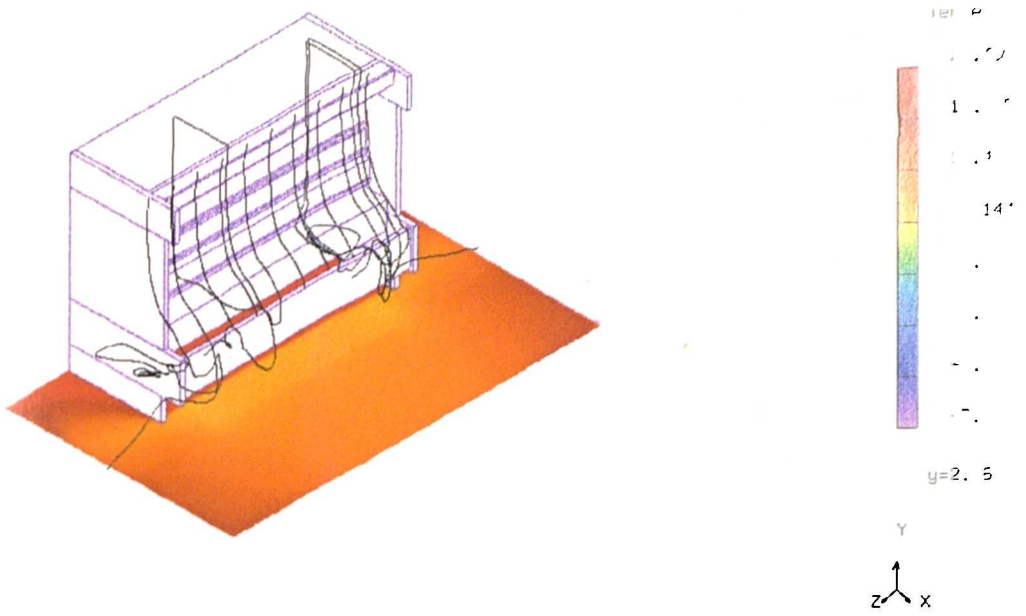

Figure 5.22 - Results of 3D Baseline Case With No Crossflow

From figure 5.22, it can be clearly seen that the air flow pattern is two dimensional along most of its length and from the uniformity of the air temperature near to the floor, it can be deduced that the overspill is virtually the same along the centre portion. Near to the ends of the case, the particle tracks show that the overspill which occurs in these regions circulates around the edges of the case. This results in more spreading of the overspilt air and therefore the air temperatures near the floor are somewhat higher.

Visualising the flow pattern in any three dimensional problem can cause a certain amount of difficulty. Therefore animations were created of the model results in order to better describe what is happening. A still from the animation for the case with no cross flow is shown in figure 5.23.

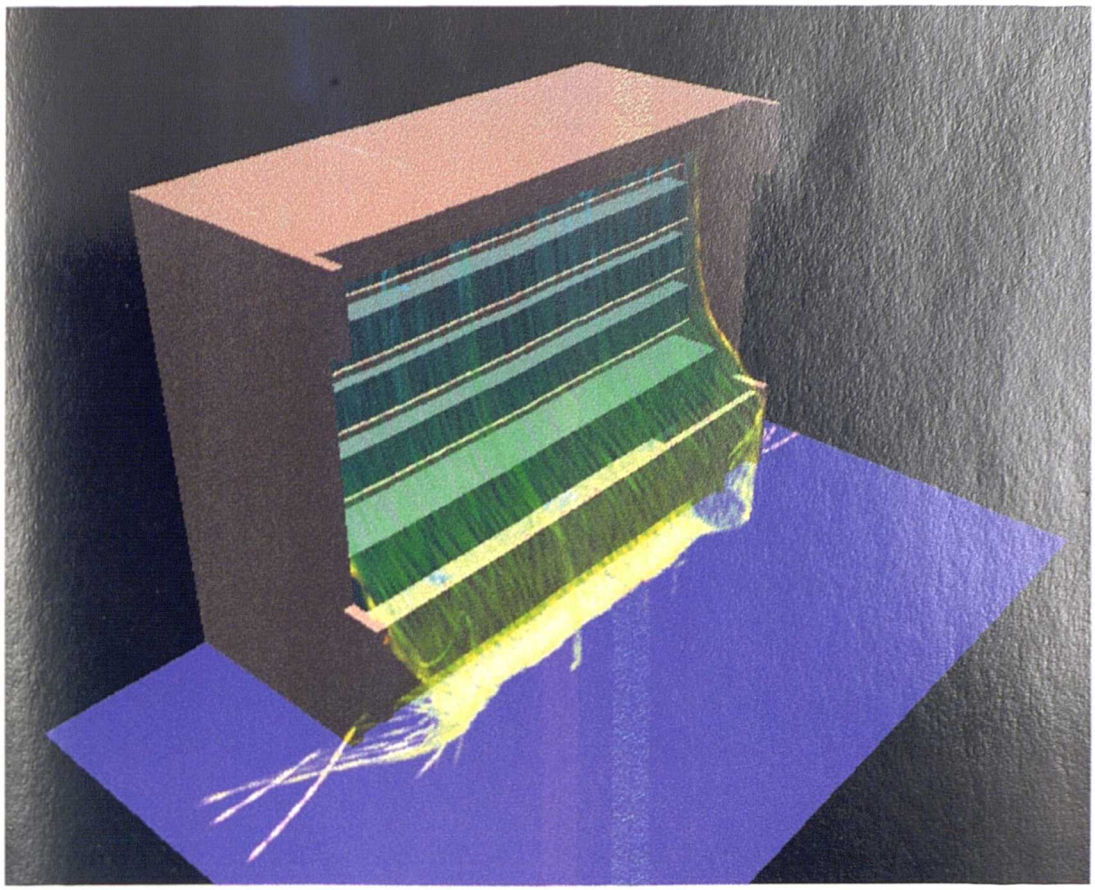

Figure 5.23 - Animation Still for 3-D Model of Baseline Case

What is not shown on the particle tracking results is that the air spilling from the case actually recirculates around, underneath the front upstand. This means that the coldest region near the floor is retained close to the front of the case. The spreading of the overspilt air at the edges is also more clearly shown.

The test standard for refrigerated display cases summarised in Chapter 3 specifies that there should be a uniform flow of ambient air across the front of the case with a velocity of 0.2 m/s. In order to ensure that CFD modelling of the case in two dimensions was valid for these conditions, a three dimensional model was constructed with such a cross flow. The temperature contours near the floor and the particle tracks from the air curtain outlet are shown in figure 5.24.

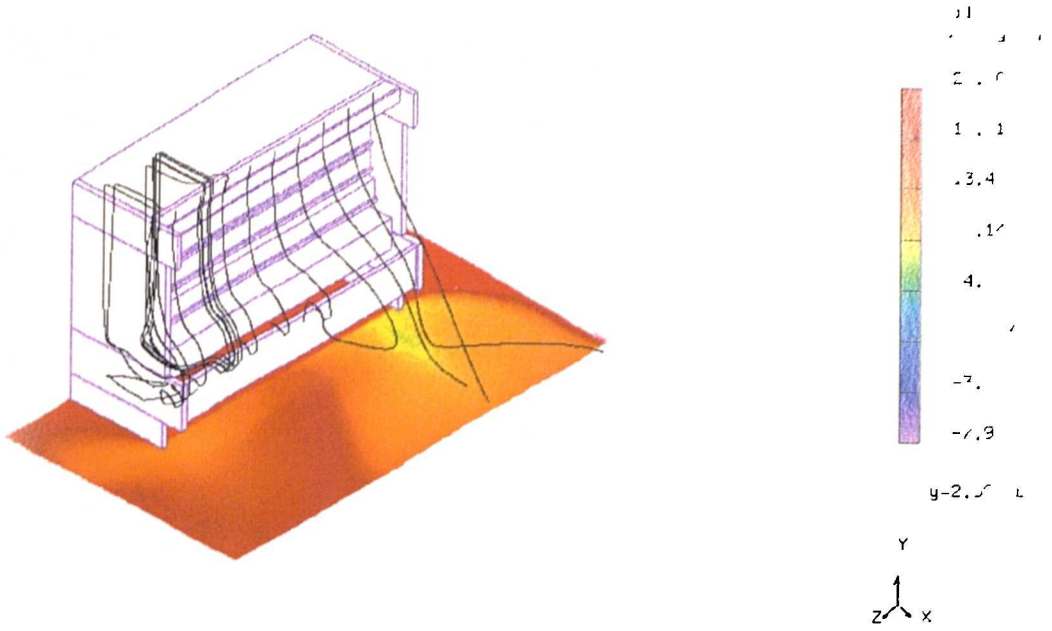

Figure 5.24 - Results of 3D Baseline Case with Cross Flow of 0.2 m/s

It is immediately possible to see that the uniformity of the air overspill has been destroyed by the addition of ambient air flowing across the front of the case from right to left. The results tend to suggest that the crossflow recirculates around the edge of the case. This recirculation forces the air issued from the air curtain upwards increasing the amount of overspill. This results in cold air reaching the floor further away from the case compared to the situation without crossflow. The animation still of this model is shown in figure 5.25 and provides a clearer picture as to the fluid dynamics of the case.

In this animation as well as the particles emanating at the air curtain outlet, a source was also provided at the right side of the domain where the cross flow was supplied from. The particles are coloured according to their temperature and the cross flow is shown up in red as being warmer ambient air.

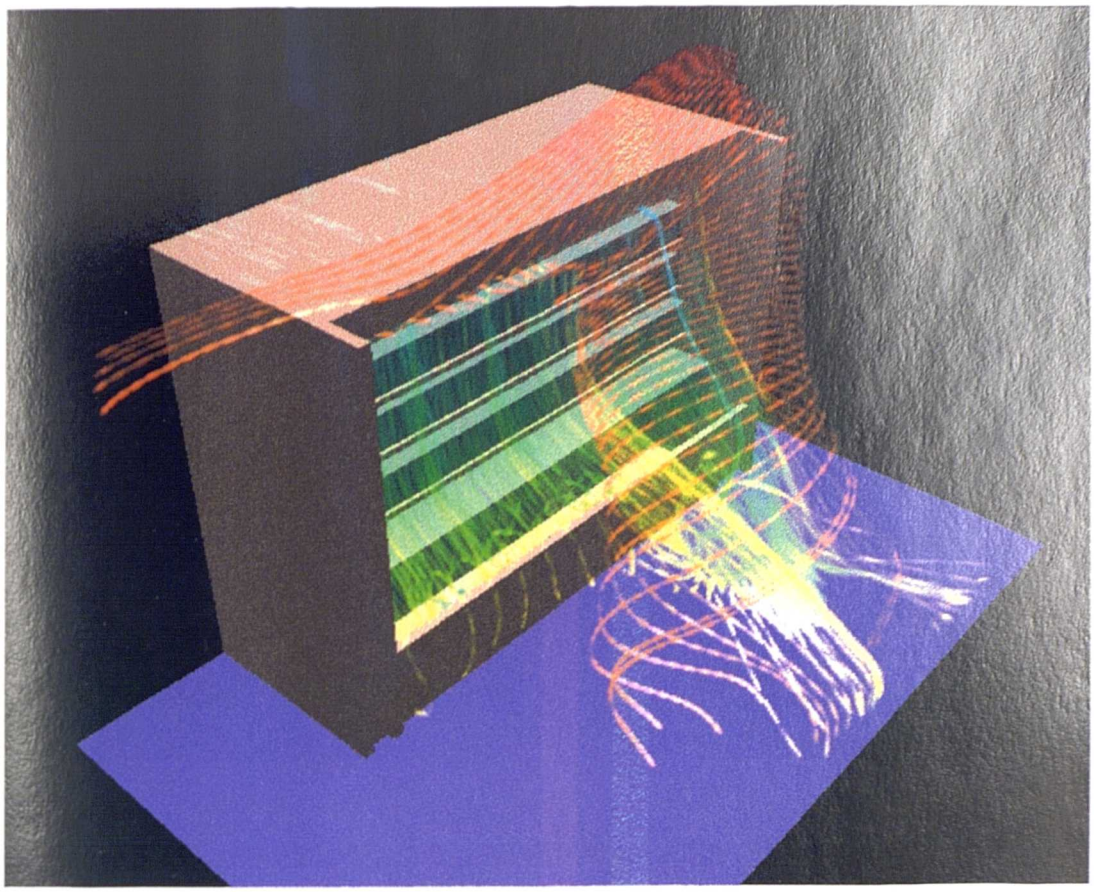

Figure 5.25 - Animation Still for Baseline Case with Cross Flow of 0.2 m/s

Figure 5.25 shows that what is in fact happening is that the ambient air flowing across the room hits the right hand end of the display case. The air then flows around the case creating a recirculation region and hence an area of low pressure. This in effect, "sucks" the air curtain away from the shelves. As the cross flow circulates around, it then passes underneath the overspilt air which pulls this away from the case. The entrainment of the ambient air at the top of the case can also be clearly seen. The low pressure region created by the cross flow recirculation is shown on figure 5.26 together with velocity vectors showing the air flow pattern. This data is taken on a plane 1 metre above the floor.

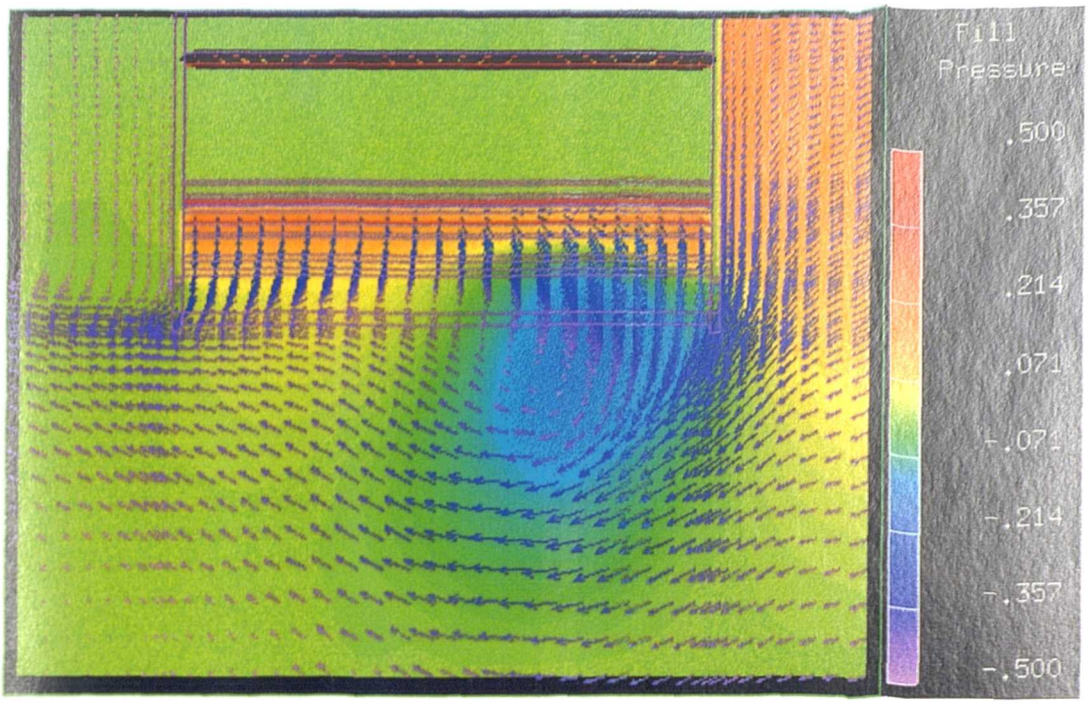

Figure 5.26 - Plan View of 3-D Model Showing Pressure and Velocity Vectors

In comparing the sensible heat transfer rate for the cases with and without the cross flow, it was found that the cross flow contributed an additional 27% on to the sensible case heat load. This is a significant effect by what is a relatively small external influence and must therefore be taken into account when locating cases near draughts caused by loading bays or doors. The effect on the air flow pattern however, remains localised close to the end of the case from which the cross flow originates. This means that the pattern of air flow within the case remains unaffected for a large proportion of its length. In a practical sense, display cases within a store normally form a line-up which may be anything up to 20 metres in length. Assuming that a draught was parallel to the front of the cases, the above results suggest that perhaps only the first metre of the line-up would be affected by a cross flow. Influences by external flows from different directions may have different effects but the study of the case on this more global scale is beyond the scope of this research project.

The design of the case itself, however, is within the remit of this project and it seems from the above results that the shape and extent of the end wall may be an influence

on the pattern of air flow and hence on the refrigeration load of the case. Figure 5.27 shows the near floor air temperatures and particle tracking results from a modelling run where the end walls of the case have been built up. This was done in an attempt to better shield the air curtain.

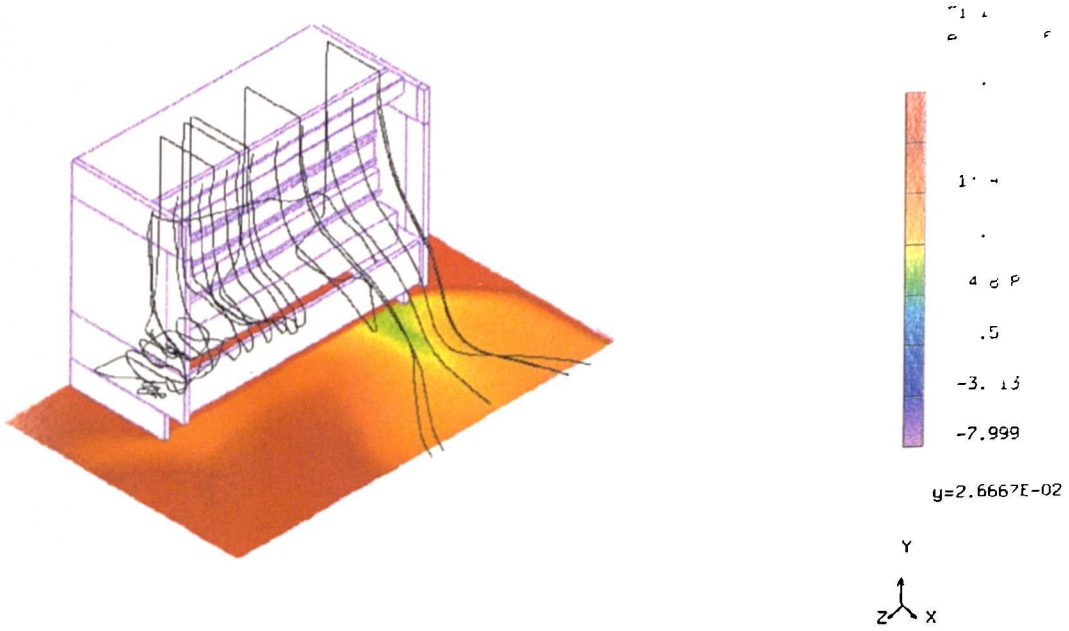

Figure 5.27 - Results of 3D Modified Case with Cross Flow of 0.2 m/s

The air flow pattern in this case is very similar to the baseline case with cross flow shown in figure 5.24. The major difference lies in the pattern of the temperature contours near to the floor. With the modified end wall, the coldest region seems to be slightly larger and closer to the front of the case. It seems, therefore, that the recirculated cross flow does not get under the overspilt air so much lifting it away from the case. This theory is better demonstrated with reference to figures 5.28 and 5.29. These show the animation still and the plan view pressure contour plot respectively.

From figures 5.28 and 5.29, it can be seen that the extended end wall means that the recirculation region created by the cross flow is moved further away from the air curtain. As the recirculated cross flow takes a wider path around the case, therefore, its influence on the path of the air curtain is somewhat reduced.

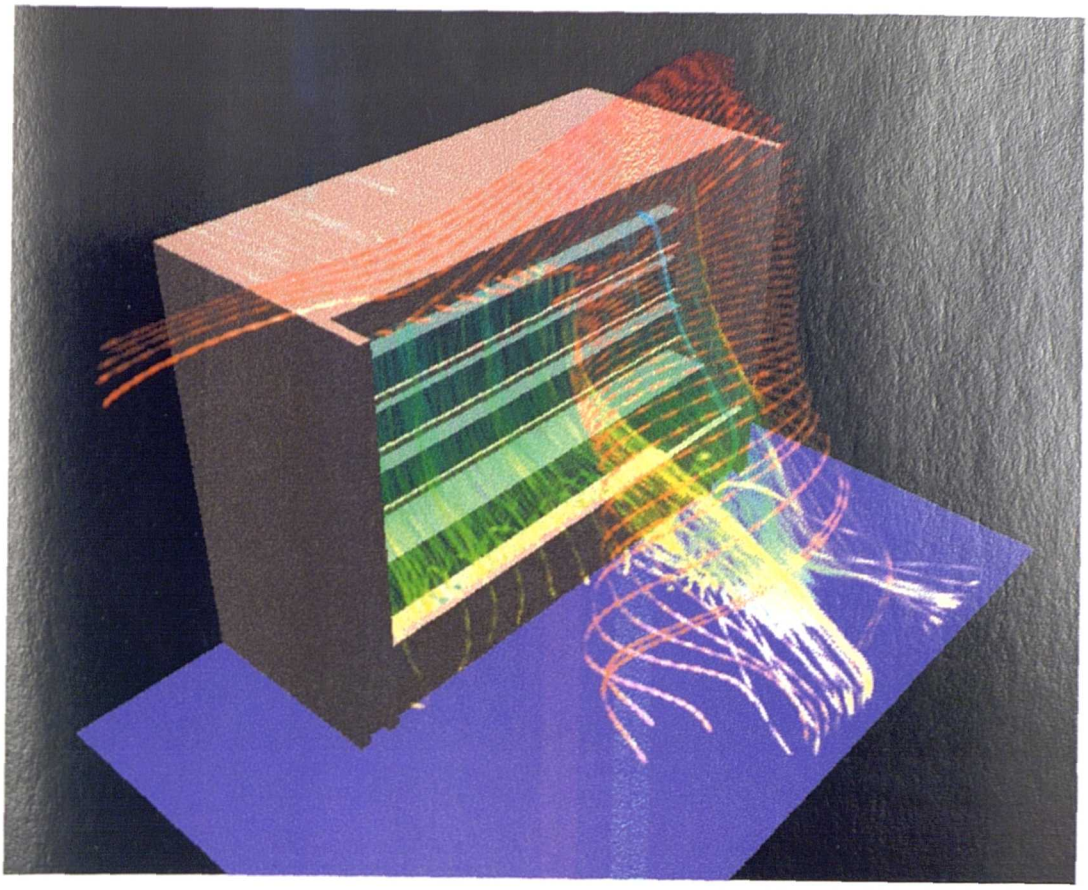

Figure 5.28 - Animation Still for Modified Case with Cross Flow of 0.2 m/s

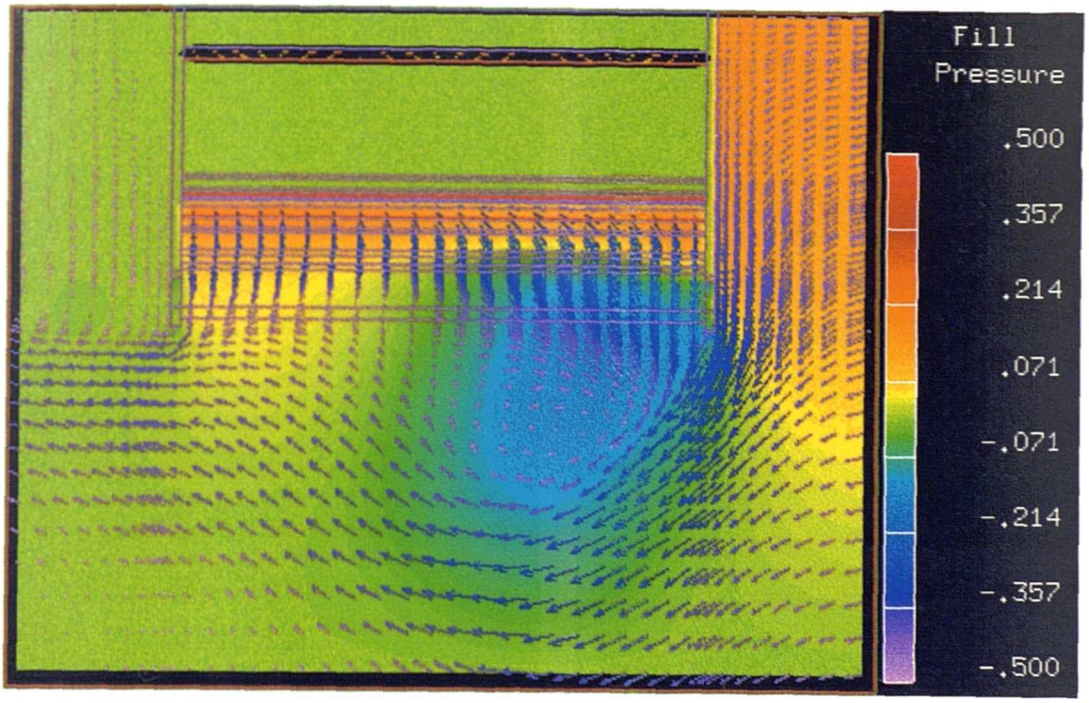

Figure 5.29 - Plan View of Modified Model Showing Pressure and Velocity Vectors

The influence of the design of the end wall can also be assessed in terms of its improvement on the case refrigeration load. Whereas the baseline case saw an increase of 27 % in the sensible load with the addition of a cross flow, the modified end wall saw a 24 % increase. Although this improvement is somewhat conservative, it demonstrates the effect that a relatively minor change can have on the performance of the display case. In reality, with line-ups of refrigerated display commonly exceeding 20 metres, the effect that the end wall has on the refrigeration load is small. This justifies the use of a two dimensional CFD model for simple parametric testing of design features.

5.9 - ASSESSMENT OF CFD MODEL

This chapter has shown the results of modelling a baseline refrigerated display case with good qualitative accuracy. With numerical modelling of any process, it must be remembered that many assumptions and simplifications are usually necessary in order to reduce the problem to one which is solvable. As a consequence, some errors must creep into the solution. Therefore, the most likely attainable goal is to model the problem to a certain degree of accuracy with consideration of the maximum acceptable error. In modelling the refrigerated display case, there is some error in the solution and this has been discussed in the preceeding sections. It is, however, considered that the discrepancies in the results are within an acceptable band of error.

It is interesting to note that numerically the CFD model falls down somewhat on the inside of the air curtain in the prediction of both velocities and temperatures. This was thought to be due to the simplifications and assumption made for the representation of the product on the shelves. As has already been explained, the main area of importance is where the turbulent mixing occurs on the outside of the air curtain. In predicting the flow and the temperature field in this region the CFD model has been shown to be successful.

Because the CFD model is to be mainly used for comparative purposes between different designs, its ultimate accuracy against the performance of an actual display

case, although important, is of limited significance. The case which has been described in this chapter therefore meets these criteria very well.

CHAPTER 6

INVESTIGATION INTO CASE MODIFICATIONS

6.1 - INTRODUCTION

In Chapter 5 a validation of the base line CFD model was carried out with comparisons of velocity and temperature profiles as well as cooling load predictions against experimental measurements. Although the results of this validation were successful in a qualitative sense, numerically there was some error between the model and the performance of the actual refrigerated display case. However, for the purposes of the current research project, it was intended that CFD techniques be used as a design tool comparing the performance of possible new designs against a baseline model. In this sense the ultimate numerical accuracy of the model, although important, is not of paramount significance.

One of the overall objectives of this research project is to assess the applicability of the use of CFD tools in the design process for refrigerated cases. To this end, tests were carried out on certain design modifications in the environmental test chamber. The purpose of these experiments was to quantify the energy savings associated with changing certain parameters and to compare these results with the predictions from the CFD model. To actually build prototypes of the case at each stage would have somewhat defeated the objective stated above. For this reason, physical testing was only carried out on modifications which could be easily implemented. For example, changing the mass flow rate of air around the case would have involved changing the fans and adding variable speed controllers. On the other hand, the removal of the honeycomb and blocking the air curtain were changes to the design which were made relatively easily.

It is, the aim of this chapter to present the results of a number of CFD modelling runs which have been carried out in order to investigate the effect of various design features.

I urther to the presentation of the CFD results, the chapter provides experimental results for a selection of the proposed modifications. The purpose of this is to demonstrate the alidity of CFD modelling in the design process.

In the following sections, the results are presented from a variety of modificatio . Considerations such as the air flow rate and temperature, number and type of air cu tai s etc. were analysed using the CFD model and experimental results in order to assess not only the energy requirements on the case but also its ability to maintain product temperatures.

The investigation is divided into two parts. Sections 6.2 to 6.8 assess parameters which are of importance in the currently accepted design of a vertical multideck display case and design modifications which have been made to this in the past.

6.2 - CASE AIR FLOW RATE

The air flow rate around the case is of critical importance, not only in terms of energy efficiency but also in maintaining product temperatures. The mass flow rate of air is far from being constant and is actually dependent on time. This is due to the fact that the propeller fans which are fitted to many contemporary designs of case are inherently inefficient against any kind of external pressure drop. Even a small amount of frost build up on the evaporator over a period of one or two hours can increase the pressure drop across the coil to such an extent that the air flow rate is affected. This can be detrimental to the performance of the case. Therefore, a refrigerated case can be designed for optimum performance at a particular air flow rate but must also then be checked against a worst case scenario simulating the pressure drop across a frosted coil. Improvements in this regard are possible with the use of axial flow fans or centrifugal fans which would even out the air flow across the upstream face of the evaporator. Such modifications are

beyond the scope of the present work but are beginning to be incorporated into case designs by the manufacturers.

Eleven runs of the CFD model were made using the baseline case geometry and varying the mass flow rate of air for the case between 0.0568 kg/s and 0.4544 kg/s. This was done by changing the inlet velocity boundary condition at the base of the back panel between 0.5 and 4.0 m/s. This enabled a performance map of the case to be drawn and this is shown in figure 6.1. The purpose of the performance map is to summarise in one diagram, the performance characteristics of a particular design of case for a series of mass flow rates. It has been chosen to summarise the performance of each case in terms of the sensible heat transfer into the calculation domain as described in section 5.6.

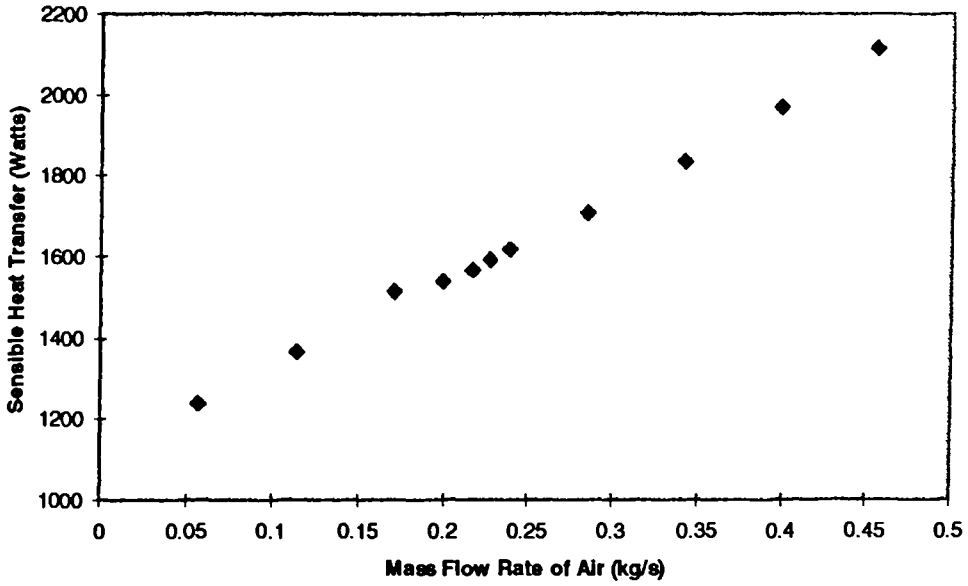

Figure 6.1 - Air Flow Rate Performance Map of Baseline Case

The performance map in figure 6.1 clearly shows that there is a linear relationship between the mass flow rate of air and the refrigeration load on the case, i.e. the higher mass flow rate of air, the higher the net heat transfer into the domain.

This is because the velocity of the air curtain governs to some extent the turbulence intensity of the air curtain and hence the amount of turbulent mixing which occurs between it and the outside air. Several runs were carried out around the mass flow rate for the actual case (0.2386 kg/s) to increase the resolution of the graph in this region. The performance map shows a fairly linear relationship between the flow rate and the refrigeration load so the question must therefore be posed; could the mass flow rate be reduced in order to save on energy?

Of course, to look at the sensible heat load without consideration of other factors would be somewhat naive. The underlying measure of the effectiveness of a refrigerated display fixture is whether or not it can maintain product temperatures. The food hygiene regulations in the United Kingdom (1995) state that chilled foods should be stored at a temperature not exceeding 8°C. Although there is no conduction calculation through the product included in the CFD model, prediction of the product temperature is possible by looking at the air temperature surrounding the product. Analysis of the modelling results showed that the highest air temperatures in the vicinity of the product occurred at the front of the shelf. Figure 6.2 shows a graph of air temperatures adjacent to the front of the product on each shelf plotted against the total mass flow rate for the case. In actual fact, in each of the modelling runs, the temperatures along the front of each shelf varied by up to 2°C. Where this was the case, the temperature shown on the graph is the maximum temperature which occurs, this giving an indication of a worst case scenario.

Figure 6.2 shows that at the lowest flow rate of 0.0568 kg/s the only product to be in accordance with the U.K. regulations is the product in the base of the display case beneath the bottom shelf. This can be explained by looking at the velocity vector plot shown in figure 6.3 with the vectors colour coded by temperature. In this case the momentum of the air is insufficient to reach the top of the back panel and therefore no air curtain is formed. In actual fact, the majority of the cold air exits the perforated back panel below the bottom shelf cooling only that product in the base well of the case.

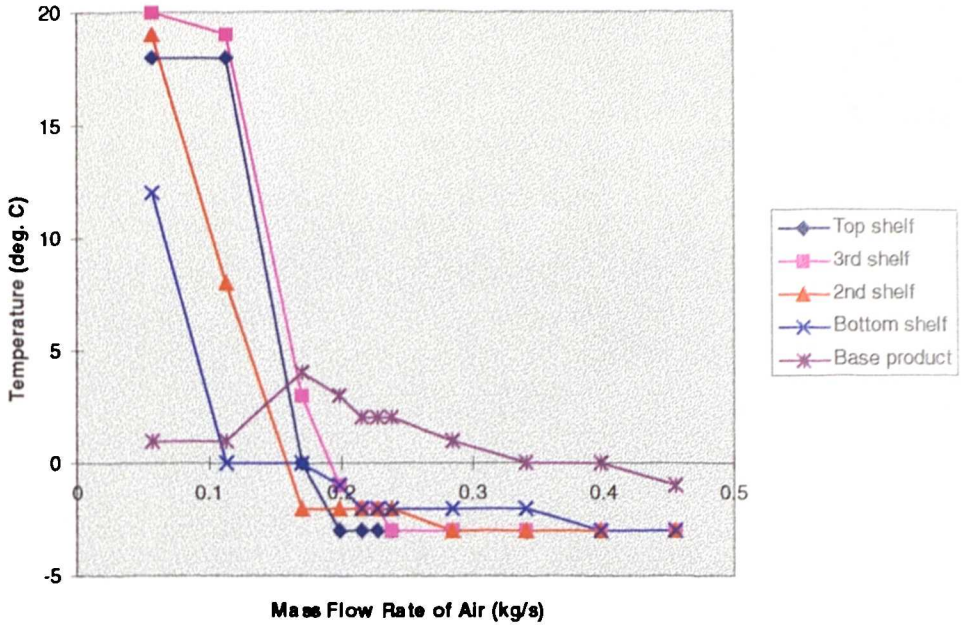

Figure 6.2 - Graph of Front of Shelf Temperatures against Air Flow Rate

The next run used a flow rate of 0.1136 kg/s with only a slight improvement on the temperatures near to the front of the product. Figure 6.4 shows the velocity vector plot for this case. Now the air has reached further up the back panel and air is being expelled over the product on the bottom shelf bringing the air temperature at the front of the product down to within regulation limits.

At a mass flow rate of 0.1704 kg/s, the momentum of the air is finally sufficient to reach the canopy of the display case as shown in figure 6.5. There is, however, too little air reaching the canopy to form an effective air curtain and most of the product protection is gained from air expelled from the back panel over the product. It then spills down over the front of the product forming a sort of air curtain. This pattern of air flow seems to be capable of maintaining temperatures within acceptable limits even before a primary air curtain has been discharged from the canopy of the case.

It is interesting to note that whereas the temperatures at the front of each shelf fall when the air flow rate is increased to 0.1704 kg/s, the temperature at the front of the product in the base well actually rises. Close examination of the velocity vector plots suggest that this is because, in the previous two models, the air has flowed from the back panel gently over the product in the base well with little disturbance. In figure 6.5 where air spills down the front of the shelves, the flow pattern across the top of the product in the base is of a similar nature as for the lower flow rates. However, the air flow in this region now has to counteract the vertical air stream which is at a higher temperature having taken up heat from the surface of the product. At the bottom of the air curtain, significant mixing has also occurred resulting in a relatively warm vertical air stream which impinges on the product in the base of the case raising its temperature. As the mass flow rate is increased, the air flow rate from the back panel is also increased. The resulting increase in momentum from the rear of the case pushes the air curtain further away from the shelves and the product. The increase in momentum of the air curtain is also increased resulting in less mixing at the bottom and a cooler air curtain. The effects of the vertical and horizontal air streams combine and hence reduce the temperature of the product in the base of the case.

Figure 6.6 shows a similar plot, this time for a mass flow rate of 0.2386 kg/s, the actual design flow rate for the case under test in the laboratory. In this case, a fully developed air curtain is projected downwards from the canopy of the case. However, the front of shelf temperatures are only a marginal improvement over those with the lower mass flow rates shown previously and in actual fact a case with a lower flow rate has been shown to be capable of maintaining product temperatures in ideal conditions.

Experiments were carried out in the laboratory to measure product temperatures using thermocouples inserted into three of the product packages on each of the shelves with an air mass flow rate of 0.2386 kg/s. the average temperatures measured over a half hour period are shown in Table 6.1.

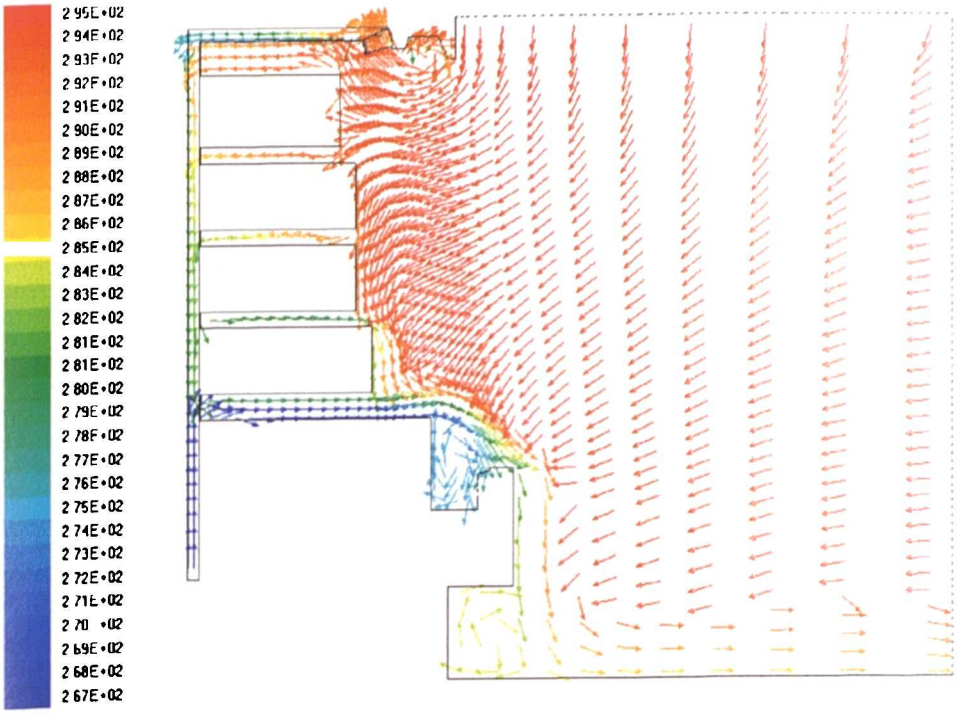

Figure 6.3 - Velocity Vector Plot for Case (Mass Flow = 0.0568 kg/s)

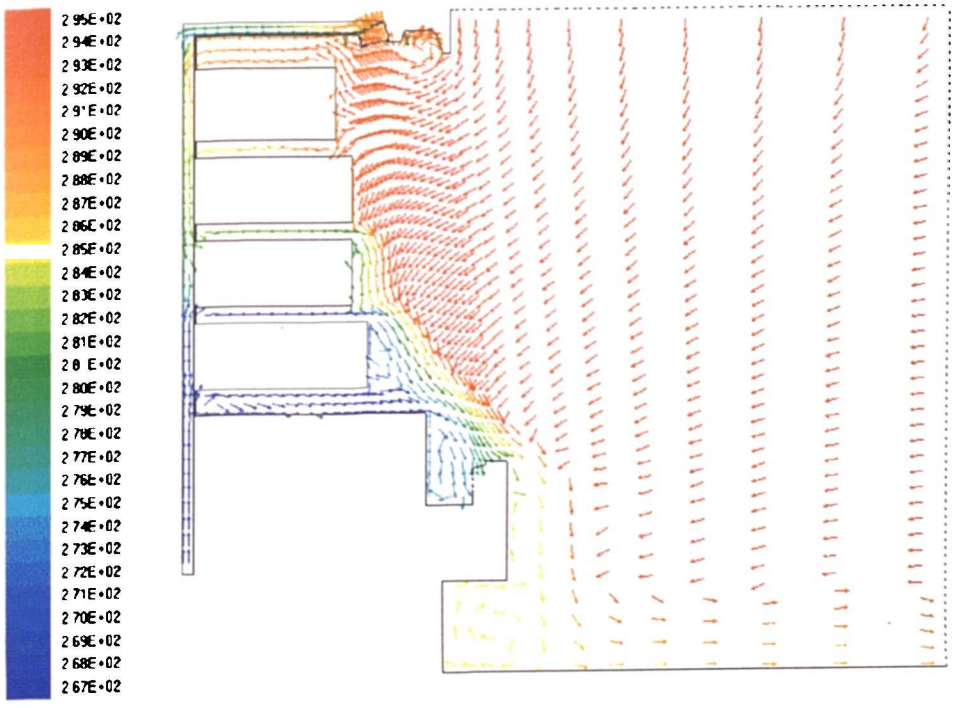

Figure 6.4 - Velocity Vector Plot for Case (Mass Flow = 0.1136 kg/s)

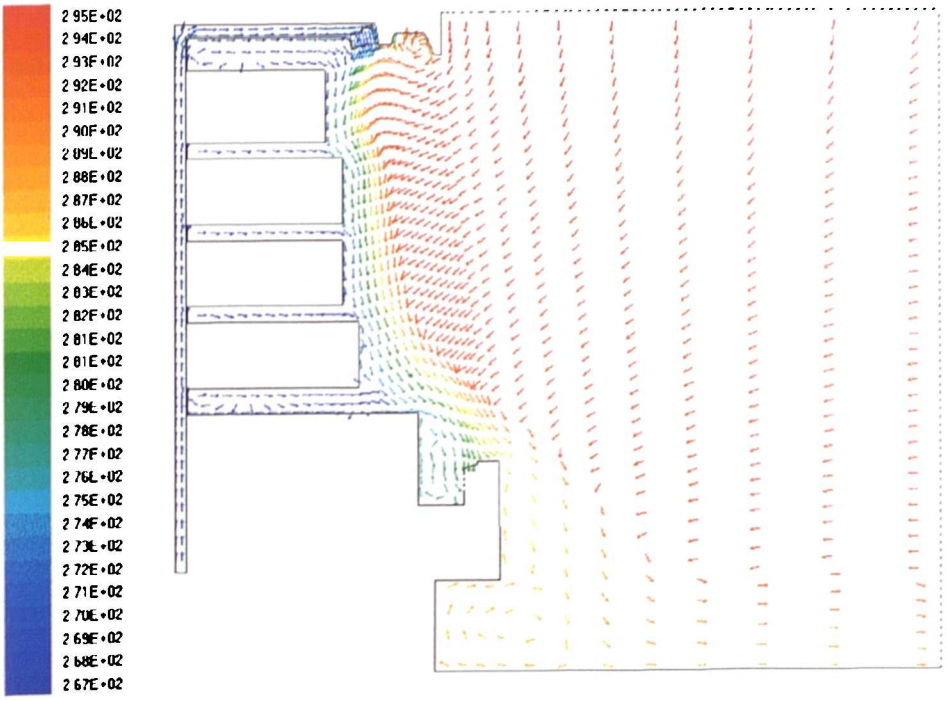

Figure 6.5 - Velocity Vector Plot for Case (Mass Flow = 0.1704 kg/s)

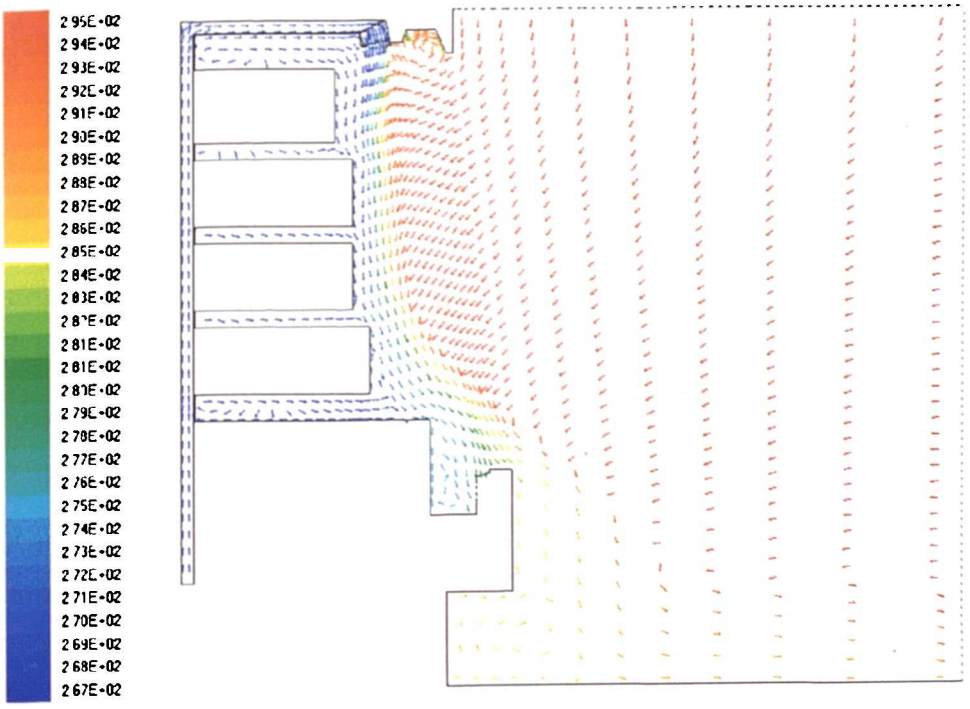

Figure 6.6 - Velocity Vector Plot for Case (Mass Flow = 0.2386 kg/s)

Table 6.1 - Product Temperatures Measured for Baseline Case (°C)			
	Left	Centre	Right
Top Shelf	-0.67	2.54	-2.66
Third Shelf	0.62	-0.87	1.82
Second Shelf	0.18	-1.16	1.81
Bottom Shelf	0.55	-0.35	1.92

Table 6.1 shows that for a mass flow rate of 0.2386 kg/s, the measured product temperatures are well within the limits set down in the U.K. food hygiene regulations. The temperatures measured are generally 2 to 3°C higher than the air temperatures predicted adjacent to the front of the product by the CFD simulation. This difference may be due to the radiation effects from the surroundings into the case and the thermal resistance between the air and the product. Indications are, therefore, that a mass flow rate of 0.1704 kg/s is sufficient to maintain product temperatures in ideal conditions whilst representing savings in the case sensible refrigeration load of 6% and similar savings in the latent load. To accept this as the design air flow rate for the case without further testing would be a bad design decision, however as an allowance must be made for the effect of frost on the evaporator. Because of the nature of the fans generally used in display cases, frost formation on the surface of the evaporator can seriously affect the mass flow rate of air around the display case. The minimum allowable air flow rate as stated above must therefore be at the condition of an evaporator immediately prior to a defrost. This means that the design air flow rate for the case will be higher than this minimum.

Another consideration is the effect that air flows external to the case may have on the air flow pattern in the case as illustrated in the three dimensional model in Chapter 5. These relatively small disturbances are less likely to affect product temperatures when the mass

flow rate of air around the case is high and this must therefore be considered when designing the display case.

Radiation to the product from the surroundings is another element worthy of consideration. This may be counteracted by increasing the convective cooling from the surface of the product by increasing the mass flow rate of air passing across it. If this flow rate were to be reduced, the product temperatures could rise from the effect of radiation.

Although all of these factors must be accounted for when designing a refrigerated display case, the above analysis does provide a tool for assessing the consequences of designing a case for a particular mass flow rate. It does this, not only in terms of the energy requirements of the case but also in terms of the ability of the case to maintain product temperatures.

From the above analysis it can be concluded that:

- There is a linear relationship between the mass flow rate of air around a multideck refrigerated display case and the refrigeration load of the case.
- Potential exists for reducing the mass flow rate of air and thus the refrigeration load for the display case whilst still maintaining product temperatures.
- Any modification, such as a reduction in air flow, must be tested either experimentally or computationally to examine the effects of the specific external conditions expected in a particular physical location on product temperatures.

6.3 - EVAPORATOR TEMPERATURE

The evaporator temperature and hence the off-coil temperature are directly related to the case temperature. For this reason, they are generally selected according to the type of product to be displayed in the case. For the dairy case under investigation, the

evaporator was designed for a temperature of -8°C giving an off coil temperature of approximately -6°C. This was applied to the CFD model by setting the inlet temperature at the base of the back panel equal to the off-coil temperature.

Several runs of the CFD model were carried out for different flow rates and figure 6.7 shows a performance map of the baseline display case compared to the same case with an off coil temperature of -10°C.

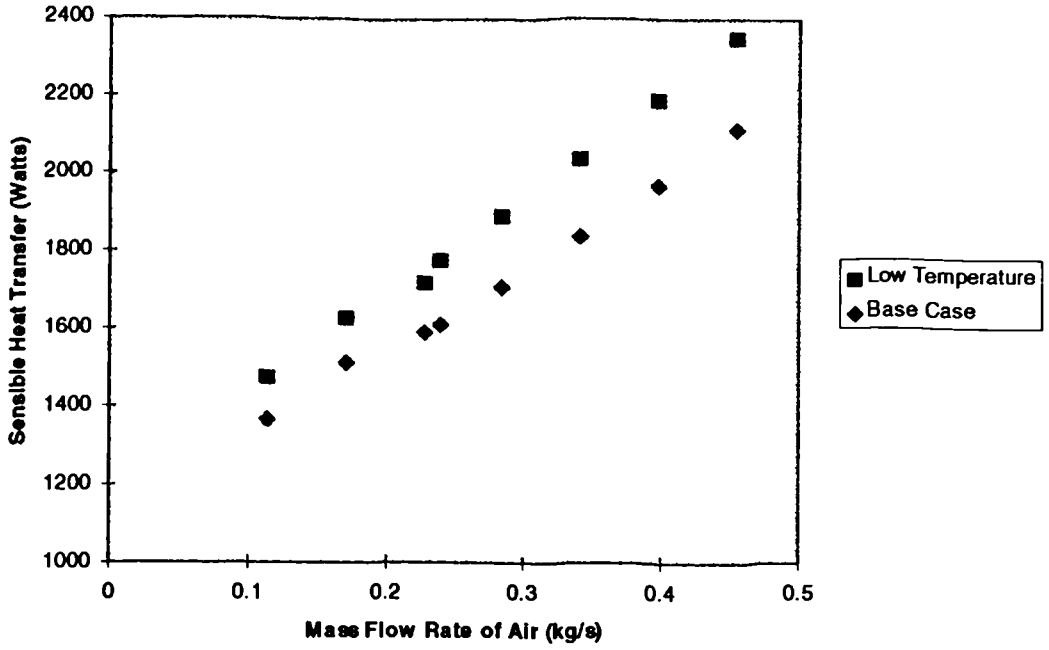

Figure 6.7 - Performance Map of Case with Lower Off-Coil Temperature (-10°C)

It is clear from the graph that lowering the evaporator temperature has a detrimental effect on the energy efficiency of the case in terms of the sensible heat transfer into the domain. In addition to this, the C.O.P. of the refrigeration cycle will also be affected in such a way that compressors will draw more power to achieve the same refrigeration effect.

This may indeed be acceptable if lowering the evaporator temperature meant that the mass flow rate could also be reduced to compensate whilst still maintaining product temperatures. Figure 6.8 shows the air temperatures adjacent to the front of the shelves plotted against flow rate.

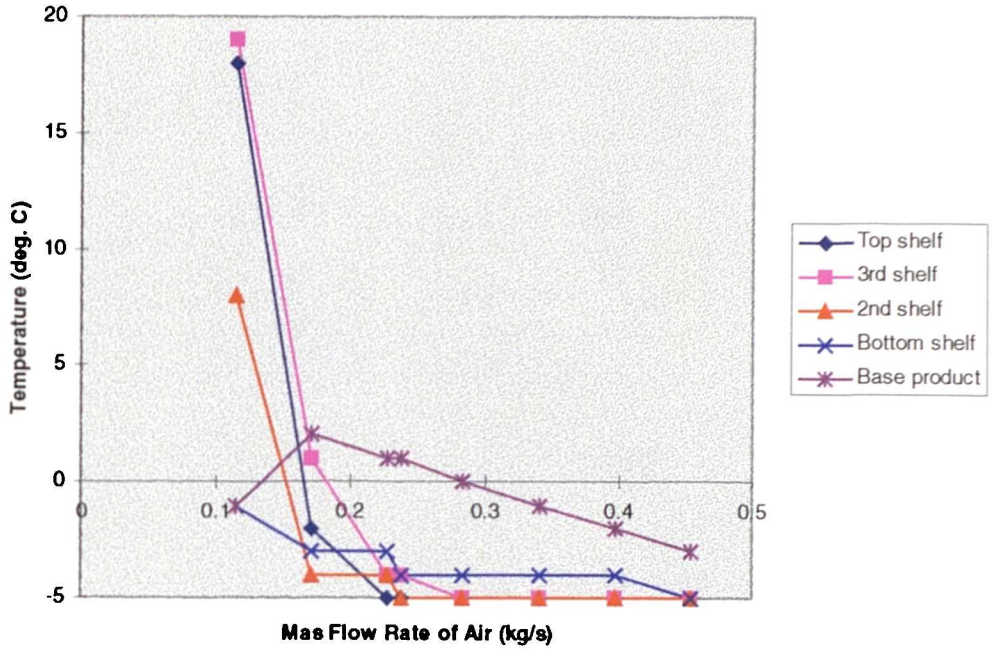

Figure 6.8 - Graph of Front of Shelf Temperatures against Air Flow Rate

It can be seen that the graph of product temperatures follows a similar pattern to that for the base line case design. The main difference is that once a full air curtain has been achieved at about 0.2 kg/s, the ultimate temperatures attainable are slightly lower. Indeed, for temperatures to fall within the food hygiene regulations, a mass flow rate of 0.1708 kg/s must be circulated, the same as for the baseline case. This means that although it may be possible to reduce the mass flow rate for a case with a lower evaporator temperature, the advantage gained by this is not enough to offset the loss in case efficiency.

For comparison with the base line solution (figure 6.6), a velocity vector plot for the case with the lower evaporator temperature is shown in figure 6.9. There is little

difference between the two vector plots. The data suggests that case temperatures are lower when the evaporator temperature is also lower. However, this seems unnecessary when a product temperature of only 8°C is required to be maintained by the food safety regulations.

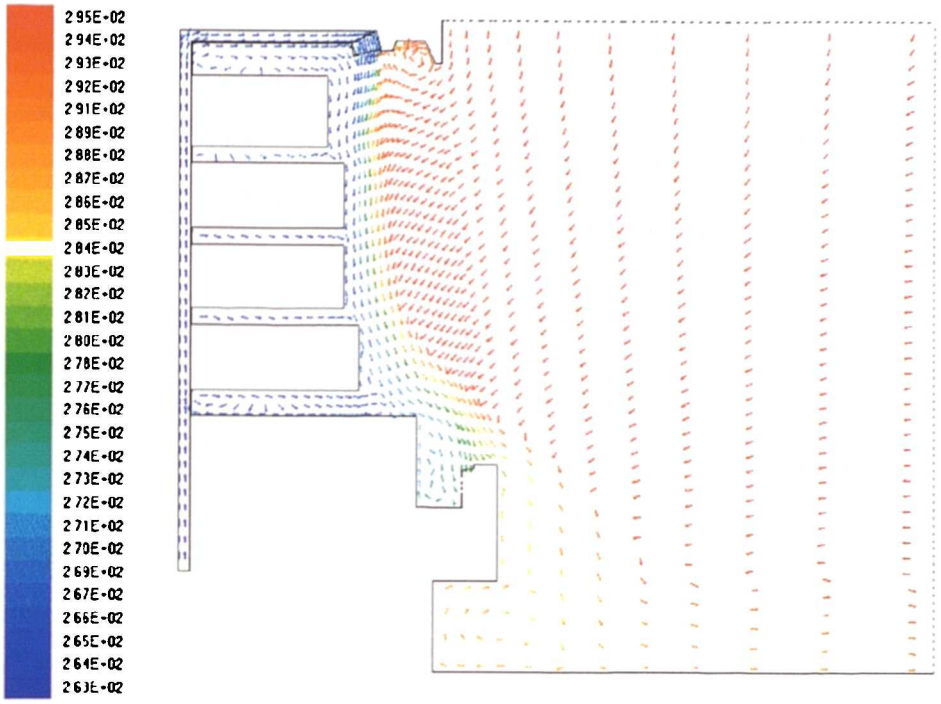

Figure 6.9 - Velocity Vector Plot for Case (Mass Flow = 0.2386 kg/s)

From the above analysis it may be concluded that:

- The evaporator should be selected on the highest possible refrigerant temperature to maintain safe food temperatures. This is both to maximise the C.O.P. of the refrigeration cycle whilst minimising, at the same time, the refrigeration load which it serves.

6.4 - IMPORTANCE OF THE HONEYCOMB

The honeycomb section located in the air curtain outlet is a design feature which has become commonplace on most contemporary designs of display case. In recent years,

however, with increasing awareness of the importance of food hygiene, concerns have heightened about the cleanliness of honeycombs and some case manufacturers now choose not to employ them on their designs. Their intricate shape and the difficulty in removing them for cleaning means that they are an ideal haven for bacteria. So does the honeycomb really improve the performance of the display case?

Figure 6.10 shows the results of eight CFD runs for different mass flow rates of air in order to compare the baseline case to one where the honeycomb had been removed. It is clear from these results that the honeycomb has little effect at lower mass flow rates with its benefits becoming more apparent as the mass flow rate increases. The reason for this is that, as with the base line case design, there is insufficient air flow at the lower mass flow rates for an air curtain to be formed. Although cold air reaches the canopy at a mass flow rate of 0.1704 kg/s, a proper air curtain is not formed until a mass flow rate of 0.2272 kg/s. It is clear that unless air is issued from the canopy there is little advantage to be gained by locating a honeycomb at the air outlet.

Once the air curtain has been formed there begins a large divergence of the performance map from that seen for the base line display case. This is because the velocity of the air curtain governs, to a large extent, the turbulence intensity of the air flow. The aim of including the honeycomb is an attempt to limit this turbulence intensity and therefore also limit the amount of turbulent mixing which occurs between the air curtain and the ambient air.

The savings achievable for the mass flow rate for the base line case (0.2386 kg/s) equates to approximately 5% and makes the inclusion of a honeycomb, a worthwhile investment. Clearly if higher mass flow rates are employed, the honeycomb becomes a necessity saving approximately 26 % on the sensible refrigeration load for a flow rate of 0.4544 kg/s.

The reason for these savings can be demonstrated by reference to figures 6.11 and 6.12. These show a comparison of the turbulent kinetic energy contours and velocity vector plots for the air curtain with and without a honeycomb at a case mass flow rate of 0.2386 kg/s.

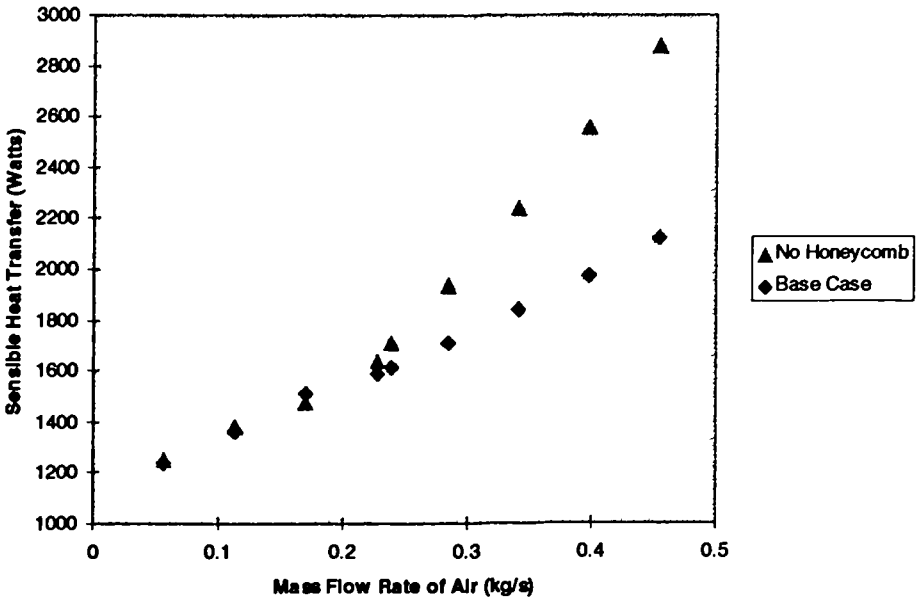

Figure 6.10 - Air Flow Rate Performance Map of Case Without Honeycomb

Figure 6.11 clearly shows that with the omission of the honeycomb, the initial turbulence intensity of the air curtain is higher than when a honeycomb is included. Howell et al. (1976) showed that the heat transfer through a vertical plane jet was largely governed by the initial turbulence intensity of the jet since this had an important effect on how the flow developed further downstream. The results from the present research seem to support this theory with a higher initial turbulence intensity resulting in higher heat transfer.

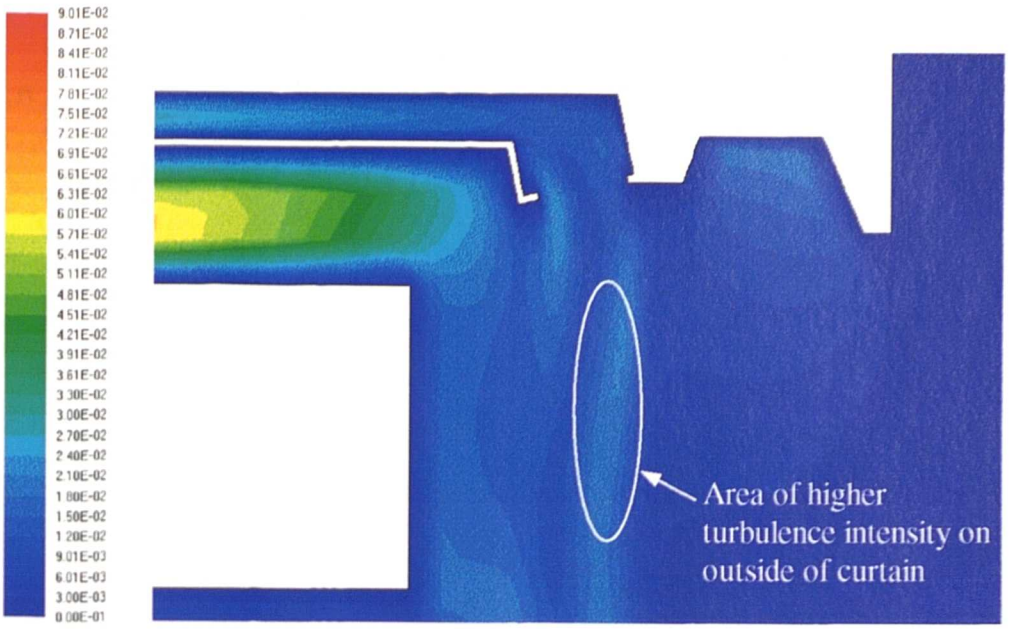

Case without Honeycomb

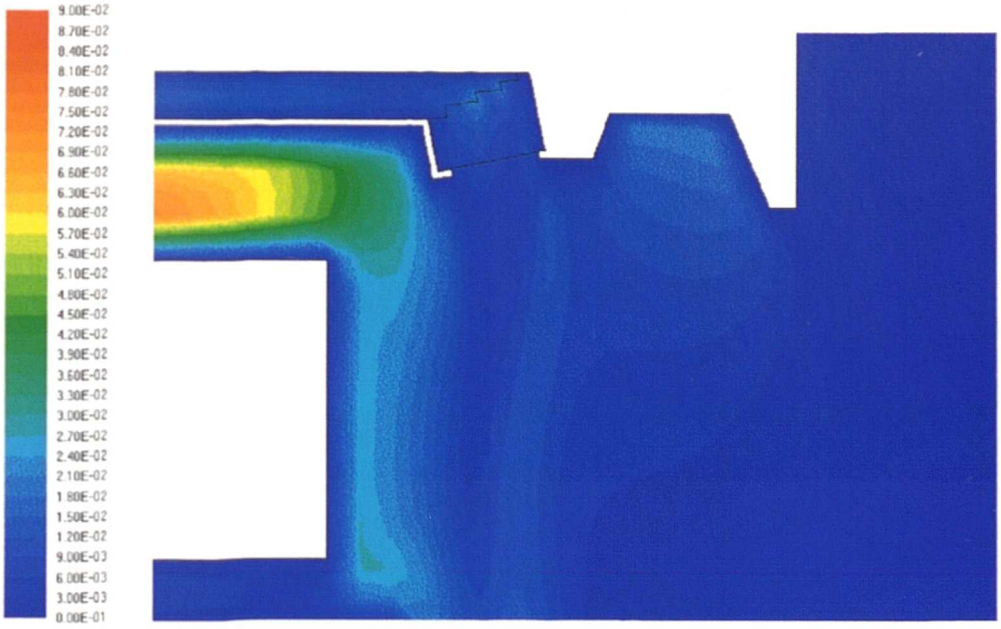

Case with Honeycomb

Figure 6.11 - Comparison of Air Curtain Turbulence Intensities

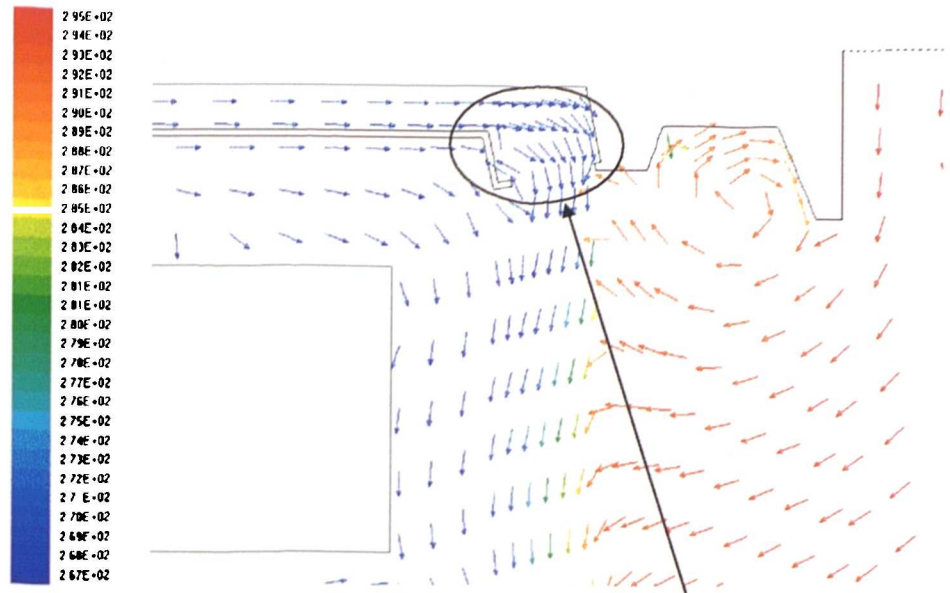

Case without Honeycomb

Area of Difference
in Flow Pattern

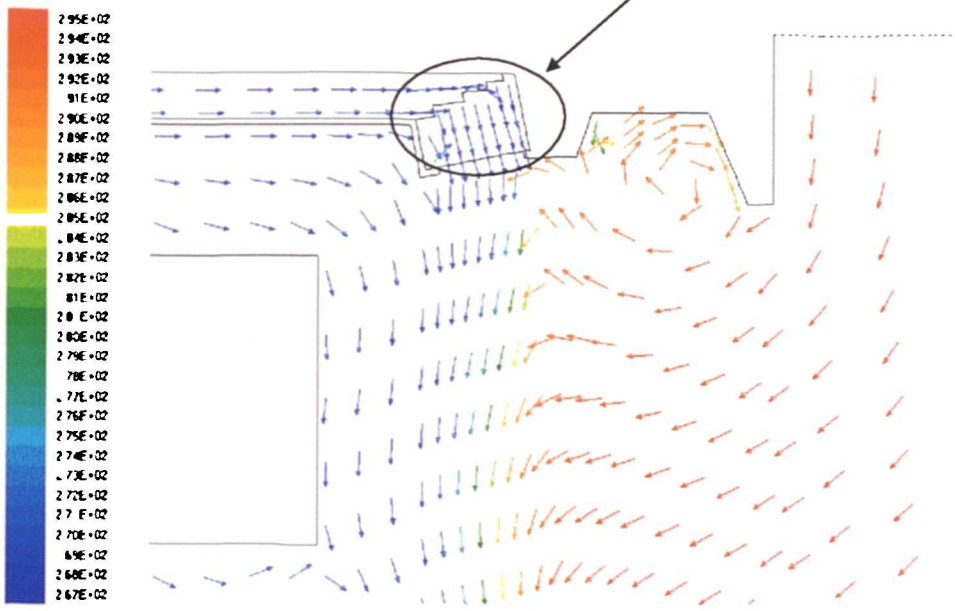

Case With Honeycomb

Figure 6.12 - Comparison of Velocity Vector Plots

The reason behind the reduction in turbulence intensity lies in the straightening characteristics of the honeycomb. The velocity vector plots shown in figure 6.12 reveal that when there is no honeycomb, the horizontal air flow through the canopy impinges on the front of the air curtain outlet. The abruptness of this transition from a horizontal to a near vertical path results in the air curtain not leaving the outlet smoothly. When the honeycomb is included in the design, the horizontally flowing air spreads over the upstream face of the honeycomb section resulting in locally contained high frequency turbulence. The transition to the vertical path then takes place over several hole diameters, limiting vastly, the transverse velocity component by the time the air reaches the downstream side.

In order to validate the results obtained from the CFD model, the honeycomb section was removed from the case on test in the laboratory. One hour runs were carried out as described in section 5.3 with data being logged in order to calculate the total refrigeration load on the evaporator. The results are shown in table 6.2.

Table 6.2 - Total Refrigeration Load Comparison for Case without Honeycomb

	Without Honeycomb	With Honeycomb
First Hour	3606 Watts	3327 Watts
Second Hour	3612 Watts	3374 Watts
Third Hour	3662 Watts	3437 Watts
Fourth Hour	3608 Watts	3508 Watts
Average Load	**3622 Watts**	**3412 Watts**

Averaging the instantaneous refrigeration loads which were logged every ten seconds, revealed that a 6.9% saving on the total load could be expected with the inclusion of the honeycomb. A direct comparison with the CFD model is not valid as it relates to the sensible load only and predicts a 5% saving in this respect.

Although in the above analysis a direct comparison between the experimental and computational results is not possible, indications are favourable that the CFD model provides a good prediction of display case performance. A prediction not only of a saving by the inclusion of a honeycomb, but also that this prediction is of the correct order of magnitude suggest that CFD could be extremely useful as a tool in case design.

From the computational and experimental results presented in this section, the following conclusions may be drawn:

- The inclusion of a honeycomb section into the air curtain outlet does have a benefit in terms of the energy efficiency of the case.
- This benefit is, however, very much dependent on the mass flow rate of air around the display case and the use of the honeycomb as a mechanism for reducing load on the evaporator must therefore be assessed on the merits of a particular design.

6.5 - THE EFFECT OF THE FRONT UPSTAND HEIGHT

Adams (1992) demonstrated that the size of the display case opening is proportional to the refrigeration load on the evaporator. For merchandising purposes there is also a requirement to maximise the opening area thus conflicting with the need for energy efficiency. One compromise lies in the use of a glass upstand on the front of the case which provides minimum obstruction between the customer and the product whilst reducing the area of the case opening.

The upstand which is occasionally seen on fresh meat display cases of contemporary design is normally double glazed to prevent condensation on the outer surface. Positioned on the front of the case adjacent to the air return grille, the upstand creates a well where cold air can collect in the base of the case. Despite the energy advantages of such a design, the main reason for the use of upstands on fresh meat displays is the

perception given to the customer of the product being contained in a more closed and therefore safe environment. This impression also comes with the benefit of allowing the customer free access to the product with the minimum of hindrance.

Two CFD models were therefore created for two heights of front upstand and computer runs completed for eight mass flow rates for each design. The two heights considered were 200mm for the low upstand and 300mm for the high upstand. The velocity vector plots for the two cases for a mass flow rate of 0.2386 kg/s are shown in figures 6.13 and 6.14. The vectors themselves are colour coded with temperature in order that this parameter can be shown in parallel.

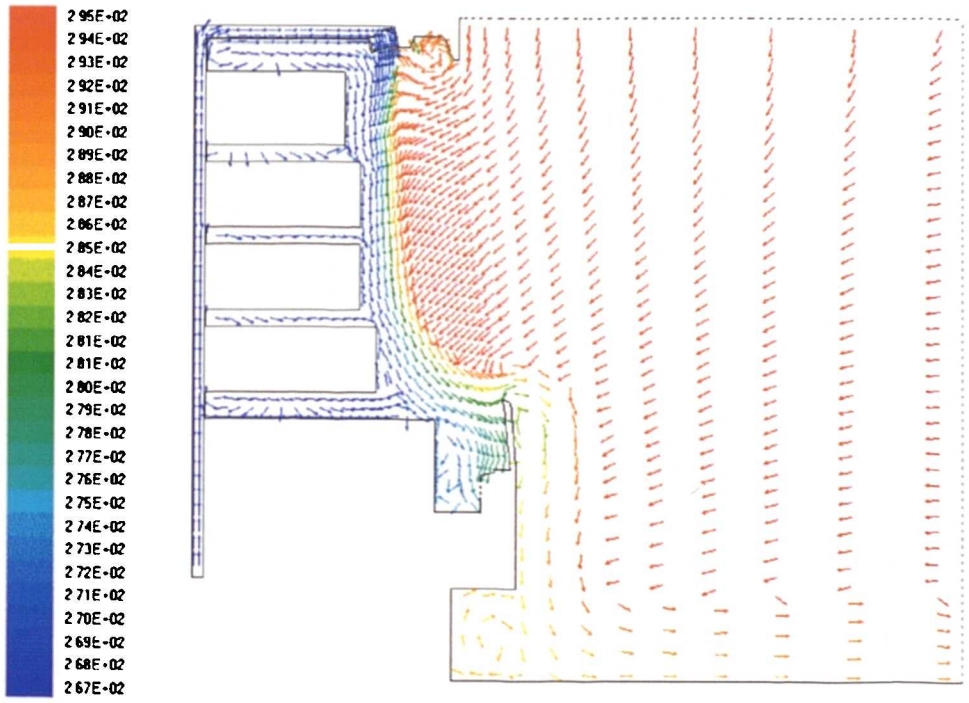

Figure 6.13 - Velocity Vector Plot for Case with 200mm Upstand

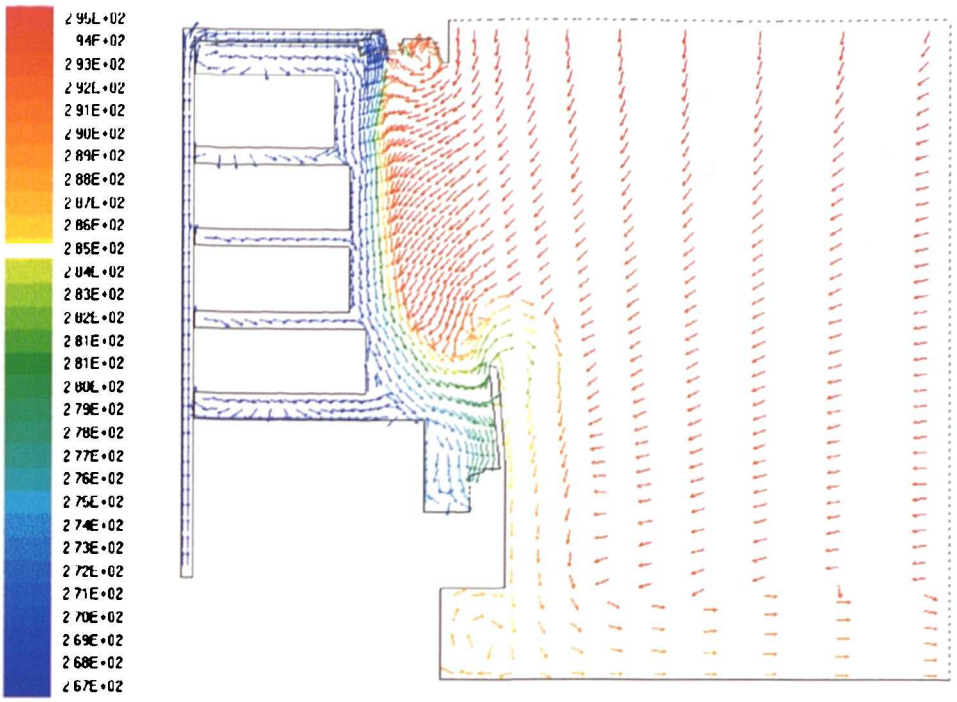

Figure 6.14 - Velocity Vector Plot for Case with 300mm Upstand

Close examination of the velocity vector plots reveals that there is very little difference between the air flow patterns seen in each of the cases. The main difference is the height at which the air spills from the case, this being governed by the height of the upstand. This, in effect reduces the length of the air curtain over which mixing can occur with the result that a higher upstand should have less sensible heat transfer across its opening. With regard to the air overspill, the perception is that by building up the front of the case higher, that this will stop overspill altogether. However, because there must be a mass balance of air across the fans, any entrainment will result in an overspill of equivalent mass. The very nature of the air curtain as a moving stream of air in a relatively still environment means that there will always be some entrainment of store air and a corresponding overspill from the front of the case.

The resulting performance maps are shown in figure 6.15. It can be seen that any upstand which is included in the display case design can be beneficial in terms of energy. Added to this is the fact that the higher the upstand the greater this energy saving can be.

Using this data, the height of such a design feature could be optimised in order that the demand for energy efficiency is balanced against the requirements of the merchandiser.

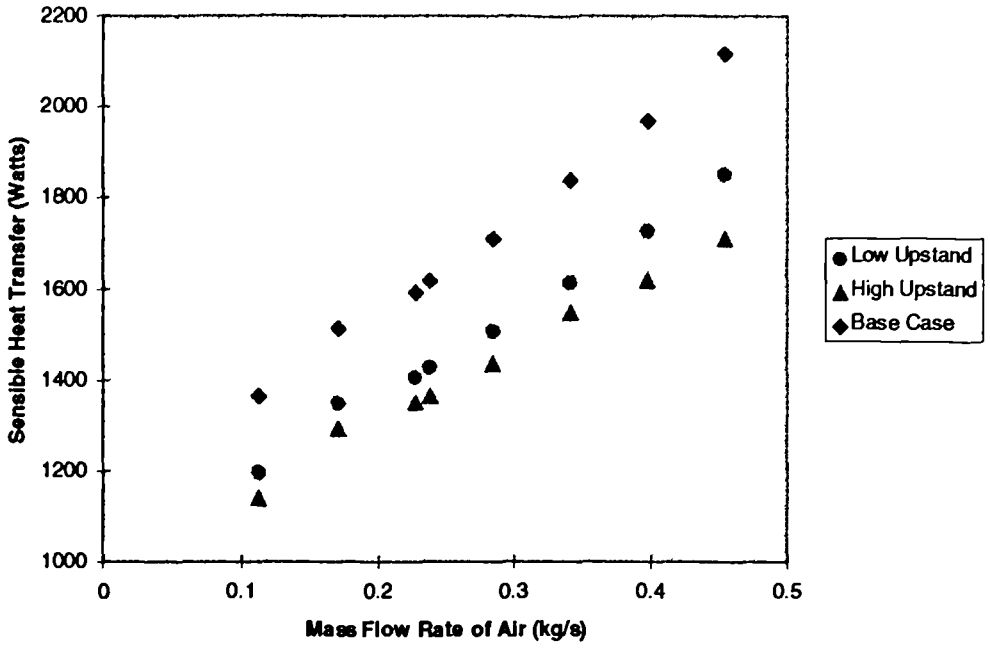

Figure 6.15 - Air Flow Rate Performance Map of Case With Front Upstand

Results from the CFD model indicate savings on the sensible refrigeration load of 11.7% for the 200mm upstand rising to 15.5% when the upstand height is increased to 300mm. These figures represent significant reductions in the energy consumption of the case and certainly should be an important consideration in case design.

In order to support these findings tests were carried out on the dairy case in the laboratory. A 225mm glazed upstand was added to the display case, the height of upstand which would normally be used in converting this make of dairy case into a fresh meat case. The results of the four one hour runs is presented in table 6.3.

Table 6.3 - Total Refrigeration Load Comparison for Case with 225mm Upstand		
	Without Upstand	With Upstand
First Hour	3327 Watts	3313 Watts
Second Hour	3374 Watts	3286 Watts
Third Hour	3437 Watts	3304 Watts
Fourth Hour	3508 Watts	3297 Watts
Average Load	**3412 Watts**	**3300 Watts**

The results of the experimental runs gave much more conservative figures for the potential energy savings which the inclusion of an upstand might provide. The saving measured for the total refrigeration load was only 3.3%, far below what was predicted by the model. Although the correlation between the two sets of results was a little disappointing the reason may lie in the simplifications made in the CFD model. In order to easily modify the CFD model, several of the live cells adjacent to the air return grille were merely changed to represent a wall. The grid construction, however, meant that the upstand was at a slight angle as shown in the velocity vector plots in figures 6.13 and 6.14. In reality, the glazed upstand used in the experiments stood vertically on the front of the case and this may or may not be a significant factor in the discrepancy between the experimental and CFD results. Therefore, although the use of an upstand has been shown to produce energy savings, more work is required into this feature in order to optimise its design.

From the analysis carried out in this section, the following conclusions may be drawn:

- The use of a front upstand on a vertical multideck display case has been shown to produce energy savings.
- The potential savings are in some way proportional to the height of the upstand.

- If the inclusion of a front upstand is to be considered, further work is required to optimise the design for the specific application in order to minimise energy consumption.

6.6 - THE EFFECT OF TWO AIR CURTAINS

The air curtain in the current case design is far from ideal. Figure 6.16 shows a comparison of velocity magnitude contour plots for the case air curtain with and without a honeycomb at the air outlet. The plot from the case without a honeycomb clearly shows that higher velocities exist at the outer edge of the air curtain outlet as the air is forced to turn through almost 90° from a horizontal path down into the trajectory required for the curtain. The addition of the honeycomb, because of pressure drop across it, tends to spread the velocity profile out but still has a greater velocity on the outer edge of the curtain.

The higher velocity on the outside of the air curtain is undesirable because it imposes a high velocity gradient in this region. High velocity gradients give rise to large shear stresses within the fluid resulting in a higher turbulence intensity and therefore more turbulent mixing.

One way of limiting the magnitude of the shear stresses occurring on the outside of the air curtain is by imposing an artificial velocity gradient on the supply air. this would have the effect of smoothing out the velocity profile of the curtain and thus restrict the amount of turbulent mixing which occurs.

The ideal air curtain would have a higher velocity on the inside to ensure good mixing on the case side and a lower velocity on the store side. It is important to remember at this juncture that if an air curtain is included at all in the case design its very nature of being a moving air stream in a relatively still environment means that entrainment of warm air

cannot be avoided. But, by limiting the degree of turbulent mixing, the heat transfer across the opening can, to some extent, be minimised. An artificially imposed velocity and temperature gradient would in effect limit the amount of shear occurring between the moving and the still air which will in turn minimise the extent of turbulent mixing. At the very least this mechanism should be capable of delaying the propagation of the fully turbulent region until further downstream.

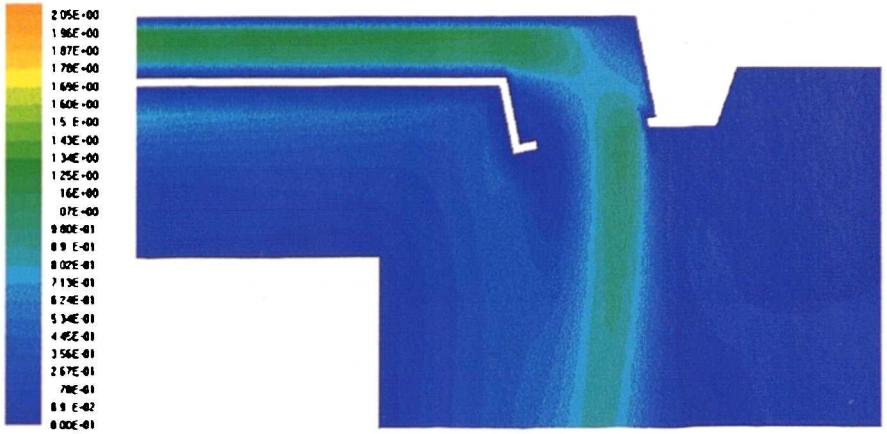

Without Honeycomb

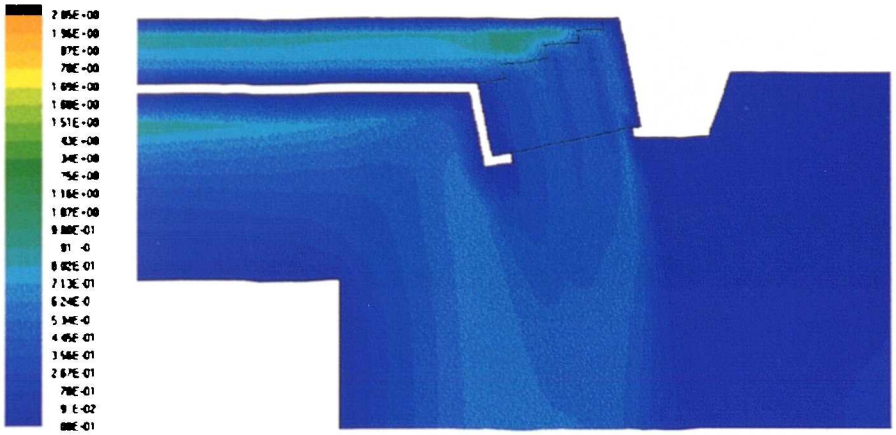

With Honeycomb

Figure 6.16 - Comparison of Velocity Contour Plots

The CFD simulations carried out in this particular investigation were done to see the advantage, if any, of increasing the number of air curtains to two. A velocity gradient was applied across the curtains by assigning each a particular flow rate. In addition, further runs were carried out to investigate the effect of also imparting a temperature gradient across the curtains. In order to create the computer model, modifications had to be carried out to the geometry whilst still maintaining a similar grid. The modified geometry and grid are shown in figure 6.17.

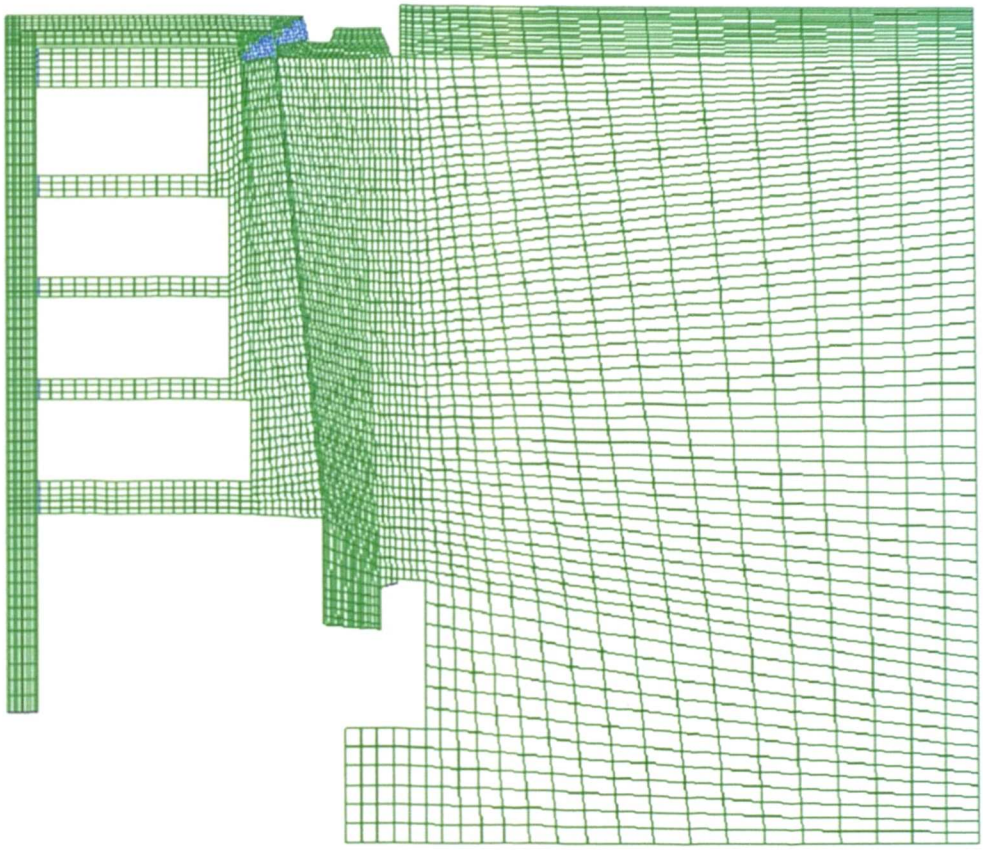

Figure 6.17 - Modified Geometry and Grid for Case with Two Air Curtains

In total, four CFD simulations were carried out. The first two were for the same temperature of -5°C for both air curtains with mass flow rates of 0.0566 kg/s for the outside curtain and 0.1132 kg/s for the inside curtain corresponding to back panel inlet velocities of 0.5 and 1.0 m/s respectively. This was followed by a model using mass flow rates of 0.1132 kg/s for the outside and 0.2264 kg/s for the inside curtain corresponding

to back panel velocities of 1.0 and 2.0 m/s respectively. This represented total mass flow rates above and below that for the baseline case. The runs were then repeated for these flow rates, this time using supply temperatures of -5°C for the inside curtain and 7°C for the outside one. The velocity vector plots for the four runs are presented in figures 6.18 and 6.19.

The velocity vectors show very little change in the air flow pattern when a temperature gradient is added to the air curtain. The most dominant difference between the four cases once again lies in the air flow rate, with higher total volume of air providing better protection of the product on the front of the shelves. However, the air temperatures adjacent to the front of the shelves are still within the limits set down in the food hygiene regulations even for the lower of the two flow rates which from foregoing analyses should be more energy efficient. A summary of the net sensible heat transfer into the domain for each case is given in table 6.4.

Table 6.4 - Summary of CFD Runs for Case with Two Air Curtains

	Curtain Temperature (°C)		Mass Flow Rate (kg/s)		Sensible Heat Transfer (% saving over base line case)
	Outside	Inside	Outside	Inside	
Run 1	-5	-5	0.1132	0.2264	1585 Watts, (2%)
Run 2	-5	-5	0.0566	0.1132	1340 Watts, (17%)
Run 3	7	-5	0.1132	0.2264	1512 Watts, (6%)
Run 4	7	-5	0.0566	0.1132	1237 Watts, (23%)

The above results from the CFD simulations suggest that the net sensible heat transfer into the domain will be lower than the base line case if two air curtains are used. This applies even at a mass flow rate above 0.2386 kg/s (for the base line case) giving greater protection to the product from external disturbances. Reducing the total mass flow rate to 0.1698 kg/s provides even more significant savings whilst maintaining product

temperatures. When a temperature gradient was applied over the air curtain together with the velocity gradient, the savings in refrigeration load were increased further.

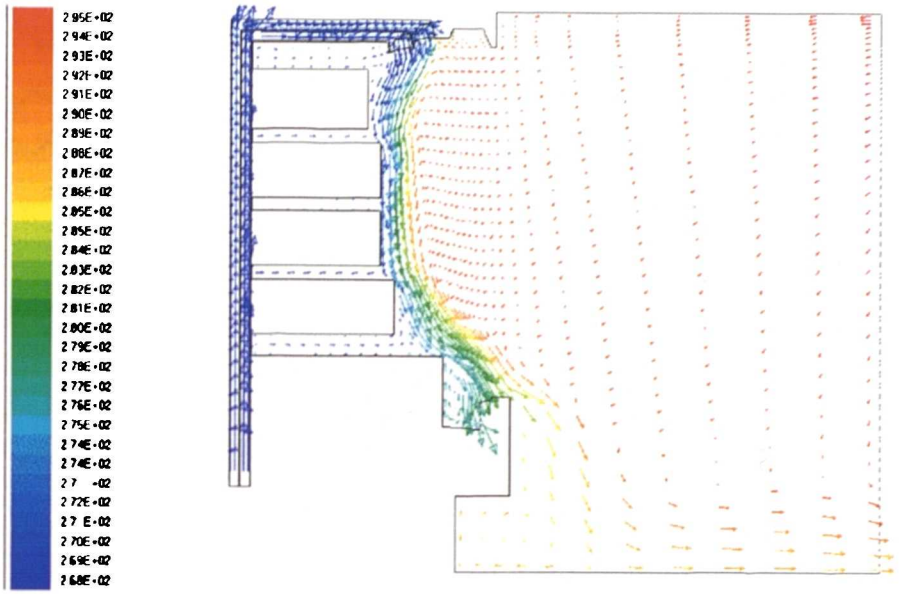

Inside curtain = 0.1132 kg/s, Outside Curtain, 0.0566 kg/s, Temperature = -5°C for Both

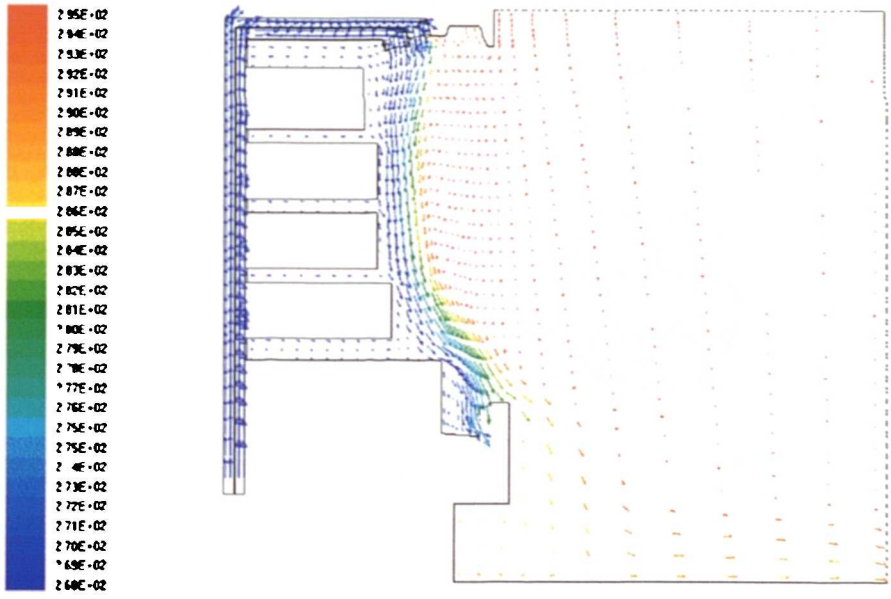

Inside curtain = 0.2264 kg/s, Outside Curtain, 0.1132 kg/s, Temperature = -5°C for Both

Figure 6.18 - Velocity Vectors for Two Air Curtains at Same Temperature

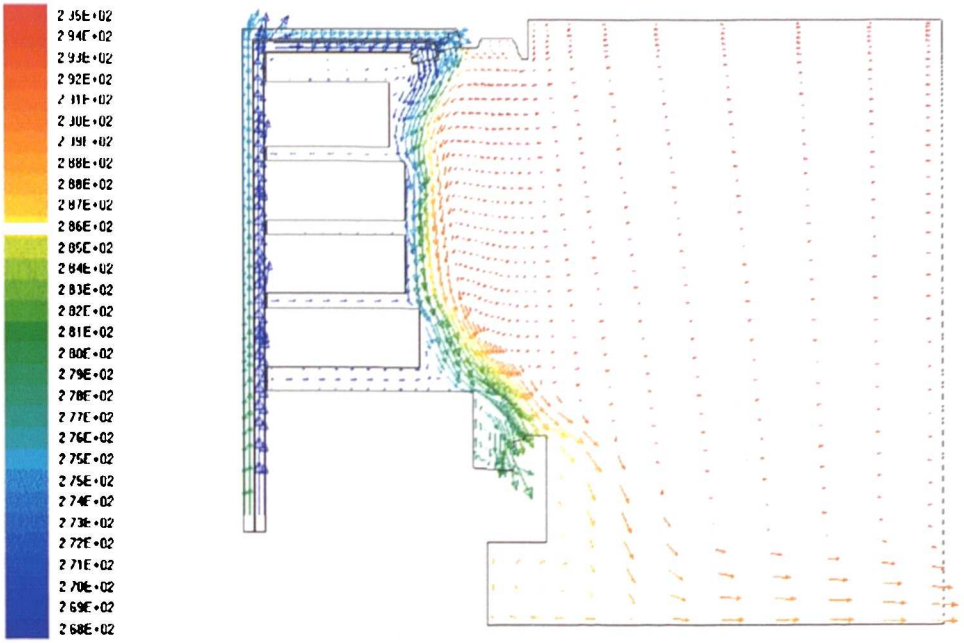

Inside curtain = 0.1132 kg/s, -5°C; Outside Curtain, 0.0566 kg/s, 7°C

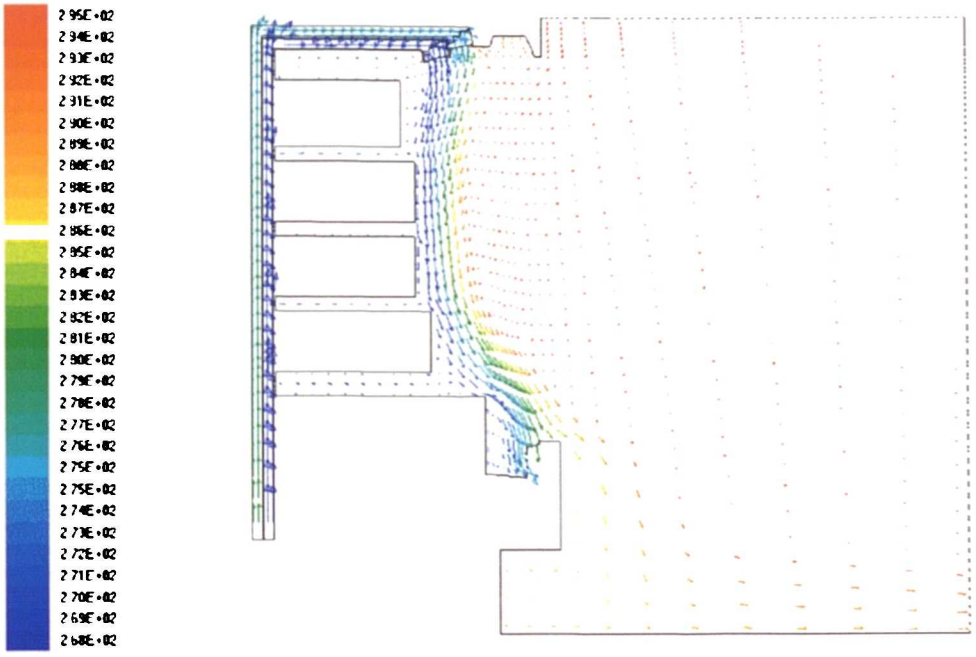

Inside curtain = 0.2264 kg/s, -5°C; Outside Curtain, 0.1132 kg/s, 7°C

Figure 6.19 - Velocity Vectors for Two Air Curtains at Different Temperatures

Figure 6.20 shows the contours of turbulence intensity for the base line case with a mass flow rate of 0.3408 kg/s compared with the case with two air curtains and a similar mass flow rate, in this case 0.3396 kg/s. The scale was kept consistent for each case in order to obtain a meaningful comparison.

Even a casual look at figure 6.20 explains the reason for the efficient performance of the case with two air curtains. The velocity gradient imposed on the outside of the curtain by the nature of the design reduces to a very large extent, the amount of fluid shear occurring in this region. This in turn means that eddies are less readily formed and the degree of turbulence on the outside of the curtain is much reduced.

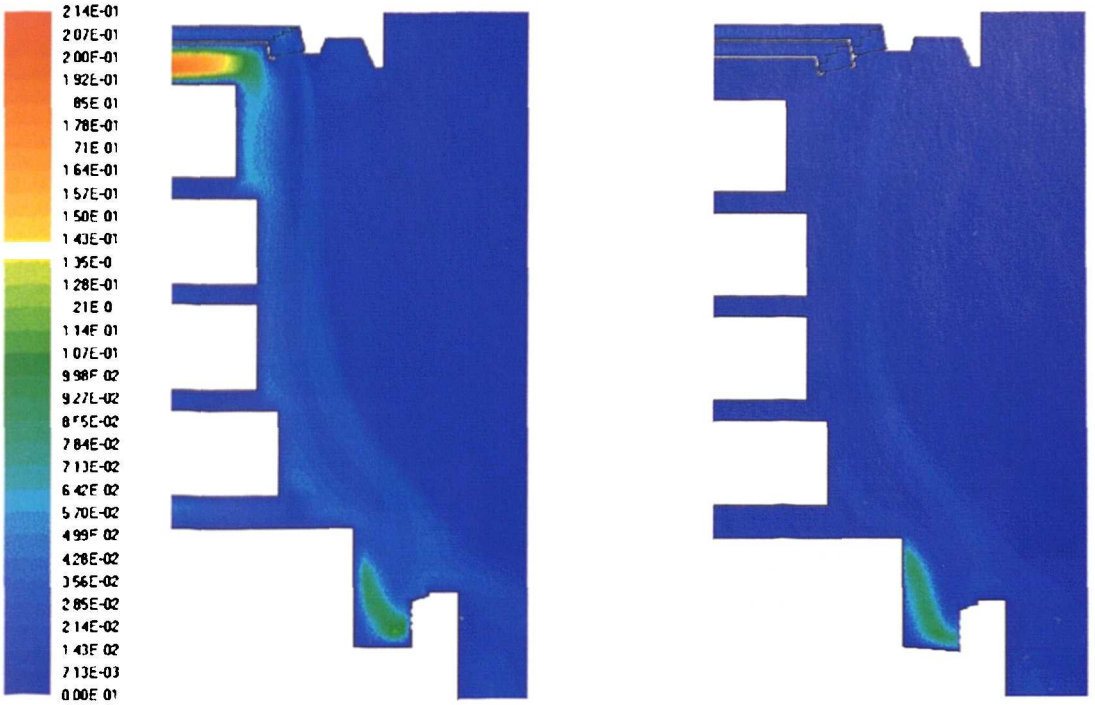

Base Line Case Design (0.3408 kg/s)

Case With Two Air Curtains at Same Temperature (0.3396 kg/s)

Figure 6.20 - Comparison of Contours of Turbulent Kinetic Energy

In running the CFD model, grid modifications meant that not exactly the same grid was used as for the base line case. This means that the results of comparing the sensible heat

transfer predicted by the two models may not be grid independent. However, the results shown in figure 6.20 do confirm the fact the turbulent kinetic energy within the air curtain has been much reduced by this modification and therefore support the findings.

From the analysis of the results presented in this section, the following conclusions may be drawn:

- Incorporating two air curtains into a display case with different velocities, the lower being on the outside of the air curtain, it has been shown that significant savings on energy are possible.
- The addition of a temperature gradient imparted across the curtain with the higher temperature being on the outside further enhances the energy savings possible.

6.7 - THE EFFECT OF REMOVING THE AIR CURTAIN

The foregoing sections have served to show that although the air curtain provides an effective barrier between the store and the refrigerated case it also imposes a cooling load on the case due to warm air entrainment. CFD simulations carried out by W.S. Atkins (1992) for Safeway Stores, investigated the consequences of removing the air curtain concept from the display case. Their analysis showed possible savings of 29% on the net sensible heat transfer into the case. Validation work then carried out at Bristol University on a similar case showed that savings in the order of 10% were more realistic. It should be remembered, however, that these two investigations were carried out on cases from different manufacturers. Whether this is the reason for the discrepancy, or there is some other explanation either in the modelling assumptions made or the experimental procedure has not been explained. It is clear though that the geometry in the region of the air curtain outlet was somewhat different between the two investigations. The current research provides the ideal vehicle to carry out further tests on this design feature, carrying out CFD simulations and experimental validation on the same case design.

The CFD model was set up using the baseline geometry and grid with several runs of the computer model being carried out for different mass flow rates. The air flow was blocked at the top of the back panel thereby still allowing diffusion through the perforations over the product but stopping air flow into the canopy. The velocity vector plot colour coded with temperature for a mass flow rate of 0.2386 kg/s is shown in figure 6.21.

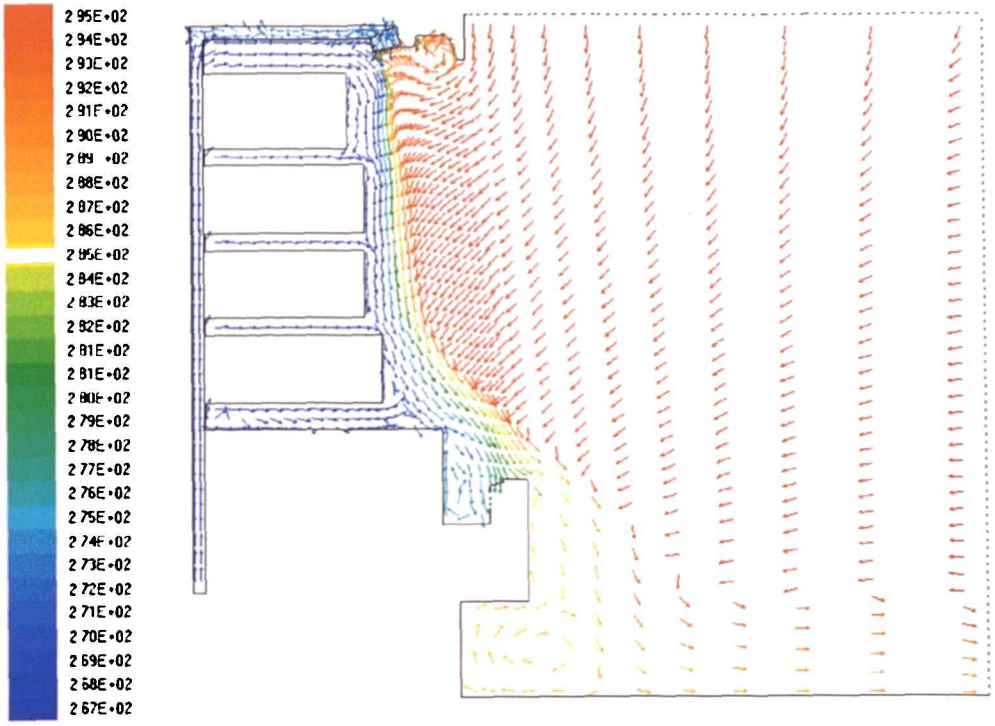

Figure 6.21 - Velocity Vector Plot for Case with the Air Curtain Removed

The velocity vectors show that generally the pattern of the air flow is very similar to that in the baseline case. A form of air curtain is still formed across the front of the product by air from the back panel on the top shelf hitting the back of the air curtain outlet and being deflected on a downward path assisted by gravity. This similarity between the air flow patterns for the case with and without the primary air curtain meant that very little difference was seen in the energy predictions for the two cases at the baseline flow rate.

The work carried out by W.S. Atkins showed that warm air encroachment presents a problem on the top shelf when designing the display case without an air curtain. The solution provided to tackle this problem was to include a fairing on the back of the air curtain outlet thus reducing the amount of space between the product on the top shelf and the canopy. Although showing significant savings, this arrangement failed to be validated satisfactorily through experiment. This is thought to be primarily due to the fact that the case modelled and the case tested were quite different in terms of the geometry of the air curtain outlet. Although, product temperatures do not seem to be a problem in the design of the case which forms the subject of this research project, it was decided to test this feature to see if it had any further advantage in terms of energy savings.

The 2D case model described above was modified with a 50 mm fairing behind the air curtain outlet and the resulting velocity vector plot is shown in figure 6.22.

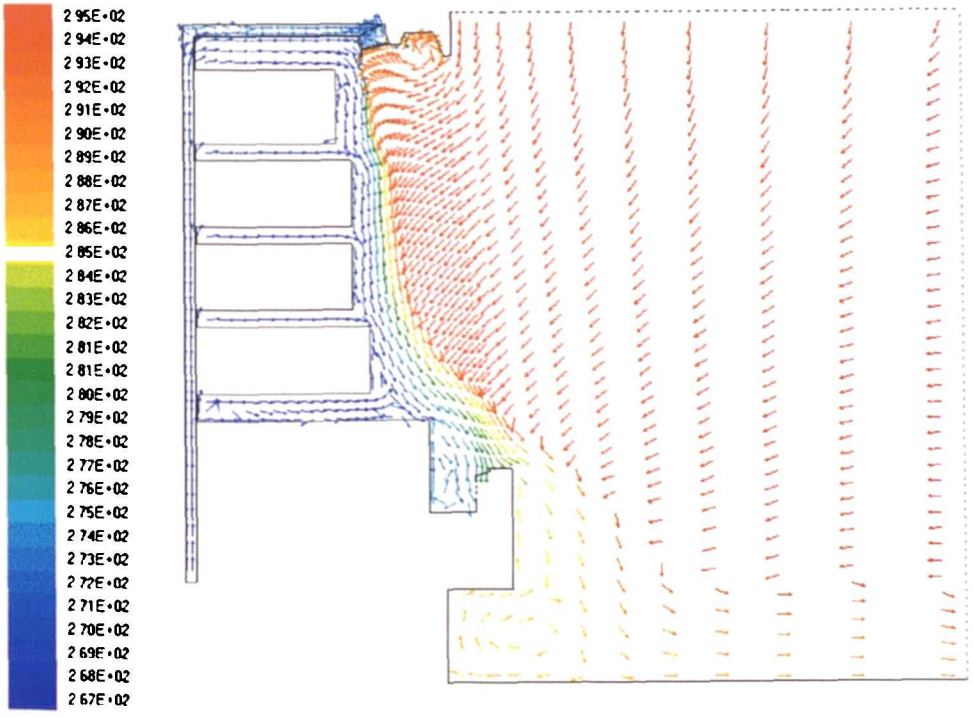

Figure 6.22 - Velocity Vectors for Case with No Air Curtain and a 50 mm Fairing

Once again, the velocity vector plot shows very little difference to the air flow pattern with the addition of the fairing. An analysis of the sensible refrigeration load on the case can be seen from the summary performance map illustrated in figure 6.23.

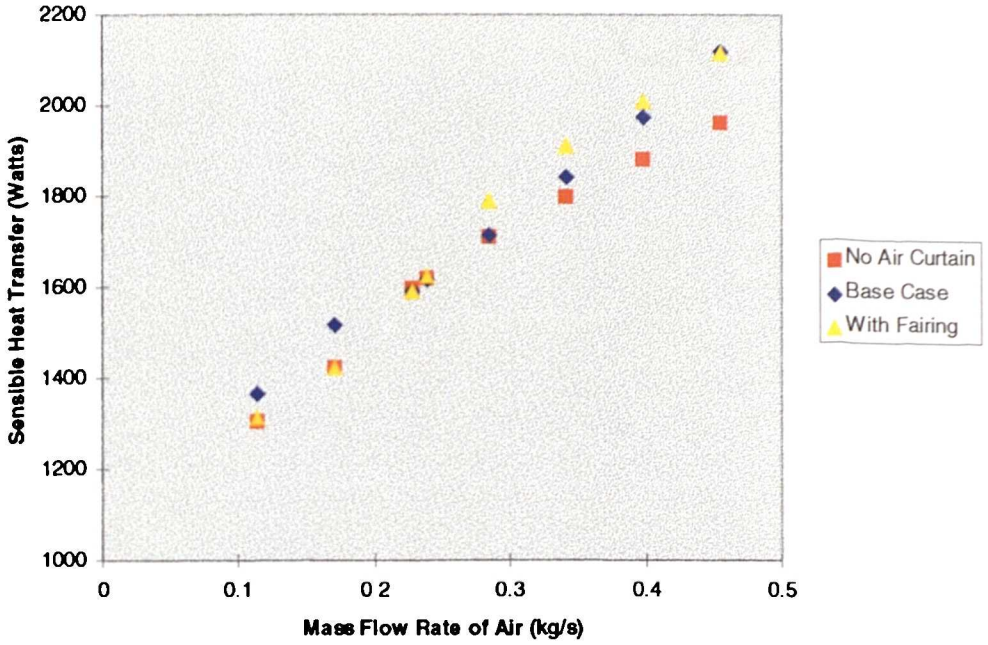

Figure 6.23 - Performance Map for Case Without Air Curtain

The performance map indicates that there is only a very small energy advantage to be gained by the omission of the air curtain and that any savings which are possible are made for cases with higher flow rates. This result will hold provided the mass flow rate remains the same for the case with and without the primary air curtain. In reality, however, this situation will not occur as an increase in flow resistance will be created by blocking off the air curtain. This, combined with the propeller fans' inability to overcome any sort of significant resistance, will mean a reduction in the case mass flow rate. As an example, if the case mass flow rate were to be reduced by 20% due to blocking the air curtain, this would correspond to a reduction of approximately 6% on the sensible heat transfer into the case. It seems, therefore, that any advantage gained in terms of the case energy consumption has little to do with the fact that the air curtain has been removed.

More likely is the fact that the air flow rate around the case has been reduced which in turn reduces the net sensible heat transfer into the case as described in section 6.2.

Far from improving the energy consumption of the case, figure 6.23 illustrates that the effect of including the 50mm fairing in the design tended to be a negative one in terms of energy efficiency. The reason for the discrepancy between these results for the fairing and the results from the W.S. Atkins work seems to be in the design of the air curtain outlet. For the case which is the subject of this project, the air curtain outlet projects down from the canopy. This provides a deflector for the horizontal air flow from the back panel, directing it downwards in a vertical path. Because of this feature, the addition of the fairing had very little effect. In the case investigated by W.S. Atkins, the design of the air curtain outlet was somewhat different finishing flush with the bottom of the canopy and thus providing no deflector for the horizontal air flow. The addition of the fairing in this case, therefore, had quite a significant effect on the air flow pattern and hence the energy consumption of the case.

In an attempt to validate the CFD runs of the case without the air curtain, it was decided to modify the case in the laboratory and carry out some experimental tests. This was done by blocking the flow from the air curtain outlet and running the case as normal. Additional tests were then carried out modifying the case to include a 50mm fairing behind the air curtain outlet. The results of these tests are summarised in table 6.4.

The total saving on energy, for the case with the air curtain omitted, measured over the base line case was of the order of 6.4%. The case which included the 50 mm fairing actually showed a small increase in the total energy consumption. These results were in line with the CFD predictions.

Table 6.5 - Total Refrigeration Load Comparison for Case Without Air Curtain			
	No Air Curtain No Fairing	No Air Curtain With 50mm Fairing	Baseline Case
First Hour	3133 Watts	3342 Watts	3327 Watts
Second Hour	3142 Watts	3456 Watts	3374 Watts
Third Hour	3284 Watts	3527 Watts	3437 Watts
Fourth Hour	3216 Watts	3468 Watts	3508 Watts
Average	**3194 Watts**	**3446 Watts**	**3412 Watts**

The analysis carried out in this section can be summarised as follows:

- CFD analysis of the display case modified by the omission of the air curtain showed only a small improvement in the energy efficiency at the baseline flow rate of 0.2386 kg/s. At higher flow rates a more significant difference was seen, the case without the air curtain consuming less energy.
- In reality, the increase in flow resistance caused by blocking the air curtain will result in a reduction in the flow rate and a corresponding reduction in refrigeration load.
- The addition of a 50 mm fairing to the back of the air curtain outlet also showed no real improvement in the refrigeration load.
- Experimental measurements showed on average a 6.4% reduction in the overall refrigeration load which was of the magnitude expected from analysis of the CFD results.

6.8 - THE EFFECT OF SHORTER AIR CURTAINS

Previous sections of this chapter have described the disadvantages of a "long" air curtain, namely, development of the air curtain leading to turbulent mixing. However, if the air curtain length were to be reduced, the effect would be to protect the product within the initial region of the jet where the centreline velocity is constant. Ejecting an air curtain

from the front of each shelf would then serve to shield the product directly beneath it in a less turbulent region of the curtain. Although this would mean that the individual curtains would overlap, it is envisaged that this would significantly enhance the performance of the case both in terms of product temperatures and energy efficiency. Another factor which contributes to this is the fact that the mass flow rate around the case can be reduced. This is because air is issued into the refrigerated environment more directly where it is required and consequently the amount of air can be controlled to a greater extent.

In the model considered, air curtains are issued at the front of each of the four shelves as well as from just behind the air curtain outlet. A mass flow rate of 0.2386 kg/s was considered. The resulting velocity vector plot is shown in figure 6.24.

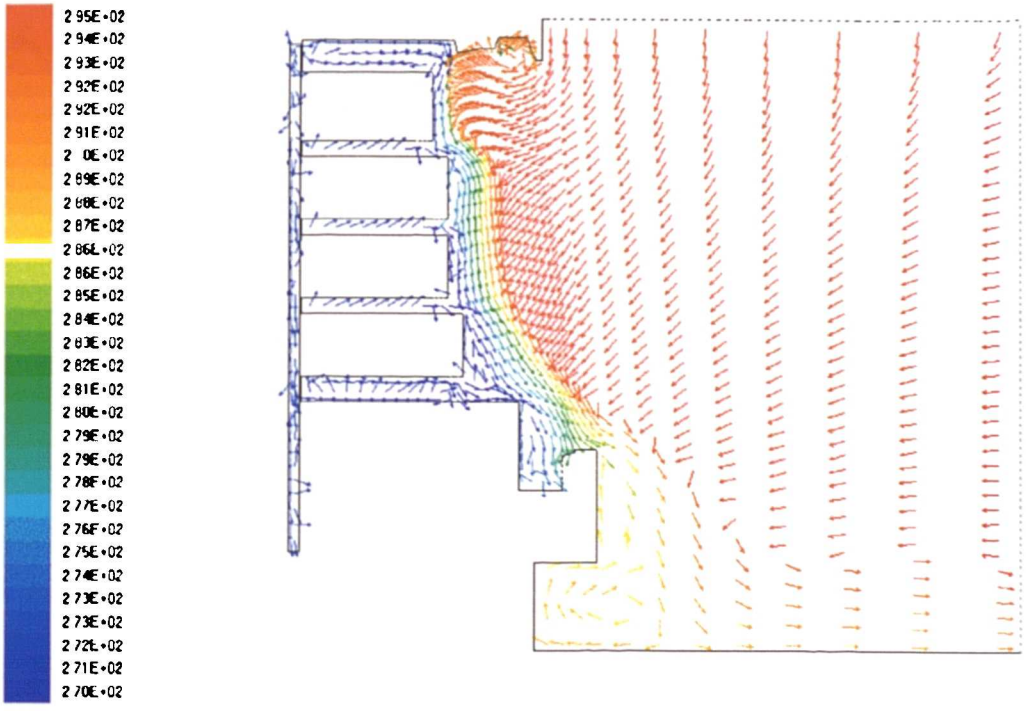

Figure 6.24 - Velocity Vector Plot with Air Curtains Issuing Beneath Each Shelf

The velocity vector plot for the modified case shows that the product is protected sufficiently so that its temperature is maintained. Some enhancements could be made at

the top shelf where temperatures adjacent to the front of the shelf are at their highest. The relative depths to each shelf may also require some investigation so that stepping of the product was perhaps not so exaggerated.

The calculation of the net sensible heat transfer into the domain showed a value of 1472 Watts, an reduction of 8.7% over the base line case which is obviously a significant saving. The reason behind this large saving can be explained with reference to figure 6.25. This shows the contours of turbulent kinetic energy for the modified case at the front of the shelves. For comparison purposes the same scale is used for both plots.

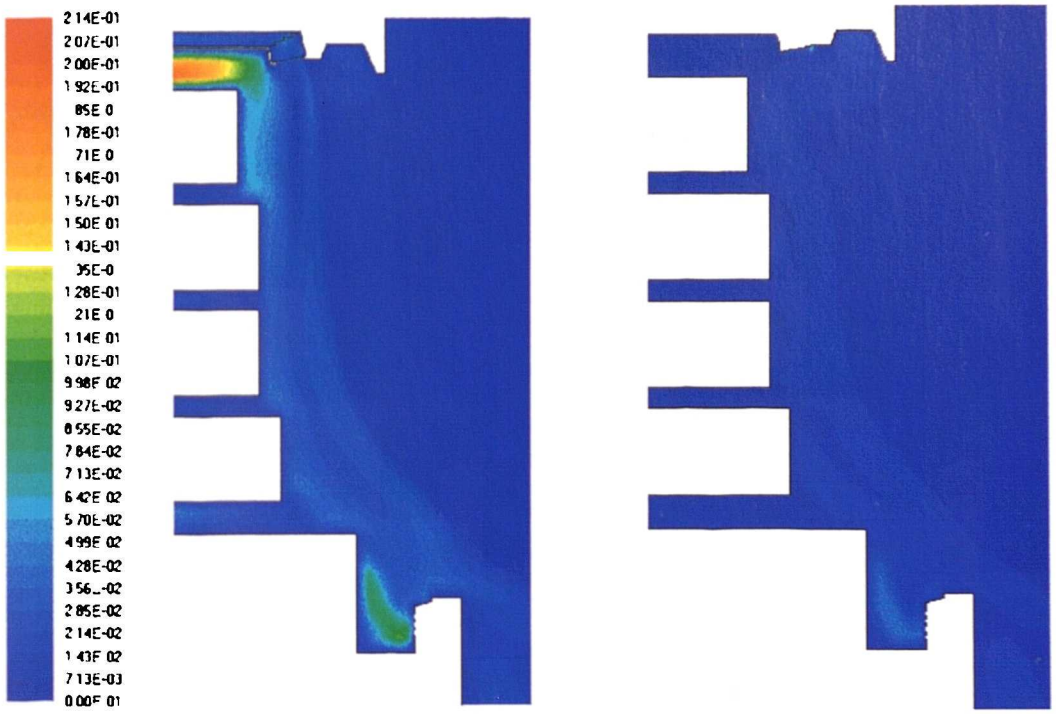

Base Line Case

Case With Series of Shorter Air Curtains

Figure 6.25 - Comparison of Turbulent Kinetic Energy for Case with Series of Shorter Air Curtains

It is clear that by the use of a series of shorter air curtains, the amount of turbulence adjacent to the front of the shelves and in the region of the air curtain has been much

reduced. Accordingly, the sensible heat load has also been reduced supporting the fact that significant savings are achievable using this strategy.

Designs of refrigerated display case incorporating shorter air curtains has been proposed by some manufacturers in the past and been granted patents accordingly. The main disadvantage of such a proposal lies in the restriction on the flexibility of shelf positioning. However, it is felt that if optimising this strategy means such savings in energy consumption are practically attainable, then a suitable design which allows, at the very least, some compromise on the flexibility of shelf positioning should be considered.

Major modifications to the actual display case are beyond the scope of this project but it is recommended that in the future, a prototype case of this design be manufactured and tested in order to quantify the savings which are practically achievable.
From the above analysis, the following conclusions may be drawn:

- CFD modelling has shown that there are potentially significant savings to be made by employing the use of multiple, shorter air curtains, issuing from the front of the shelves.
- Some optimisation of the design is required in order to fully maximise this potential and ensure that product temperatures are maintained.
- It is recommended that a prototype case following this operating strategy be built and tested in order to validate the CFD model.

6.9 - APPRAISAL OF CFD MODELLING INVESTIGATIONS

This chapter has used both the technique of CFD modelling and physical testing to look at several design features and operating strategies of refrigerated display cases. From these investigations, it has been possible to draw a number of conclusions regarding the

design of such display equipment. Some modifications have shown considerable reductions in the refrigeration load on the case while, equally, some have been worse than the present design.

Chapter 7 will summarise the conclusions which have been drawn from this investigation and assess, their practical significance on the process of the design of refrigerated display cases.

CHAPTER 7

CONCLUSIONS AND RECOMMENDATIONS FOR FURTHER WORK

7.1 - CONCLUSIONS

A detailed numerical and experimental investigation has been carried out into the fluid dynamics and heat transfer characteristics of a vertical multideck refrigerated display case. This has been done using commercially available computational fluid dynamics (CFD) software as a design tool and then validating this numerical model with experimental measurements obtained in a custom design test facility.

The design and construction of the test facility formed a major portion of this research project. It comprises an $80m^3$ environmental chamber conditioned by an air handling unit and capable of maintaining conditions between 0°C and +40°C and 30 to 95% RH. The refrigeration side of the rig has been designed to mimic as closely as possible, in its operation and control strategy, a contemporary commercial refrigeration system in order that future research can be carried out into this area.
From the results of the project, a number of conclusions can be drawn as follows:

1) A linear relationship exists between the mass flow rate of air around a multideck refrigerated display case and the refrigeration load on the case. This relationship is such that a 17% reduction in mass flow rate results in a 5% reduction in the sensible refrigeration load on the case with product temperatures still maintained below the limit set down in the food hygiene regulations.

2) Although potential exists for reducing the mass flow rate of air there is a lower limit on the amount of air flowing around the case. In general, as long as the mass flow rate is sufficient to form an air curtain across the front of the product, any further increase wastes energy without providing any improvement in the product temperature.

3) The evaporator should be selected on the highest possible refrigerant temperature to maintain safe food temperatures. This is to both maximise the C.O.P. of the refrigeration cycle and minimise at the same time the refrigeration load which it serves.

4) The inclusion of a honeycomb section into the air curtain outlet has a benefit in terms of the energy efficiency of the case. This benefit, however, is very much dependent on the mass flow rate of air around the display case. The use of the honeycomb as a mechanism for reducing load on the evaporator must therefore be assessed on the merits of a particular design.

5) The use of a front upstand on a vertical multideck display case has been shown to improve the energy efficiency of the case. The potential savings from this feature are in some way proportional to the height of the upstand. Further work is required on this design feature to optimise the design for the specific application and thereby minimise energy consumption.

6) Incorporating two air curtains into a display case with different velocities, the lower being on the outside of the air curtain, has been shown to produce energy savings. This is due to the velocity gradient imposed on the outside of the air curtain which limits the degree of fluid shear in this region. The result of this is less turbulent mixing between the curtain and the warmer store air.

7) CFD analysis of the display case modified with the omission of the air curtain showed only a small improvement in the energy efficiency at the baseline flow rate of 0.2386 kg/s with a slightly more significant improvement at higher flow rates. In reality, the increase in flow resistance caused by blocking the air curtain will result in a reduction in the flow rate and a corresponding reduction in the refrigeration load. For instance if the mass flow rate of air around the case was reduced by 17% by blocking off the air curtain outlet, the resulting saving would be of the order of 7% in the sensible refrigeration load. Experimental

measurements showed on average a 6.4% reduction in the overall refrigeration load by the omission of the air curtain.

8) The addition of a 50mm fairing at the back of the air curtain outlet showed no significant improvement in the refrigeration load. It was originally though that the inclusion of a 50mm fairing would limit the ingress of warm store air into the top of the case. However, due to the nature of the case design being investigated, this was not an important factor.

9) CFD modelling has shown that there are potentially significant savings to be made by employing the use of multiple, shorter air curtains, issuing from the front of the shelves. This model has yet to be validated but it is thought that some optimisation of the design is required in order to fully maximise this potential and ensure that product temperatures are maintained.

10) It has been demonstrated that some potential exists for reducing the energy consumption of the food retail sector through better design of refrigerated display cases. As well as these commercial issues, however, this research has enabled a better understanding of how refrigerated cases work and some of the issues that surround them. For instance, fluid theory says that when a moving stream of air enters a relatively still environment there will be entrainment into the jet. This applies equally for display cases and consequently it is virtually impossible to stop at least some entrainment of store air alongside the primary air curtain.

11) If it is clear that some entrainment of store air will occur, the next step in reducing the case load is to prevent mixing between the cold and warm parallel air steams. The degree of mixing is a function of the degree of turbulence intensity contained within the air curtain. These levels of turbulence can be reduced by means of honeycombs, reducing air flow rates and thus velocities and by reducing the velocity gradient by means of multiple air curtains. Since the eddies within the curtain cascade, increasing the turbulence intensity further down the curtain, the degree of mixing is also a function of curtain (or opening) height.

12) The overspill of cold air has always been an issue with the use of vertical multideck display cases. It is clear that as long as there is some entrainment of store air, there will be some overspill at the front of the case due to there being a mass balance across the fans. The temperature of this spilled air is a function of the amount of mixing which has occurred with the cold air curtain.

The research carried out during the course of this project makes a contribution to the overall effort towards the improvement of the energy efficiency of retail refrigeration systems in two ways. Firstly, through a combination of numerical modelling and experimental validation, computational fluid dynamics has been shown to be a valuable tool in the design of refrigerated display cases. Secondly, a number of conclusions have been drawn as to the operating strategy of an existing case design and the effectiveness of certain design features. For example, it has been shown that the inclusion of a honeycomb, the air mass flow rate around the case, and the number of air curtains are all important parameters in the energy efficient design of a display case.

7.2 - RECOMMENDATIONS FOR FURTHER WORK

While several suggestions have been made towards ways in which the operating efficiency of display cases can be improved, these have been in broad terms with little attempt at optimising a particular design feature. It is logical that this be the next step towards designing a more energy efficient display case.

The assumption during this research has been of steady state operating conditions with a constant mass flow rate. This is a fair approximation as any change to the operating conditions occurs very slowly. It should be remembered, however, that the actual operation is not steady state, mainly due to frosting and defrosting. It is therefore suggested that once an optimal design is achieved, this be tested against the extreme conditions which are likely to occur during the course of an evaporator frosting e.g. maximum and minimum mass flow rates and air off temperatures. In this way, the

performance of the case can be assessed in terms of the operating parameters which will occur in practice.

All the investigations carried out during the course of this project have been done with consideration of standard test conditions as a representative ambient environment for the operation of the display case. However, within the actual environment of the supermarket, the display case is subject to a whole range of randomly occurring conditions with cross draughts, the disturbance of customers walking past, product overstacking, re-merchandising etc.. Accordingly, it is suggested that some course of work is carried out to investigate some of these conditions and the interaction between the case and its environment.

APPENDIX A

SUMMARY OF PLANT SPECIFICATIONS

ENVIRONMENTAL CHAMBER

Manufacturer	Cryotec Coldroom, The London Refrigeration Company, Refrigeration House, Grays Park Road, PO Box 133, Slough, Berks SL2 4BL
Wall Insulation	75mm of fire retardant high density virgin bead expanded polystyrene Internal Finish:- Good quality white plastisol steel sheeting to the walls and ceiling External Finish:- Good quality white plastisol steel sheeting
Fittings	One Dual glazed inspection window 1.5m x 1m Two vapour sealed twin 1.8m fluorescent fittings
Internal Dimension	7m x 3.5m x 3m

DAMPER WALL

Manufacturer	Brooke Air Sales, J C House, Hurricane Way, Wickford Business Park, Wickford, Essex SS11 8YB
Damper type	Opposed blade (OB type)
Size	3.5m x 3m

FILTER WALL

Manufacturer	Farr Europe, Farr Filtration Limited, 272 Kings Road, Tyseley, Birmingham B11 2AB
Type	DGF90 Disposable Panel Filter
Size	3.5m x 3m

SUPPORT FOR AIR HANDLING UNIT

Manufacturer	Air-Con-Duct Ltd, Bridge Works, Iver Lane, Cowley, Uxbridge UB8 2JG

CHILLER

Manufacturer	Liebert Europe, Globe Park, Marlow, Bucks SL7 1YG	
Model	CSU3000	
Serial No.	C04051A	
Refrigerant	R22	
Cooling Capacity per Module (kW)	Low/Med Capacity	9.9
	High Capacity	19.0
Coolant Flow Rate-l/s	0.57	
Leaving Water Temp °C	11	
Supply	380 Volts, ph 3, 50 Hz	
Coolant Pump	0.75 Hp	
No. of Compressors	2 (100% redundant system)	
Design High Pressure	20.4 Bar	
Design Low Pressure	10.2 Bar	

CONDENSER

Manufacturer	Liebert Europe, Globe Park, Marlow, Bucks SL7 1YG
Model	CSC 065

AIR HANDLING UNIT

Manufacturer	Reycol SVC Ltd, Unit 20, Moor Park Industrial Centre, Tolpits Lane, Watford, Herts WD1 8SR
Model Type	MPU5
Supply Volume	$3m^3/s$
External Static	$100 N/m^2$

Fan type	Centrifugal (Forward Curved Impeller)
Shaft Speed	657 rpm
Absorbed Power	1.723 kW
Total Efficiency	55%
Motor Type/kW	2.20
Motor Voltage	415 volt/3phase/50 Hz
Full load current	4.90 amps
Speed	1400 rpm
Humidifier	Housing only
Cooling Coil	EAT 23/17,12LAT20.4716.1
Cooling Media	Water @ 5/11°C 15% Glyc.
No. Rows/Stages	1 Row
Water Flow Rate	0.410 kg/sec
Water Pressure Drop	8.382 kPa
Connections	0.75 inch bsp flow & return
Construction	Copper tubes - Aluminium fins
Heating Coil	
Capacity	12 kW total load
Heating Media	Electric @ 415/3 @ N Supply
No. Rows/Stages	1 Stage
Construction	Black Heat Sheathed
Pre-Filter	Disposable Panel
Filter Efficiency	EU4
Anti-Vibration	Air Damped Springs (Isolation) 97% @ 20 Hz
Mixing Box	Hand operated

HUMIDIFIER

Manufacturer	JS Humidifiers, JS Industrial Services Ltd, Rustington Trading Estate, Artex Avenue, Rustington, West Sussex BN16 3LN
Type	4/6 stage step sequence direct steam injection
Model	Eurovap ELS - 8 (Super)
Serial No.	72337
Electric Supply	240V, 50Hz a c
Power max	6.9 kW
Capacity	8 Litres/hour

CHAMBER TEMPERATURE PROBE

Manufacturer	Status Instruments Ltd, Green Lane, Tewkesbury, Gloucestershire GL20 8HE
Model	SEM105P (Temperature)
Sensor	Platinum Resistor to BS1904 Class B
Output	4-20mA, 2 wire
Supply	10 to 33V DC
Range	0-50°C
Accuracy	± 5°C

CHAMBER HUMIDITY PROBE

Manufacturer	Status Instruments Ltd, Green Lane, Tewkesbury, Gloucestershire GL20 8HE
Model	SEM105H-3
Measuring Range	Humidity 0 to 100% RH
Response Time	60 secs (90% change less than 15 secs)
Stability	< 2% RH/year
Output	4-20mA linearly proportional to 0 to 100% RH
Supply	12 to 32 V DC
Accuracy	Humidity ± 3% (10 to 90% RH)

COMPRESSORS

Manufacturer	DWM Copeland
Re-Manufactured by	Trumetic Refrigeration Service, Unit 5, 7 & 9, Dodgson Street, Rochdale OL16 5SJ

Compressor 1

Model	DKJ-75
Refrigerant	R22
Cylinders	2
Electrical Supply	380-420 V, 3Phase, 50 Hz
Displacement	5.14 m^3/h
Nominal Speed	1450 min^{-1}, 50 Hz

Compressor 2

Model	DKJ-100
Refrigerant	R22
Cylinders	2
Electrical Supply	380-420 V, 3Phase, 50 Hz
Displacement	5.14 m^3/h
Nominal Speed	1450 min^{-1}, 50 Hz

Compressor 3

Model	DKJ-150
Refrigerant	R22
Cylinders	2
Electrical Supply	380-420 V, 3Phase, 50 Hz
Displacement	6.33 m^3/h
Nominal Speed	1450 min^{-1}, 50 Hz

CONDENSERS

Manufacturer	Searle Manufacturing Company, Newgate Lane, Fareham, Hampshire PO14 1AR

Model	MDS 3-4
Type	Air cooled
Refrigerant	R22

CABINET 1 (CASE ON TEST)

Manufacturer	Hussmann Manufacturing Ltd, Rosyth Road, Glasgow G5 0XZ	
Model	Eurovision EV-78-M-20 Case	
Application	Dairy	
Operating Temp.	0 / +3°C	
Type	Air fin type fitted with EEV and TEV	
Case Length	2.5 Metres	
Refrigerant	R22	
Extraction Rate	With Shelf Lights	3722 Watts
	No Shelf Lights	3443 Watts
Evaporating Temp.	-8 °C	
Electrical Load	Total Fans	120 Watts
	Total Lights	420 Watts
	Total Defrost(Def. Heater)	3000 Watts
	Total Refrigeration	540 Watts
	Gas Defrost	540 Watts
	Electric Defrost	3540 Watts

CABINET 2 (ADDITIONAL LOAD)

Manufacturer	Carter Refrigeration Display Ltd, Redhill Road, Birmingham B25 8EY
Model	CHV
Case Length	2.5 Metres
Type	Air fin type fitted with TEV
Refrigerant	R22
Extraction Rate	3280 Watts

Cabinet Temperature	2°C		
Evaporator Temp.	-12°C		
Electrical Loading:	Lighting Canopy	Twin Row	200 Watts
		Single Row	100 Watts
		Shelves	80 Watts
	Fans		208 Watts
	Electronic Controls & Valves		100 Watts
	Electric Defrost		2200 Watts

HEAT EXCHANGER

Manufacturer	Alfa Laval Thermal Ltd, Great West Road, Brentford, Middlesex TW8 9BT	
Model	CB26-34H(h21, b21)	
Serial No.	198976	
	Water	R22
Mass flow rate (kg/s)	0.4754	0.06272
Fluid Condensed/vapourised (kg/s)	0.000	0.04704
Temperature In/Out (°C)	10.0/5.0	-4.3/0.0
Operating Pressure In/Out (bar)		4.2934/4.188
Heat Exchanged (kW)	10.00	
Heat Transfer Area (m^2)	0.80	
Mean Temperature Difference (°C)	8.1	

LIQUID RECEIVER

Manufacturer	Schultze, ESK System Component, Germany
Model	SGS 18 /22 -22L
Volume	18 Litres
Refrigerant R22 charge	18 kg
Pressure Max	28 bar
Weight	15 kg

OIL SEPARATOR

Manufacturer	Schultze, ESK System Component, Germany
Model	OS-3/4"
Max Operating Pressure	28 bar
Test Pressure	31 bar
Temp. Max	100°C
Volume	3.5 Litres
Pre-Charge Ref. Oil	0.6 kg
Material	Steel

OIL RESERVOIR

Manufacturer	Schultze, ESK System Component, Germany
Model	OSA - 7.5
Max Operating Pressure	25 bar
Test Pressure	31 bar
Temp. Max	100°C
Volume	7.5 Litres
Volume low level sight glass	2.91 Litres
Material	Steel

PRESSURE TRANSDUCER

Manufacturer	Danfoss, Nordborg, Denmark
Type and Code	AKS32, 060G2083
Serial No.(P1), (P2) & (P3)	00084273, 00032143 & 00034143
Pressure range	1 - 24 bar
Max Pressure	40 bar
Supply / Output	15 - 30 V dc / 0 - 10 V
Type and Code	AKS32, 060G2082
Serial No. (P4) & (P5)	00103273 & 00099273

Pressure range	1 - 9 bar
Max Pressrue	33 bar
Supply / Output	15 - 30 V dc / 0 - 10 V

THERMOCOUPLES (K-TYPE)

Manufacturer	TC Ltd, PO Box 130, Cowley Mill Training Estate	
	Longbridge Way, Uxbridge UB8 2YS	
Type Reference	12-K-150-118-1.0-2I-3P6M-ACF 76S	
Type No.	12	
Calibration	K Nickel Chromium vs Nickel Aluminium	
Outer diameter	1.0 mm	
Length	150 mm	
Fitting	Adjustable compression, ACF 76S	
Temperature Range	Continuous (°C)	0 to +1100
	Short term (°C)	-180 to +1350
Response Time	0.15 sec	
Accuracy	±2.5°C	

THERMOCOUPLES (T-TYPE)

Supplier	RS Components Ltd, The Fairway Estate, Green Lane
	Hounslow, Middlesex TW4 6BU
Type	T (Welded Tip Thermocouple PTFE insulated)
Material	Copper / Copper Nickel
Wire Diameter	0.8 mm
Wire Length	1 m
White Sleeve (positive)	Copper
Blue Sleeve (negative)	Copper-Nickel
Temperature Range	- 50 to + 200°C
Accuracy	±1.0°C

MASS FLOWMETER

Manufacturer	Krohne Measurement & Control Ltd, Rutherford Drive, Park Farm Industrial Estate, Wellingborough, Northants NN8 6AE
Model	MFM 4085K
Protection	IP67
Transducer	MFS4000 - 10G
Connections	DN15 / PN40
Pressure Test	1.5 × Connection Rating
Wetted Parts	Titanium
Signal Converter	MFC085K
Supply Voltage	240 V ac
Cable Connection	PG16
Output	No.1 - 1 × Analog, 1 × Pulse, 1 × Status

Configuration

Display Units	kg/min
Analogue Output	4 - 20 mA
Output Range (1)	0 - 12 kg/min

Process Data

Fluid	R22
Density	1200 - 1500 kg/m^3
Temperature	10 - 30°C
MaximumPressure	15 bar gauge

POWERMETERS

Manufacturer	Polymeters Response International Ltd, PRI House, Moorside Road, Winchester, Hampshire SO23 7RX
Model	Prime 500
Product Code	PR528225 (Assy No.)

Serial No	100354
Analogue Output	kW, kVA, I
Supply	240V, 5A, 3ph, 4 Wire, 50Hz

ELECTRICAL PANEL AND CONTROL SYSTEMS

Manufacturer	Global Panels Ltd, Unit3, Hill Farm, School Road, Henley, Ipswich, Suffolk, IP6 0SA

CASE AND PACK CONTROLLER

Manufacturer	Elm Ltd, 80 Johnstone Ave, Cardonald North, Hillington Business Park, Glasgow G52 ANZ

THREE AXIS POSITIONING ROBOT

Manufacturer	CAM Systems Ltd, Unit 3, Rougham Industrial Estate, Bury St. Edmunds, Suffolk, IP30 9ND.

APPENDIX B

THEORETICAL CALCULATION OF REFRIGERATION LOAD

1.0 - Heat Transfer Through Fabric, Q_{wall}:

Calculated from the formula:

$$Q_{wall} = U\,A\,\Delta T$$

Where:

Approximate area of walls = 12.13 m^2.

Walls are constructed from 50 mm expanded polystyrene with a thermal conductivity of 0.035 W/ m K. Surface heat transfer coefficients are assumed to be 9.0 W/m^2K on the outside and 11.0 W/m^2K on the inside.

$$\frac{1}{U} = \frac{1}{h_{si}} + \frac{l}{k} + \frac{1}{h_{so}}$$

Therefore U = 0.613 W/m^2K.

$\Delta T = T_{ambient} - T_{case}$

$= 22 - 0 = 22°C$

$\Rightarrow Q_{wall} =$ <u>164 Watts</u>

2.0 - Heat Transfer by Radiation, Q_{rad}:

Radiative heat transfer occurs across the opening of the case which has an area of 3.05 m^2. The problem can therefore be simplified into radiation exchange between two flat, grey, parallel plates of the following specifications.

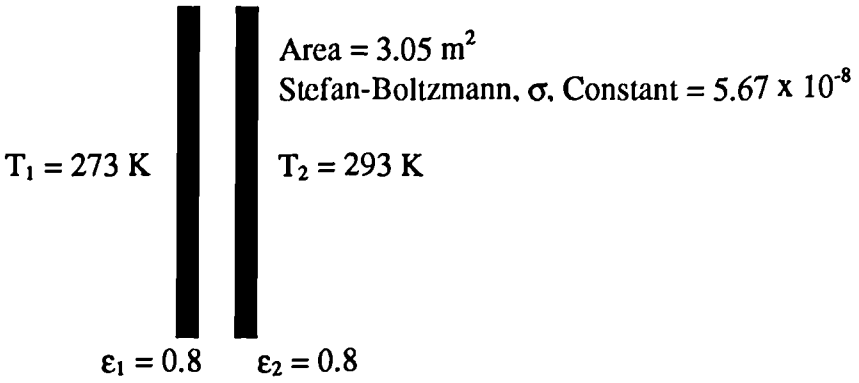

$$Q_{rad} = \frac{\sigma . A . (T_2^4 - T_1^4)}{1/\varepsilon_1 + 1/\varepsilon_2 - 1}$$

$$\Rightarrow Q_{rad} = \underline{313 \text{ Watts}}$$

3.0 - Latent Heat Transfer, Q_{lat}:

During experimental runs on the display case, 9 Litres of condensate was measured over a period of six hours and over two defrost cycles.

Therefore, mass flow rate of vapour into case = 0.000417 kg/s

Latent heat required to condense water vapour to a liquid = 0.000417 x 2500 kJ/kg
= 1.04 kW.

Latent heat required to freeze water = 0.000417 x 333.5 kJ/kg
= 0.139 kW.

$$\Rightarrow Q_{lat} = \underline{1179 \text{ Watts}}$$

4.0 - Fan Load, Q_{fan}:

Electrical load on fans from manufacturers information = 120 Watts per fan.

Assuming that one third of this is given out in heat for each of the fans, the refrigeration load affected by the fans = <u>120 Watts.</u>

APPENDIX C

PUBLICATIONS

Stribling D., Tassou S.A. & Marriott D. "The use of computational fluid dynamics in the minimisation of air overspill from refrigerated display cases" Proceedings of the CIBSE National Conference, October 1995.

Stribling D., Tassou S.A. & Marriott D. "Optimisation of the design of refrigerated display cases using computational fluid dynamics" Proceedings of The Institute of Refrigeration, Session 1995-96.

Stribling D., Tassou S.A. & Marriott D. "An experimental investigation of refrigerated display case performance" Proceedings of the International Refrigeration Conference, Purdue University, Indiana, 1996.

Stribling D., Tassou S.A. & Marriott D. "A Two-dimensional CFD model of a refrigerated display case" ASHRAE Transactions, 1997, V. 103, Part 1.

REFERENCES

Adams P. "Merchandising vs. energy consumption in the supermarket" Heating/ Piping/ Air Conditioning, April 1992, p. 53-58.

Adams P. "The intereffect of supermarket refrigeration and air conditioning" ASHRAE Transactions, 1985, V. 91, Part 1, p.423-433.

Adams P. "Intereffects in supermarkets" ASHRAE Journal, October 1985,pp.38-40.

Adams P. & Trieb S.E. "Convenience store refrigeration: self contained or remote?" Heating / Piping / Air Conditioning, November 1985, pp.103-107.

Asker G. & Berner E. "Industrial air curtain units - Part I - for reduction of temperature and moisture exchange in open doorways to freezers and coolers" Berner Industries Inc., Bulletin 32265, 1965.

Boussinesq J. "Theorie de l'ecoulement Tourbillant" Mem. Pre. Par Div. Sav., 23, Paris, 1877.

Cox R.L., Haberl J.S. & Claridge D.E. "*A study of energy use in grocery stores*" ASHRAE Transactions: Symposia p.1301-1314.

Evans J.A., Russell S.L. & Gigiel A.J. "Verification of CFD predicted reductions in energy consumption due to modifications of a multideck refrigerated display cabinet" University of Bristol, Food Refrigeration & Process Engineering Research Centre (FRPERC), 1993.

Görtler H. "Berechnung von aufgaben der freien turbulenz auf grund eines neuen naherungsansatzes", ZAMM, 1942, V. 22, p. 244.

Hanjalic K. & Launder B.E. "Sensitising the dissipation equation to irotational strains", 1981, Journal of Fluids Engineering, V. 12, p.34.

Hawken P.J., Hearty P.F. & Lemal C. "The influence of two-phase flow on a coriolis effect mass flow meter", ASHRAE Transactions, 1985, V.91, Part1B, p.310-321.

Hetsroni, G. "Heat transfer through an air curtain" PhD Thesis, Michigan State University, East Lansing, 1963.

Hetsroni G. & Hall C. W. "Further studies of the air curtain" Quarterly Bulletin of the Michigan Agricultural Experimental Station, 1964, V.46, Part 3, pp. 438-452.

Howell R.H. "Calculation of the humidity effects on energy requirements of refrigerated display cases" ASHRAE Transactions, 1993, V. 99, part 1, p.679.

Howell R.H. "Effects of store relative humidity on refrigerated display case performance" ASHRAE Transactions, 1993, V. 99, part 1, p.667.

Howell R.H. & Adams P. "Effects of indoor space conditions on refrigerated display case performance" Final Report, ASHRAE-596RP, 1991.

Howell R.H. & Shibata M. "Heat transfer thru air doors on heated and cooled buildings" Proc. 4th International Symposium on the use of Computers for Environmental Engineering Related to buildings, Tokyo, 1983, p.140.

Howell R.H. & Shibata M. "Optimum heat transfer through turbulent recirculated plane air curtains" ASHRAE Transactions, 1980, V. 86, part 1, p.188.

Howell R.H., Van N.Q. & Smith C.E. "Heat and moisture transfer through turbulent recirculated plane air curtains" ASHRAE Transactions, 1976, V.82, part 2, pp.191-205.

Launder B.E., Reece G.J. & Rodi W., Journal of Fluid Mechanics, 1975, V. 68, p.537.

Launder B.E. & Spalding D.B. "The numerical computation of turbulent flows", Comput. Meth. Appl. Mech. Eng., 1974, Vol. 3, p. 269-289.

Loerke R.I. & Nagib H.M. "Control of free stream turbulence by means of honeycombs: a balance between suppression and generation" Trans. of ASME, September 1976, p. 342.

Lumley J. L. "Passage of a turbulent stream through honeycomb of large length to diameter ratio" Transactions of ASME, June 1964, pp.218-220.

Lumley J. L. & McMahon J. F. "Reducing water tunnel turbulence by means of a honeycomb" Transactions of ASME, December 1967, pp.764-770.

McGuirk J.J. & Rodi W., Proc. of 1st Symposium on Turbulent Shear Flow, Penn. State Univ., USA, 1977.

Patel J. "Simulation of honeycomb sections using the porous media model", 1996, Final year project, Brunel University, London.

Powlesland J. W. "New uses continue to be found for air curtains" Canadian Mining Journal, October 1971, pp.84-93.

Ratkowsky D.A., Olley J., McMeekin T.A. & Ball A. "Relationship between temperature and growth rate of bacteria cultures" Journal of Bacteriology, V. 149, No.1, January 1982, pp.1-5.

Reichardt H. "Gesetzmassigkeiten der Freien Turbulenz" VDI-FORSUNGSHEFT, 1942, p. 414.

Reynolds O., Phil. Trans. of the Royal Society London, Series A, Vol. 186, 1874, pp.123-161.

Rodi W., Proceedings of 2nd Symposium on Turbulent Shear Flows, London 1979.

Schlichting H. " Boundary Layer Theory" McGraw-Hill Book Co., New York, 1955.

Taylor G. & Adams E. "An evaluation of methods of controlling the environment adjacent to multideck refrigeration display cases" Proceedings of the CIBSE National Conference, 1994, pp.216-226.

Tyler T. "Open display cases - control natural drafts in the area" ASHRAE Journal, September 1960, p.63.

Van N.Q. "Influence of the initial turbulence intensity on the heat and moisture transfer through a recirculated air curtain" PhD Thesis, University of Missouri-Rolla, Rolla , MO, 1975.

Van N.Q. & Howell R.H. "Influence of initial turbulence intensity on the development of plane air curtain jets" ASHRAE Transactions, 1976, V. 82, part 1, p.208.

Versagi F. J. "Supermarkets are uncomfortable" Air Conditioning & Refrigeration News, 14th April 1969, p.12.

Walker D.H., Tsaros T.L. & Deming G.I. "Guide for the selection of supermarket refrigeration systems" Electric Power Research Institute (EPRI), Final Report CU-6740, March 1990.

"Night blinds on refrigerated cabinets" March Consulting Group for the Energy Efficiency Office, Good Practice Case Study 223, 1994.

"Safeway stores plc chilled multideck cabinet airflow study" Report by W.S. Atkins Engineering Sciences, November 1992.

BS 6148: 1981: British standard methods of test for commercial refrigerated cabinets.

European Standard EN 441-1, 1995, Refrigerated display cabinets.

"The Food Safety (Temperature Control) Regulations 1995" Statutory Instrument No. 2200, 1995.

GB Patent No. 865147, "Display Case with Adjustable Refrigerated Shelves" Application date: February 3rd 1958 by Hussmann Refrigerator Company.

GB Patent No. 1011175, "Refrigerated Display Unit" Application date: December 30th 1963 by MaCray Refrigerator Company.

GB Patent No. 1134399, "Refrigerated Display Apparatus" Application date: December 13th 1966 by Litton Industries Inc.

GB Patent No. 1544584, "Refrigerated Display Case" Application date: August 15th 1977 by Emhart Industries Inc.

BIBLIOGRAPHY

1. **Gosney W.B.** "Principles of Refrigeration" Cambridge University Press, 1982

2. **Dossat R.J.** "Principles of Refrigeration" Prentice-Hall Editions, 3rd edition, 1991.

3. "CFC Phase Out: Advice on alternatives and guidelines for users" March consulting group for the DTI, March 1993.

4. **Awbi H. B.** "Ventilation of buildings" E. & F. N. Spon, 1991.

5. Fluent Users Manual.

6. Flovent Reference Manual.